The amygdala regulates information flow from the prefrontal cortex to the nucleus accumbens

By

Vincent B. McGinty

Bachelor of Arts, Johns Hopkins University, 2001

Submitted to the Graduate Faculty of Arts and Sciences

in partial fulfillment of the requirements for the degree

Doctor of Philosophy in Neuroscience

University of Pittsburgh

2008

UNIVERSITY OF PITTSBURGH

SCHOOL OF ARTS AND SCIENCES

It was defended on

29 May 2008

and approved by

Germán Barrionuevo, M.D.

Joel P. Gallagher, Ph.D.

Bita Moghaddam, Ph.D.

Susan R. Sesack, Ph.D.

Peter L. Strick, Ph.D.

Dissertation advisor: Anthony A. Grace, Ph.D.

The amygdala regulates information flow from the prefrontal cortex to the nucleus accumbens

Vincent B. McGinty, Ph.D.

University of Pittsburgh, 2008

Motivated behaviors are mediated by a neuronal circuit that includes the amygdala, prefrontal cortex and nucleus accumbens. The amygdala signals the affective significance of cues in the environment, and the prefrontal cortex and accumbens contribute to planning and selecting actions. Thus, the physiological interactions within this circuit may be neural correlates for the interface between motivation and voluntary movement. Using in vivo electrophysiological recordings, we measured the effects of amygdala activation on excitatory transmission in the prefrontal cortex-to-nucleus accumbens pathway. In the prefrontal cortex, a subset of neurons that projected to the accumbens was excited by amygdala stimulation. Prefrontal-to-accumbens projecting neurons were also excited by Pavlovian conditioned odors, suggesting a role for this pathway in the expression of conditioned fear. In neurons of the accumbens, amygdala input facilitated and shifted the latency of spikes elicited by prefrontal cortex stimulation. Facilitation was greatest when amygdala and prefrontal cortex were stimulated nearly synchronously at subthreshold intensities, suggesting that accumbens neurons integrate both the timing and strength of their afferent inputs. In additional accumbens recordings, high intensity amygdala activation induced an activity-dependent depression of prefrontally elicited spiking; thus, the amygdala is able to modulate prefrontal-to-accumbens transmission by several mechanisms. Taken together, these findings show that the amygdala can influence neuronal transmission at two critical motor-related sites in the brain. In this way, affective information may constrain and gate action, resulting in optimal behavioral responses to salient motivational stimuli.

TABLE OF CONTENTS

LIST OF TABLES

LIST OF FIGURES

ACKNOWLEDGEMENTS

I've always liked showing things with pictures, so first, I'd like to illustrate acknowledge the family that has loved and supported me in the past seven years:

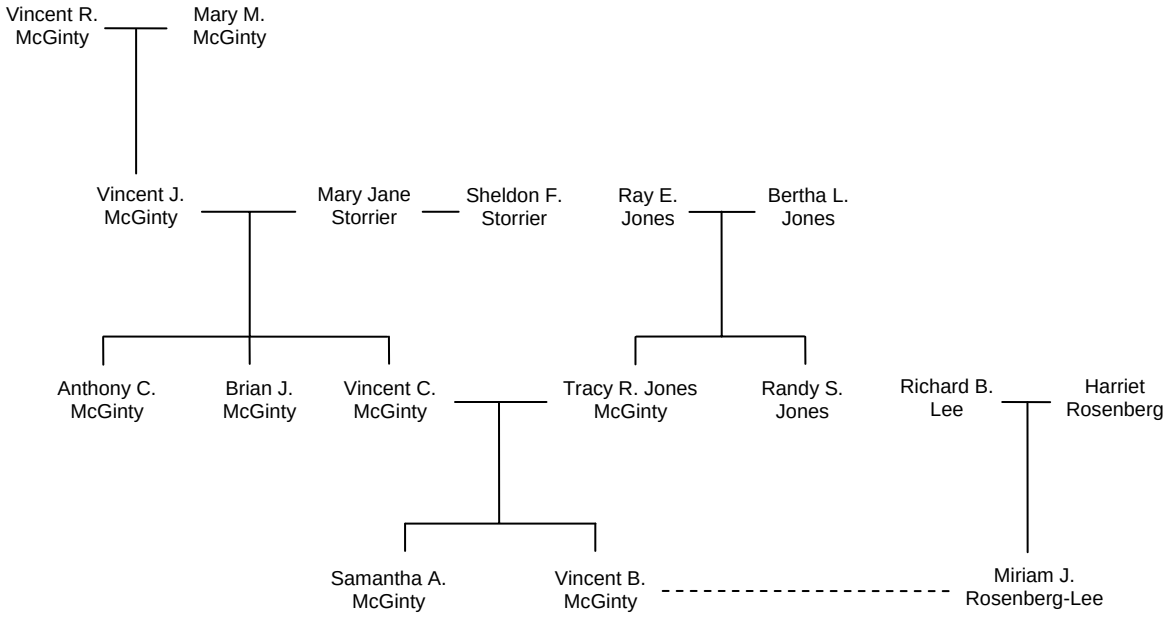

This work is dedicated to them, because not a word of it would have been written without their understanding, encouragement, and faith in me. Although we live far apart, I see every day how fortunate I am to have such people in my life. I especially want to thank my parents, who have recognized the joy and wonder that I find in my work, and who have believed in me even at my most challenging times. I also want to thank Miriam, my friend and partner. Because of her, these years have been some of the best and happiest in my life; I hope for many more to come.

I would also like to acknowledge my academic family, the colleagues and mentors with whom I've had the honor of working:

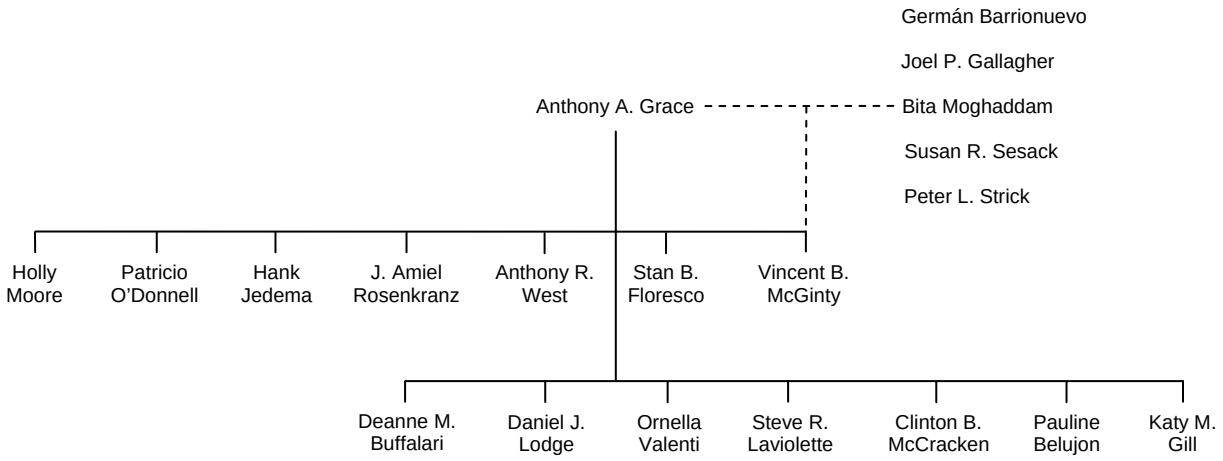

In particular, I am most grateful to my mentor, Tony Grace, for his insight, wisdom and kindness; to my committee chair, Bita Moghaddam, who has challenged and inspired me; to Germán Barrionuevo, for his insightful discussions; and to Susan Sesack and Peter Strick, who have served on my committees throughout my time here, and who have shown immense patience and understanding. Also, I am grateful to my outside examiner, Joel Gallagher, for his excellent questions and discussion at my defense. Among the members of the Grace lab, I thank Deanne Buffalari Tennant, Stan Floresco, Dan Lodge and Clint McCracken for their friendship and for their help and advice on this dissertation. In addition, I am indebted to Nicole Macmurdo, Christy Smolak, Emily Mahar, and Brian Lowry for their invaluable technical assistance.

I wish to thank my colleagues and friends in the Pittsburgh neuroscience community as well, particularly Alan Sved, Marc Sommer, Richard Clarke, Annie Cohen, Harvey Morris, Brittanie Sather Eggan, and Stephen Eggan. For their tireless work and warm friendship, I am indebted to Joan Blaney, Patti Argenzio, Marlene Nieri, Mary Spanoudakis and the entire office staff. Finally, I have received generous financial support from the NIH, the Center for the Neural Basis of Cognition, and the Andrew Mellon Fellowship program.

CHAPTER 1: A CIRCUIT FOR MOTIVATION AND ACTION: THE AMYGDALA, PREFRONTAL CORTEX AND NUCLEUS ACCUMBENS

The brain organizes our actions, allowing us to survive, reproduce and maintain homeostasis. Actions can be motivated by salient primary rewards, such as an appetizing food or an aggressive foe; however, primary rewards are not always necessary. Sensory cues that predict pleasant or unpleasant consequences – yet are not themselves rewarding – can influence behavior just as potently as primary reinforcers. As a result, animals (particularly mammals) can plan and act using cues that represent, or are separate in time and space from their goals – and undertake equally elaborate actions to meet those goals. Thus, we can engage in motivated behaviors even when what we seek is not immediately before us.

The brain systems dedicated to motivated behaviors include circuits through nearly all levels of the cerebrum. While some simple behaviors (such as feeding and drinking) rely on spinal cord and brainstem circuits, more complex motivated behaviors require many interacting brain regions. For example, foraging for food (a deceptively simple activity) uses information about hunger (brainstem and hypothalamus), the places where food may be found (hippocampal formation), the palatability of the food available (insular cortex), the sounds and smells of approaching predators (sensory cortex), etc. Yet, this multitude of information ultimately produces a unified, fluid sequence of movements.

In this way, complex motivated behavior is made possible by brain circuits that link sensation and cognition with volition and action. What then are the specific circuits that create this link? And how do the neurons within these circuits interact?

1.1 NUCLEUS ACCUMBENS, AMYGDALA, AND PREFRONTAL CORTEX

1.1.1 The limbic-motor interface revisited

One of the most influential accounts of how motivation leads to action was presented in a landmark paper by Mogenson and colleagues (1980). Citing recent anatomical work, they observed that amygdala, hippocampus, and other structures involved in motivated behaviors ("limbic" regions) directly project to ventral striatum; and that the ventral striatum (or nucleus accumbens (NAcc)) in turn directly innervates the ventral pallidum, a major part of the basal ganglia motor system. Supported by corroborating behavioral and electrophysiological evidence, they posited that the NAcc was a critical gateway between motivation-related inputs and motor-related outputs, and thus called the NAcc a "limbic-motor interface" (Mogenson et al. 1980). The core of their hypothesis has been largely validated, as subsequent studies have demonstrated that the NAcc is crucial for many kinds of reward-directed behavior (Robbins and Everitt 1996; Cardinal et al. 2002).

In their original description of the limbic-motor interface, Mogenson and colleagues included the amygdala, hippocampal formation, hypothalamus, septum, ventral tegmental area (VTA), and the primitive cortex surrounding the corpus callosum as part of the "limbic system"

(as described by MacLean 1952). This definition of the limbic system has become somewhat deprecated, as not all of these regions mediate emotion, homeostasis or basic drives. Indeed, as Ledoux (2000) notes:

> The limbic system theory began to run into trouble almost immediately when it was discovered, in the mid-1950s, that damage to the hippocampus, the centerpiece of the limbic system, led to severe deficits in a distinctly cognitive function, long-term memory (Scoville & Milner 1957).

Thus, the NAcc appears to be more than an interface for motivational information and action; rather, it is a gateway for many diverse afferent nuclei – including affective, contextual and motor centers – to influence behavior (Grace 2000).

This thesis will investigate the regulation of the NAcc by two of its most important afferent nuclei: the amygdala and the medial prefrontal cortex (mPFC). The amygdala, given its role in emotion, fits the classical mold of a "limbic" region. In contrast, the mPFC contributes to the planning and execution of goal-directed movement. Therefore, the interface between motivation and action may critically depend on the interactions of these regions. We will address two of these interactions: the convergence of amygdala and mPFC afferents in NAcc neurons, and the direct amygdala innervation of the mPFC. Because the amygdala influences two motor-related nuclei, the interface between motivation and action may be better characterized as a multi-synaptic circuit, rather than a single brain nucleus as originally proposed by Mogenson (1980).

1.1.2 The basolateral amygdala encodes learned reward value

The amygdala is a multi-part gray matter nucleus deep in the temporal lobe. Its nuclei are physiologically heterogeneous, and appear to derive from distinct embryological tissues (Swanson and Petrovich 1998). Multimodal sensory information from thalamus and cortex selectively innervate the lateral and basal amygdala nuclei (basolateral amygdala or BLA), and the BLA in turn projects back to sensory cortex (Pitkanen 2000). Glutamatergic neurons of the BLA also project heavily to the NAcc and mPFC. Because BLA is the only amygdala nucleus to innervate these areas, it will be the exclusive focus of this thesis. Nonetheless, other amygdala nuclei are necessary for some aspects of motivated behaviors (LeDoux et al. 1988; LeDoux 2000).

In classical conditioning experiments, BLA neurons fire action potentials in response to a conditioned stimulus (CS, such as a tone or odor) only after that stimulus has been paired with a reinforcing unconditioned stimulus (such as a foot shock) (Rosenkranz and Grace 2002; Maren and Quirk 2004; Tye and Janak 2007). In instrumental conditioning experiments where several CSs are paired with different positive and negative rewards, distinct CSs activate separate populations of BLA neurons. Importantly, when the CS/reward associations are reversed, BLA neuronal responses also reverse after several trials (Schoenbaum et al. 1999). In this way, BLA neurons appear to encode the motivational significance (rather than just the identity) of a CS. In behavioral experiments, BLA lesions and disconnection of the BLA from its target regions impair the ability of CSs to guide behavior (Killcross et al. 1997; Baxter et al. 2000; Floresco and Ghods-Sharifi 2007). Thus, the BLA supports motivated behaviors by signaling to motor nuclei (such as the mPFC and NAcc) the learned affective value of otherwise neutral cues.

1.1.3 The medial prefrontal cortex contributes to voluntary movement

Prefrontal cortex is defined as the cortical areas recipient of projections from the medial dorsal thalamus. In the rat, this includes the agranular cortical areas on the medial wall of the hemisphere, rostral to the genu of the corpus callosum (among other areas, Krettek and Price 1977a). These medial prefrontal cortical areas receive input from VTA, medial dorsal and periventricular thalamus, amygdala, hippocampus, and orbitofrontal cortex (Conde et al. 1995). MPFC efferent projections are diverse, including reciprocal innervation of amygdala, thalamus and orbitofrontal cortex, as well as dense output to brainstem, hypothalamus and the NAcc (Sesack et al. 1989; Floyd et al. 2000, 2001).

The mPFC is important for many motivated behaviors. While its projections to hypothalamus and brainstem influence autonomic and visceral motor function (Neafsey 1990; Price 1999), the mPFC also has a clear role in planning and executing somatic motor behavior. Disruption of mPFC impairs spatial navigation and working memory (Floresco et al. 1997), effort-based decision making (Floresco and Ghods-Sharifi 2007), switching between stimulus-response modalities (Birrell and Brown 2000), and learning and exploiting action-outcome associations (Dalley et al. 2004). Importantly, these more complex behaviors rely on mPFC connectivity with its cortical, subcortical and striatal outputs (Floresco et al. 1999; Cardinal et al. 2002). In this way, the mPFC innervation of the NAcc may be a critical motor-related input to this structure (Floresco et al. 1999). As we will review below, disruption of the mPFC-to-NAcc projection often produces behavioral deficits similar to bilateral mPFC or NAcc lesions alone.

1.1.4 The BLA influence on the mPFC and NAcc: a circuit for motivation and action

The affect-related BLA-to-NAcc projection and the motor-related mPFC-to-NAcc projection converge within single medium spiny neurons (O'Donnell and Grace 1995; Wright and Groenewegen 1995; French and Totterdell 2002, 2003). In this way, the interface of motivational and motor information takes place within the NAcc, as well as in the NAcc's output to the ventral pallidum as originally conceived by Mogenson (1980). In addition, the BLA projects densely to the mPFC, suggesting that affective information can influence motor output at two sites. Therefore, we propose that the "limbic-motor interface" – the route by which motivation can influence action – is not a single nucleus; rather, it is a circuit, composed in part by the BLA, mPFC, NAcc, and the connections between them.

1.2 ANATOMICAL AND FUNCTIONAL CONNECTIVITY WITHIN THE CIRCUIT

As outlined above, the affective significance of sensory stimuli is encoded by the BLA, and thus the BLA's projection to the mPFC and NAcc may allow affective information to influence behavior. In support of this, we will review how the connectivity within this circuit is specific and topographically conserved, and how communication between components of the circuit supports motivation-based decision making.

1.2.1 A closed loop

The BLA and mPFC share direct, reciprocal projections, and both project directly to the NAcc. All of these projections are thought to use glutamate as the primary neurotransmitter, exciting neurons in their post-synaptic target regions (Groenewegen et al. 1990). These projections are abundant and highly specific with respect to the subregions of the BLA, mPFC and NAcc that are innervated. First, many BLA-to-mPFC projection neurons reside in the caudal basal nucleus (Krettek and Price 1977b; Hur and Zaborszky 2005). They collateralize at a high rate, with ~50% sending a second axon to the NAcc (Shinonaga et al. 1994); thus, both NAcc and mPFC are likely to receive similar signals encoded by BLA neuron firing. These efferents of the BLA terminate with specificity: in the mPFC, BLA inputs terminate most densely in layer V of infralimbic cortex (IL) (Krettek and Price 1977b; Gabbott et al. 2006), where many projection neurons to NAcc reside (Ding et al. 2001). In the NAcc, inputs arising from caudal basal BLA terminate preferentially in the shell (Groenewegen et al. 1990; Shinonaga et al. 1994). Finally, the NAcc shell is the primary striatal territory innervated by the IL cortex (Sesack et al. 1989). Thus, the connections between BLA, mPFC and NAcc form a closed topographic loop, with the most dense connectivity between caudal basal BLA, IL cortex and NAcc shell.

Within the NAcc shell, the inputs from BLA and mPFC exhibit further specificity by converging preferentially within the "cell clusters" of the dorsomedial shell (Wright and Groenewegen 1995). Furthermore, both anatomical and electrophysiological evidence suggests that BLA and mPFC afferents synapse on single NAcc medium spiny neurons (O'Donnell and Grace 1995; Finch 1996; French and Totterdell 2002, 2003). Thus, the architecture of this circuit suggests that its component regions may be strongly interdependent. Emotional or motivational

information signaled by the BLA will reach both IL cortex and NAcc shell neurons, and thereby influence cortico-striatal information flow and motor output.

1.2.2 Disrupting the circuit disrupts some motivated behaviors

Lesioning or inactivating the BLA, mPFC or NAcc in rodents can impair their ability to use affective information to guide behavior (Cardinal et al. 2002). Moreover, asymmetric "disconnection" lesions that disrupt communication between two components of the circuit often have similar effects as bilateral lesions of either component alone. For example, the presentation of a cue that has been associated with a reward (drugs or food) can stimulate reward seeking behavior; NAcc disruption, BLA disruption, or disconnection of the BLA and the NAcc reduce reward seeking in response to the cue (Di Ciano and Everitt 2004; Ambroggi et al. 2007). The BLA-to-mPFC pathway may be involved in effort-based decision making, as BLA disruption or BLA/mPFC disconnection in rats decreases their preference for larger yet harder to obtain rewards (Floresco and Ghods-Sharifi 2007). Finally, the mPFC-to-NAcc pathway was shown to mediate the effects of aversive task feedback (a time-out period) on the performance of a continuous attention task, with mPFC/NAcc disconnection and bilateral NAcc disruption having similar effects (Christakou et al. 2004).

Thus, for some functions attributed to the BLA, mPFC and NAcc, the integrity of the connections between them appears to be essential. Although the experiments above used different paradigms, in all cases disconnection reduced the ability for affective information (the reward associated with a cue, the promise of a large reward, unpleasant feedback) to produce

optimal behavior. This is consistent with our hypothesis that the BLA-mPFC-NAcc circuit supports the linking of motivational information and action.

1.3 ELECTROPHYSIOLOGICAL CORRELATES OF BLA-MPFC-NACC INTERACTIONS

These three regions are anatomically interconnected, and their connectivity is important for complex motivated behaviors. In order to ultimately account for how this circuit mediates these behaviors, it is necessary to understand how neuronal activity in one nucleus affects activity in the others.

1.3.1 The BLA influence on the mPFC

BLA afferents invade deep and shallow layers of the mPFC (Krettek and Price 1977b), and glutamatergic terminals synapse on putative pyramidal neurons and identified interneurons (Bacon et al. 1996; Gabbott et al. 2006). Consistent with this, electrical stimulation of the BLA evokes both excitatory and inhibitory responses in mPFC neurons, attributed to direct monosynaptic input and di-synaptic interneuron input, respectively (Perez-Jaranay and Vives 1991; Ishikawa and Nakamura 2003; Dilgen and O'Donnell 2004; Orozco-Cabal et al. 2006; Floresco and Tse 2007). BLA-evoked excitation has been reported in mPFC layer V pyramidal neurons (Orozco-Cabal et al. 2006), and both excitation and inhibition have been shown in mPFC-to-NAcc projecting neurons (Floresco and Tse 2007).

While this suggests that the BLA may directly influence the mPFC output to NAcc, the distribution, magnitude and specificity of this influence is not known. These details are critical, as they will determine whether affective signals from BLA facilitate, inhibit, or filter motor-related activity in mPFC. In addition, we have recently shown that BLA input allows mPFC neurons to encode the presence of Pavlovian conditioned odors, and that this encoding is necessary for the conditioned response (Laviolette et al. 2005). If mPFC-to-NAcc projection neurons also encode conditioned stimuli, it would suggest a previously unappreciated role for this pathway in conditioned fear.

1.3.2 The convergence of BLA and mPFC inputs in the NAcc

The NAcc contains medium spiny neurons similar to those found in the dorsal striatum (Chang and Kitai 1985; O'Donnell and Grace 1993). Like striatal medium spiny neurons, those in the NAcc are thought to require a large amplitude of convergent glutamatergic synaptic activation in order to fire (Wilson and Kawaguchi 1996; Wickens and Wilson 1998; Blackwell et al. 2003). Thus, how NAcc neurons integrate their many converging subcortical and cortical inputs, and how this integration leads to spike firing is a crucial functional feature of the NAcc.

The direct convergence of BLA and mPFC afferents on single NAcc neurons (O'Donnell and Grace 1995; Finch 1996; French and Totterdell 2002, 2003) is evidence that affect- and motor-related information are integrated at the single-cell level. Stimulation of these afferents evokes fast excitatory responses consistent with their presumed glutamatergic nature (Yim and Mogenson 1982; Finch 1996; Brady and O'Donnell 2004), and convergence of excitatory responses in single neurons has been shown for BLA, mPFC, hippocampal, thalamic and

entorhinal cortical inputs (O'Donnell and Grace 1995; Finch 1996; Mulder et al. 1998; Goto and O'Donnell 2002).

While these electrophysiological observations corroborate the anatomical evidence for convergence, they do not explain how input integration gives rise to action potential firing. Furthermore, results obtained from different preparations do not allow a single account of input integration to be formed. In NAcc neuron slices, simultaneous activation of a few adjacent dendritic spines produces supralinear summation of excitatory responses, whereas activating a larger number of presumably separate spines results in linear input summation (Carter et al. 2007). In NAcc neurons in vivo, simultaneous BLA and mPFC inputs sum sublinearly (Goto and O'Donnell 2002). As a result, how converging inputs elicit spiking is not clear. Indeed, very few studies have observed spiking evoked by multi-input activation (Finch 1996), and there exist no studies where these responses were systematically measured or characterized.

In addition, glutamatergic inputs to NAcc neurons may also recruit dopamine to induce synaptic plasticity in afferent pathways. In neurons receiving both BLA and hippocampal inputs, high frequency stimulation of hippocampal afferents released dopamine in the NAcc and induced a dopamine-dependent depression of BLA inputs (Floresco et al. 2001b). High frequency stimulation of BLA may also increase NAcc dopamine, and induce dopamine-dependent potentiation of BLA inputs. (Floresco et al. 2001a; Howland et al. 2002). Thus, the integration of BLA and mPFC inputs in single NAcc neurons may also be influenced by activity-dependent dopamine release.

1.4 SUMMARY AND HYPOTHESES

Given the anatomical and behavioral evidence reviewed here, we propose that the "limbic-motor interface" is not a single nucleus, but a circuit of interdependent nuclei. Specifically, we posit that the BLA's connection with the mPFC-to-NAcc axis is crucial for actions that are driven by affective information. By examining the electrophysiological interactions between the elements of this circuit, the functional properties of this interface may be better understood.

There is clear electrophysiological evidence from in vivo recordings that affective information from BLA could impact the motor-related mPFC-to-NAcc pathway. In the mPFC, BLA afferent inputs can excite or inhibit mPFC-to-NAcc projecting neurons; however, the specificity of this influence is not known. In the NAcc, convergent excitatory BLA- and mPFC-evoked responses occur in single neurons; but the regulation of spike firing by these inputs (through glutamatergic and possibly dopaminergic mechanisms) has not been investigated. Thus, important functional properties of these circuits have not been characterized. Furthermore, previous studies have typically focused on a single synaptic pathway (e.g. BLA-to-NAcc), so there is very little understanding of how BLA, mPFC and NAcc interact with one another at the circuit level. To this end, we studied the functional connectivity within this circuit in two primary experiments.

In the first experiment (Chapter 2), we tested the influence of the BLA on mPFC neurons that were identified as projecting to the NAcc. Recent work from our group demonstrated that the excitatory BLA input to mPFC signals the presence of conditioned odors, and enables mPFC neurons to express excitatory responses to those cues. Disrupting these mPFC excitatory responses disrupts the expression of conditioned fear. Given the importance of mPFC-to-NAcc

transmission in behavior, we hypothesized excitatory conditioned cue responses would occur in the neurons that compose this pathway. Thus, we recorded from identified mPFC-to-NAcc projecting neurons, and measured responses elicited by electrical and chemical stimulation of the BLA, as well as by Pavlovian conditioned odors. To assess the specificity of these responses, a non-overlapping, cortically-projecting population of mPFC neurons was also tested.

In the second series of experiments, we recorded from NAcc neurons, focusing on neurons that received converging BLA and mPFC inputs. The integration of subthreshold excitatory inputs in NAcc neurons has been investigated; however, there have been no rigorous studies of spikes evoked by activation of multiple NAcc afferents. Based on existing electrophysiological evidence, we hypothesized that BLA inputs would facilitate mPFC-evoked spiking via timing-dependent summation of monosynaptic excitatory responses. Therefore, we first measured how BLA stimulation modulated the evoked spiking elicited by mPFC stimulation in single NAcc neurons (Chapter 3). There is also evidence that strong afferent input to the NAcc can release dopamine and induce dopamine and NMDA-dependent plasticity. Thus, we tested the effects of high intensity BLA train stimulation, which we hypothesized would depress mPFC-evoked spiking via a timing-independent, dopamine-mediated mechanism (Chapter 5). Finally, to assess the encoding of emotional information in the NAcc, Pavlovian conditioned odor responses were also measured in these neurons (Chapter 4).

CHAPTER 2: SELECTIVE ACTIVATION OF MEDIAL PREFRONTAL-TO-ACCUMBENS PROJECTION NEURONS BY AMYGDALA STIMULATION AND PAVLOVIAN CONDITIONED STIMULI*

2.1 ABSTRACT

Medial prefrontal cortex (mPFC) neurons respond to Pavlovian conditioned stimuli, and these responses depend on input from the basolateral amygdala (BLA). In this study, we examined the mPFC efferent circuits mediating conditioned responding by testing whether specific subsets of mPFC projection neurons receive BLA input and respond to conditioned stimuli. In urethane-anesthetized rats, we identified mPFC neurons that projected to the nucleus accumbens (NAcc) or to the contralateral mPFC (cmPFC) using antidromic activation. Stimulation of the BLA and Pavlovian conditioned odors selectively activated a subpopulation of ventral mPFC neurons that projected to NAcc, but elicited virtually no activation in mPFC neurons that projected to cmPFC. BLA stimulation typically evoked inhibitory responses among non-activated neurons projecting to either site. These results suggest that the ventral mPFC-to-NAcc pathway may support behavioral responses to conditioned cues. Furthermore, because projections from the BLA (which also encode affective information) and the mPFC converge within the NAcc, the BLA

* Published previously by Oxford University Press: Cerebral Cortex 2007; doi: 10.1093/cercor/bhm223

may recruit the mPFC to drive specific sets of NAcc neurons, and thereby exert control over prefrontal cortical-striato-thalamocortical information flow.

2.2 INTRODUCTION

The medial prefrontal cortex (mPFC) is involved in emotional associative learning, in which actions or stimuli become associated with pleasant or unpleasant consequences. Recently we reported that a subpopulation of mPFC neurons encode emotional stimuli in a Pavlovian fear conditioning paradigm (Laviolette et al. 2005). Interference with mPFC function by blocking dopamine D4 or cannabinoid receptors prevents the encoding of emotional information in these neurons, and reduces the expression of conditioned fear (Laviolette et al. 2005; Laviolette and Grace 2006). However, the precise role of the mPFC in associative learning is complex, and may depend on the type of learning to which the animal is exposed (Garcia et al. 2006; Quirk et al. 2006). Thus, while the mPFC appears critical for fear conditioning, it is not known how the mPFC supports this type of learning.

The ability of the prefrontal cortex to represent emotional stimuli depends on input from the basolateral amygdala (BLA)(Schoenbaum et al. 2003; Laviolette et al. 2005). MPFC neurons fail to encode conditioned stimuli when the BLA is inactivated during conditioning, and only mPFC neurons that receive excitatory input from BLA respond to conditioned stimuli (Laviolette et al. 2005). Since BLA input to mPFC overwhelmingly targets spiny dendrites, many BLA- and conditioned stimulus-responsive neurons are likely to be projection neurons (Bacon et al. 1996;

Gabbott et al. 2006); however, it is unclear whether these neurons correspond to subpopulations with distinct projection targets.

The capacity of the mPFC to mediate the expression of conditioned fear depends on its efferent targets, and one target likely to play a role in fear conditioning is the nucleus accumbens (NAcc). As is the case with BLA and mPFC, manipulations of the NAcc can disrupt associative learning (Cardinal et al. 2002). The BLA, mPFC and NAcc share dense, topographic, glutamatergic interconnections (Krettek and Price 1977b; Groenewegen et al. 1990; Wright and Groenewegen 1995), and functional disconnection of two of these regions often mimics bilateral lesions of either region alone (Coutureau et al. 2000; Parkinson et al. 2000; Setlow et al. 2002; Floresco and Ghods-Sharifi 2007). Thus, the connections among these three regions appear to play critical roles in the integration of emotional information and the expression of motivated behaviors.

We propose that the BLA, mPFC and NAcc form a functionally interconnected neuronal circuit that encodes emotional information, and that it is the mPFC output neurons that target the NAcc (PFC-to-NAcc) which receive input from the BLA and respond to conditioned stimuli. To test this hypothesis, we recorded PFC-to-NAcc neurons during stimulation of the BLA and during Pavlovian fear conditioning and compared their responses to those of a comparable, but largely non-overlapping subpopulation of mPFC neurons projecting to the contralateral mPFC (PFC-to-PFC) (Pinto and Sesack 2000).

2.3 MATERIALS AND METHODS

All experiments were performed in accordance with the National Institutes of Health *Guide for the Care and Use of Laboratory Animals* and were approved by the University of Pittsburgh Animal Care and Use Committee.

2.3.1 Subjects and Surgery

Experiments were performed on male, Sprague-Dawley rats (290-400g). For the BLA stimulation experiments, 81 rats were anesthetized with a single intraperitoneal injection of urethane (1.4-1.5g/kg in deionized water), which provided stable anesthesia throughout the experiments (maximum experiment duration was 8 hours). In these 81 rats, urethane was preferred over other available anesthetics because it was found in preliminary experiments (not shown) to produce the least depression of spontaneous mPFC neuron activity. For the 14 rats used in odor conditioning experiments, chloral hydrate (400mg/kg in water intraperitoneally, maintained via supplemental injections through a femoral vein catheter), was used in order to duplicate the conditions of previous studies (Rosenkranz and Grace 2002; Laviolette et al. 2005). Comparative studies have shown that chloral hydrate and urethane have similar effects on evoked cortical responses (Angel and Gratton 1982).

When the rats no longer displayed a reflexive withdrawal in response to a foot pinch, they were placed in a stereotaxic apparatus (David Kopf Instruments, Tujunga, CA). Burr holes were drilled in the skull overlying the electrode implantation targets, and the underlying dura was carefully removed. Up to four electrodes were then lowered (1mm/min or less) into the brain: a

recording electrode in the right side mPFC, a combination stimulating electrode/guide cannula (chemotrode) in the ipsilateral BLA, and stimulating electrodes in either the ipsilateral NAcc, contralateral mPFC (cmPFC), or both (Figure 2.1A). In a small number of experiments, the mPFC was stimulated and the BLA was the recording site. All coordinates are given relative to the bregma landmark, with the axes abbreviated as follows: AP for anterior-posterior; ML for medio-lateral; DV for dorso-ventral.

The recording electrodes were pulled (Narishige, Tokyo, Japan) from 2mm outside-diameter filamented borosilicate glass tubing (World Precision Instruments, Sarasota, FL). The electrode tips were broken back under microscopic control, and the electrodes were filled with the recording solution (2M NaCl with Pontamine Sky Blue, impedance 6-12MΩ measured in situ through the amplifier (Fintronics WDR-420, Orange, CT)). The recording electrodes were

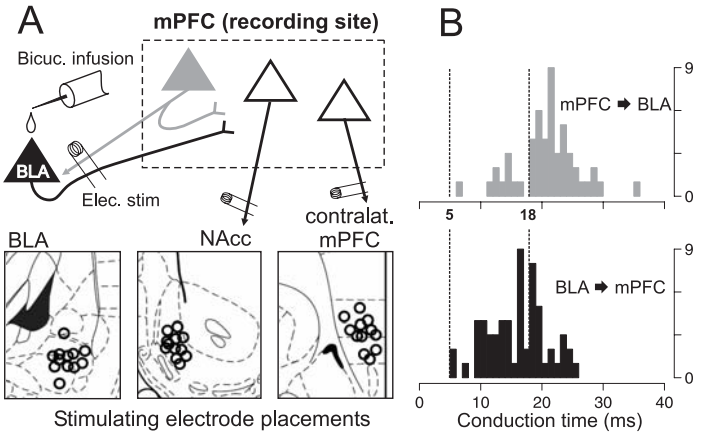

Figure 2.1 Experiment schematic, electrode placements, and conduction time histograms A A diagram illustrating representative electrode placements for BLA stimulation experiments. The primary recording site was the mPFC, where neurons were recorded and identified as projecting to the NAcc, cmPFC or BLA by antidromic stimulation. In addition, in a small number of experiments, the BLA was the recording site, and BLA neurons projecting to mPFC were identified by antidromic stimulation of the mPFC (not illustrated). **B** Histograms of antidromic latencies for BLA-to-mPFC projection neurons (bottom) and for mPFC-to-BLA projection neurons (top); Y-axis is number of neurons. The latency distributions suggest that BLA stimulation causes orthodromic activation of the BLA-to-mPFC pathway prior to the antidromic activation of PFC-to-BLA neurons. Therefore, to isolate orthodromic responses, only responses that occurred within 5-18ms of BLA stimulation were analyzed.

lowered slowly through the mPFC (AP +2.5 to +3.5mm; ML 0.3 to 0.9mm; DV -3.0 to -5.5mm) using a hydraulic microdrive (Narishige).

The BLA was implanted with chemotrodes (combined guide tube and stimulating electrodes, Plastics One C313G-MS303/2) with a stimulating electrode protruding 2mm beyond the guide tube (0.7-1.0mm exposed at tip), and an accompanying infusion cannula that projected 1.6mm beyond the guide tube. The chemotrodes were placed such that the negative pole was in the posterior BLA (AP -3.6mm; ML 4.8 to 5.0mm; DV 9.0mm), the positive pole was in the anterior BLA (AP -2.6mm, rest same) and the guide tube was located between the two poles. The NAcc stimulating electrodes (Rhodes Medical Instruments, Woodland Hills, CA, electrode type NEX-100) were placed in NAcc shell (AP +1.2 to 1.6mm; ML 0.7 to 0.9mm; DV -8.2mm). The cmPFC stimulating electrodes (Rhodes Medical Instruments, SNEX-100) were placed in the infralimbic (IL), dorsal peduncular (DP), and medial orbital (MO) cortical areas (AP +2.7 to 3.3mm; ML 0.3 to 0.7mm; DV -5.0 to -5.3mm).

2.3.2 Electrophysiological procedures and neuron identification

Extracellular action potentials from mPFC neurons were amplified and filtered (1000x gain, 100-4000Hz band pass, Fintronics WDR-420, Orange, CT), passed to an oscilloscope and audio monitor for real time monitoring, and to a computerized data acquisition system (Microstar Laboratories, Bellevue, WA) for storage and off-line analysis with custom software (Neuroscope) and routines for the R software language (R Development Core Team, 2005). Electrical stimulation was controlled with a software pulse generator (Neuroscope) and the Master-8 stimulator and stimulus isolation units (A.M.P.I., Jerusalem, Israel). The pulse

duration was 0.25ms for all stimulation sites, and the currents applied varied with the stimulated region, as described below.

The neurons of interest, identified by antidromic stimulation, were those mPFC neurons projecting to the NAcc (PFC-to-NAcc), those projecting to the mPFC contralateral to the recording site (PFC-to-PFC), and in some cases those projecting to the BLA (PFC-to-BLA). Neurons projecting to both NAcc and cmPFC or to both NAcc and BLA were found infrequently (Pinto and Sesack 2000) and were only tested for responses to BLA electrical stimulation. Action potentials were confirmed as antidromic if they met two of three criteria: a spike latency that varied by 2ms or less over 20 trials; the ability to follow two stimulation pulses delivered 2.5ms apart (400Hz, preferred for silent or slow-firing neurons); and the collision of the antidromic response with spontaneous spikes (preferred for spontaneously active neurons) (Fuller and Schlag 1976). As the recording electrode was lowered through the mPFC, a cell searching procedure (Floresco and Grace 2003) was used to find antidromically responding neurons. Stimulation pulses were delivered one at a time to the NAcc, cmPFC and/or BLA at an overall rate no greater than 0.5Hz, with maximum currents of 500, 400 and 700μA, respectively. Neurons that were confirmed as projecting to the NAcc or cmPFC were then subjected to electrical and/or chemical stimulation of the BLA, or to conditioned odors (see 2.3.5). For the odor conditioning experiments, only projection neurons with baseline firing ≥ 1Hz were recorded in order to adequately measure inhibitory responses. For neurons confirmed as projecting to the BLA, only antidromic response latency was measured.

2.3.3 BLA electrical stimulation

Once a suitable neuron was isolated, the baseline activity was recorded, and then the BLA was stimulated for 2-5 minutes with the following pattern: a continuous 0.3Hz pulse train, with intermittent 20Hz trains (1sec train duration) every 20 seconds. These two frequencies fall within the range of firing rates observed in BLA principal neurons in freely moving rats; low frequency firing is typically observed at rest, while higher frequency firing occurs in the presence of conditioned stimuli (Schoenbaum et al. 1998, 1999). Thus, neuronal responses to both low and high frequency BLA stimulation may relate to mPFC function in different behavioral states. The BLA stimulation current used in this part of the experiment was typically 400μA; however, if a neuron exhibited a 100% response ratio at this current intensity, the current was lowered to produce a 50-80% response ratio.

2.3.3.1 Minimizing the effects of antidromic activation One potential artifact of BLA stimulation is the antidromic activation of terminals of mPFC neurons that project to the BLA, which may cause recurrent excitation of mPFC neurons. However, we minimized the impact of antidromic/recurrent excitation in the current study by measuring only responses likely to be orthodromic. We measured the antidromic latency (conduction time) of 60 PFC-to-BLA neurons (mean 20.8±0.7ms), and of 52 BLA neurons projecting to mPFC (BLA-to-mPFC, mean 16.2±0.6ms, significant difference by t-test, $p < 10^{-5}$), recorded during preliminary BLA recording/mPFC stimulation experiments. Thus, BLA neurons projecting to the mPFC exhibited faster conduction times on average than reciprocally projecting neurons; a difference which is consistent with that reported in two previous studies (Likhtik et al. 2005; Floresco and Tse

2007). The majority (60%) of BLA-to-mPFC neurons had conduction latencies between 5 and 18ms, but only 19% of PFC-to-BLA neurons had conduction latencies in this range (Figure 2.1B). Therefore, within 5-18ms after a BLA stimulation pulse, the majority of orthodromic input reaches the mPFC, but only a small portion of recurrent antidromic inputs have been activated. Based on this differential distribution of conduction times, we limited our analyses to only the spikes that occurred within 5-18ms of a BLA stimulation pulse. Although this window does not completely eliminate the contribution of antidromic activity, it minimizes antidromic effects and maximizes the measurement of orthodromic BLA-to-mPFC activation. Furthermore, the threshold current for most antidromically activated PFC-to-BLA neurons was greater than the 400μA current used during the BLA stimulation part of the experiment (510±21μA mean threshold current; 84% had thresholds greater than 400μA). Therefore, it is likely that few PFC-to-BLA neurons were activated antidromically by 400μA BLA stimulation amplitude.

While these criteria minimize the measurement of recurrent/antidromic activity due to BLA stimulation, they do not eliminate the contribution of recurrent/*orthodromic* activity – i.e. of local polysynaptic excitation. Although not monosynaptic, such excitation may nonetheless reflect an important component of the excitatory BLA input to the mPFC. Thus, the excitatory responses that occur between 5 and 18ms after BLA stimulation are interpreted as being due to orthodromic, monosynaptic excitation, with a possible contribution from local polysynaptic excitatory circuitry.

2.3.3.2 Population analysis of BLA-evoked responses The change in probability of spike discharge evoked by BLA electrical stimulation was calculated by subtracting the pre-pulse spike probability (-200 to 0ms, calculated from 0.3Hz stimuli only) from the post-pulse spike

probability (+5 to +18ms); the pre-pulse probability was scaled to be comparable to the shorter post-stimulus window. To assess excitatory responses across the population of neurons recorded, cells with greater than 1% increase in spike probability to either 0.3Hz or 20Hz stimuli (approximately the smallest detectable increase) were grouped together, and the mean pre- and post- stimulus spike probability were calculated. Because the baseline firing rate was typically low, inhibitory responses were not reliably detectable in all neurons (Floresco and Tse 2007). Therefore, to assess inhibitory responses across the population, neurons that did not exhibit a spike probability increase and that also had a pre-stimulus spike probability greater than or equal to 1% were grouped together, and the mean pre- and post-stimulus spike probabilities were calculated. A 1% pre-stimulus spike probability is equivalent to a spontaneous firing rate of 0.8Hz.

2.3.3.3 Single neuron analysis of BLA-evoked responses We also assessed whether single mPFC neurons exhibited significant excitation in response to BLA stimulation using statistical criteria similar to previous studies (Maunsell and Gibson 1992; Hanes et al. 1995; Bisley et al. 2004; Gifford et al. 2005). For each neuron, the pre-stimulus spike count was fitted to a Poisson distribution. This distribution was used to calculate a post-stimulus spike count threshold, *t*, such that the number of post-stimulus spikes was expected to be *t* or fewer for 95% of the time based on pre-stimulus firing (i.e. we found *t* such that $P(X \leq t) < 0.95$, where X is a random sample from the Poisson fit). Thus, a neuron was considered to exhibit a significant level of excitation if the actual number of post-stimulus spikes for either 0.3 or 20Hz stimuli was greater than its 95% threshold *t*, corresponding to a significance level of $p < 0.05$. Among these significantly excited neurons we also identified a subset of "highly excited" neurons, whose post-stimulus spike

counts exceeded a 99.9% threshold (the spike count exceeded *t* such that $P(X \leq t) < 0.999$), corresponding to a significance level of $p < 0.001$.

Because most neurons recorded exhibited low spontaneous activity, this method was not appropriate for determining the significance of inhibitory responses. Specifically, in low firing neurons, even a total cessation of firing would not surpass a significant threshold for inhibition. Given the stimulation and analysis parameters used in this study, a spontaneous firing rate of 2.6Hz or greater would typically be needed to identify a meaningful (i.e. non-zero) inhibition threshold; only 11 of the 136 PFC-to-NAcc and PFC-to-PFC neurons recorded exhibited sufficient spontaneous firing to calculate such a threshold. Therefore, although we observed apparent inhibitory responses, we did not attempt to report the significance of inhibition in single neurons.

2.3.4 BLA chemical stimulation (bicuculline infusion)

To further rule out the contribution of activation of terminals or fibers of passage, in some experiments the BLA was stimulated chemically with a direct infusion of the $GABA_A$ antagonist bicuculline. Bicuculline-evoked field potential activity in BLA was recorded simultaneously with projection neuron single unit activity in mPFC. Bicuculline (20-50ng in 500nl Dulbecco's phosphate buffered saline) was infused into the BLA over a two minute period through a cannula (Plastics One) fitted into the chemotrode guide tube, and coupled to polyethylene tubing, a Hamilton syringe, and motorized syringe pump. At most, two infusions separated by 90-180 minutes were performed in the same animal. Using the electrode leads of the BLA chemotrode, extracellular field potentials were recorded and amplified (Cygnus, 10-1000Hz band pass, 1000x

gain). Within 30-120 seconds after bicuculline infusion, isolated epileptiform discharge events (EDs) appeared, representing the vigorous firing of many nearby neurons (Steriade et al. 1998). The EDs were characterized as spontaneous, all-or-none voltage deflections with an initial negative phase, followed by a large amplitude positive phase. The EDs occurred at a rate of 0.1-0.5Hz and persisted for 15-25 minutes following the infusion. Unlike previous studies (Steriade et al. 1998; Steriade and Contreras 1998), the EDs were not followed by seizure activity, and the rats did not display outward signs of seizure. These previous studies used a different general anesthetic, injection site, and species than the current study, which may explain the lack of seizure activity in our experiments. Infusion of 500nl buffered saline vehicle did not cause EDs (not shown).

ED times were used as reference times to construct peri-event time histograms of mPFC projection neuron activity. The ED times were defined as the peak of the initial negative phase of the voltage deflection. Previous studies have shown that the peak of the initial negative phase of the ED corresponds to the strongest firing in nearby neurons. Therefore, based on the orthodromic BLA-to-mPFC conduction times (5-26ms, see 2.3.3.1, Figure 2.1B), post-ED spikes that occurred within 5-26ms were interpreted as being consistent with monosynaptic, orthodromic input from the BLA.

2.3.5 Pavlovian conditioning experiments

Two groups of male Sprague Dawley rats (285-365g) were subjected to Pavlovian odor conditioning. The first group, consisting of 14 rats, was conditioned while awake, with recordings subsequently performed under anesthesia (see 2.3.5.2); before the recording

procedure, 9 of these 14 rats were subjected to a very brief duration test for the retention of fear conditioning. The second group, consisting of 8 rats, was conditioned while awake and then subjected to more thorough testing for the retention of conditioned fear, similar to that described previously (Laviolette et al. 2005; Laviolette and Grace 2006). None of this latter group was subjected to recording procedures to avoid potential extinction effects of the longer exposure. The protocols and equipment used in these experiments were similar to previous studies from our group (Otto et al. 1997; Rosenkranz and Grace 2002; Laviolette et al. 2005). Rats were allowed to habituate individually in the conditioning room for 20-30 minutes, and were then put in the conditioning chamber: a fan-ventilated Plexiglas box, with a metal shock grid floor and open top (Coulbourn, Allentown, PA). After 10 minutes, the first of two distinct odors (almond or peppermint (McCormick, Hunt Valley, MD)) was presented for 10 seconds, and two minutes later, the second odor was presented (no shocks were given during these initial presentations). Subsequently, the two odors were presented in alternation at two-minute intervals. One odor (CS+) was consistently paired with a 3 second foot shock (0.4-0.6mA), and the other odor was presented alone (CS-). The rats received a total of six odor/shock pairings. CS+ identity (almond or peppermint) and CS order (CS+ first or CS- first) were counterbalanced across subjects. The rats remained in the chamber for 20 minutes following the last odor presentation, and were then removed and returned to their home cage for the rest of the day. The conditioning chamber was cleaned and deodorized after each use.

2.3.5.1 Behavioral testing On the day after conditioning, rats in both groups were tested for freezing in the presence of the CS+ odor (9/14 rats from the first group, 8/8 rats from the second group). Testing was performed in the same room and chamber as conditioning; however, the

conditioning chamber was altered to reduce contextual cues that might cause a fear response in the absence of any odor: the ventilating air flow was redirected, the shock grid was reoriented, construction paper was applied to the otherwise clear walls, and the open top was partially occluded.

Rats from the first group (9 of 14, which comprised the group from which recordings were made) were tested with a single, brief CS+ presentation to prevent extinction of the conditioned fear response (Shipley 1974): After 20-30 minutes habituation in the conditioning room, rats were placed in the chamber. After 6 minutes, the rats were presented with the CS- odor, then CS+ odor (without shock), then CS- odor again (20sec each, eight minutes between odors). Rats remained in the chamber for an additional 6 minutes, and were then returned to their home cage for the rest of the day. The fear response was determined by measuring freezing: a crouching posture with no visible movement other than breathing. Percent freezing (i.e., time freezing divided by total time) was scored and measured over the 60 second period that followed odor presentation (the two CS- periods were averaged). The 20 second period *during* odor presentation was not included because most rats actively sampled the odor (sniffing and whisking) during this time. One rat did not show any freezing throughout the entire testing period, and was excluded from analysis.

Rats from the second group (n=8, not recorded from) were tested with longer CS+ and CS- presentations, as had been employed in previous studies (Laviolette et al. 2005; Laviolette and Grace 2006). After 20-30 minutes of habituation to the conditioning room, the rats were placed in the chamber. After 10 minutes, the first odor (either CS+ or CS-, counterbalanced) was presented for five minutes; 10 minutes after the first odor onset, the second odor was presented for five minutes. Freezing was measured over the five minute CS+ and CS- presentations in bins

of one minute. In addition to freezing, in this group of 8 rats exploratory and grooming activity was also measured using a scoring system adapted from previous studies (Rosenkranz et al. 2003; Laviolette et al. 2005). For each one minute bin, rats were assigned a score based on ambulatory activity: 0 points for no movement; 1 point for movement across one side of the chamber; 2 points for 2 sides of the chamber; 3 points for all four sides of the chamber; 4 points for all four sides and center of the chamber. To this score, one point was added if the rat engaged in grooming behavior, and one point was added if the rat explored the chamber by rearing, for a total possible score of 6 points.

2.3.5.2 Electrophysiological responses to conditioned odors in anesthetized rats In the group of rats subjected previously to odor-based Pavlovian fear conditioning (n=14), PFC-to-NAcc and PFC-to-PFC neuron responses to the CS+ odor (previously paired with foot shock) and the CS- odor (unpaired) were recorded. Recordings took place 24 hours after conditioning in 5/14 rats; recording took place 48 hours after conditioning (24 hours after behavioral testing, see above) in 9/14 rats. After the baseline firing of each neuron was measured, the rat was presented with the CS- odor, followed by the CS+ odor, followed again by the CS- odor (10sec each). In 8 rats, the baseline recording period and the time between odors was 4-5 minutes, and in the remaining 6 rats, it was 8-10 minutes. Typically, 3 or 4 neurons were recorded in each animal. To reduce habituation of the odor-evoked neural response, the interval between odor presentation sequences was typically 45-60 minutes.

As with the electrical stimulation experiments, two analyses were performed. First, to assess the response across the population of recorded neurons, the firing rate immediately before odor presentation (30sec) was subtracted from the firing rate during odor presentation (10sec) for

each neuron. The odors typically evoked both excitatory and inhibitory responses, and the top and bottom quartiles of responses (i.e. greatest excitatory and inhibitory responses) were analyzed separately using ANOVA. Second, single neurons were analyzed to determine whether they exhibited significant excitation by the CS+ or CS- odor: for each neuron the pre-odor firing rate was fitted to a Poisson distribution, and a spike count threshold of 95% (t such that $P(X \leq t) < 0.95$) was calculated. Neurons with spike counts during the odor presentation that exceeded this threshold were deemed "significantly excited" ($p < 0.05$). Neurons that were "highly excited" ($p < 0.001$) were similarly identified using a 99.9% threshold (t such that $P(X \leq t) < 0.999$).

2.3.6 Electrode marking and histological processing

The recording electrode location was marked by iontophoretic ejection of Pontamine Sky Blue dye (-10μA, 40-60 minutes). Stimulating electrode locations were marked by passing current between the electrode poles (200μA (reversed polarity), 10sec). The rats were then killed with an overdose of anesthetic and decapitated, and the brains removed and placed for 48 hours in paraformaldehyde with 1% potassium ferricyanide. The brains were transferred to a cryoprotectant solution of 25% sucrose. After two days they were sliced coronally and Nissl stained using standard histological procedures.

The locations of electrodes were assessed using the atlases of Paxinos and Watson (1998; 2005) and plotted onto a typical mPFC section. For clarity, the locations of only a representative sample of 33 out of the 66 PFC-to-NAcc neurons recorded during BLA stimulation are shown (Figure 2.3C), including 11/12 excited PFC-to-NAcc neurons. Because of damage to some

tissue sections, 1 of the 12 excited PFC-to-NAcc neurons that were located in IL cortex (Figure 2.3C) could not be precisely plotted onto the representative section.

2.3.7 Statistics

Differences between groups were assessed using ANOVA with Tukey's Honest Significant Difference post hoc testing (Norman and Streiner 2000), or with paired t-tests or Wilcoxon rank sum tests as appropriate. Multiple p-values were corrected with Holm's stepwise Bonferroni correction (Norman and Streiner 2000).

2.4 RESULTS

2.4.1 Electrical stimulation of BLA

Projection neurons in the mPFC were identified using antidromic stimulation from their projection sites (Figure 2.1A, Figure 2.2A). Two analyses of excitatory BLA-evoked responses were performed. First, using a population analysis the average excitatory response was found to be significantly greater in PFC-to-NAcc neurons than in PFC-to-PFC neurons (Figure 2.3). This was particularly evident for 20Hz BLA stimulation, where the response ratio increased by 16.8±7.2% (spikes per stimulus) in PFC-to-NAcc neurons, and decreased by 0.7±0.7% in PFC-to-PFC neurons ($p<0.002$ Wilcoxon rank sum test). In PFC-to-NAcc neurons there was no

difference in the average excitation evoked by 0.3 and 20Hz stimuli (Figure 2.3B); however the onset latency of 0.3Hz responses was typically 1-2msec shorter than for 20Hz responses (Figure 2.3A). Second, analysis of the excitatory response of individual neurons revealed that a larger portion of PFC-to-NAcc neurons (12/66, 11 rats) had significant increases in spike probability (exceeded a 95% threshold, see 2.3.3.3) than did PFC-to-PFC neurons (4/70, 4 rats, $p < 0.04$, Fisher exact test for proportions) (Table 2.1). In addition, 9/66 PFC-to-NAcc neurons (8 rats) fell into the "highly excited" category (exceeded 99.9% threshold), compared to only 1/70 PFC-to-PFC neuron ($p<0.008$, Fisher exact test).

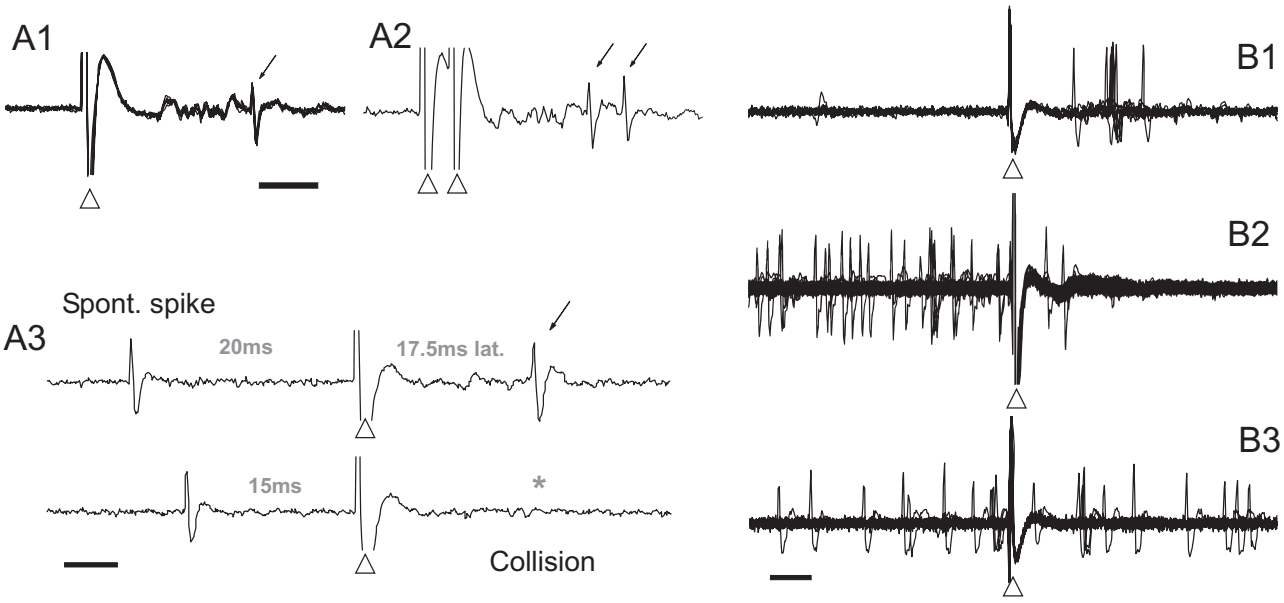

Figure 2.2 Examples of orthodromic and antidromic evoked spikes A Antidromic responses (thin arrows) to cmPFC or NAcc stimulation were confirmed using three criteria: a constant latency response (**A1**, six overlaid traces) to stimulation (arrowheads); the ability to follow 400Hz paired pulse stimulation (**A2**); and the collision of evoked spikes with spontaneous spikes (**A3**, asterisk). Scale bars = 5ms. **B** Projection neurons exhibiting spikes in response to BLA stimulation (arrowheads) were classified as "excited" (**B1**, 10 overlaid traces from a single PFC-to-NAcc neuron). Neurons classified as "non-excited neurons with spontaneous firing" were typically inhibited (**B2**, 270 traces from a PFC-to-NAcc neuron) or showed no response (**B3**, 90 traces from a PFC-to-NAcc neuron) to BLA stimulation. The remaining neurons exhibited few spontaneous or evoked spikes (not shown). Scale bar = 5ms.

Although PFC-to-NAcc neurons were recorded throughout the mPFC, all of the significantly excited PFC-to-NAcc neurons were located in the ventrally situated IL or DP areas (Figure 2.3C). The average antidromic latency of PFC-to-NAcc neurons in the more dorsal prelimbic cortex (PL) was 12.0±0.7ms and in IL or DP was 8.9±0.5ms (significant difference $p<0.001$, t-test). Among IL/DP neurons, there was no latency difference between significantly excited (8.7±0.9ms) and non-excited neurons (9.1±0.6ms, $p<0.7$, t-test).

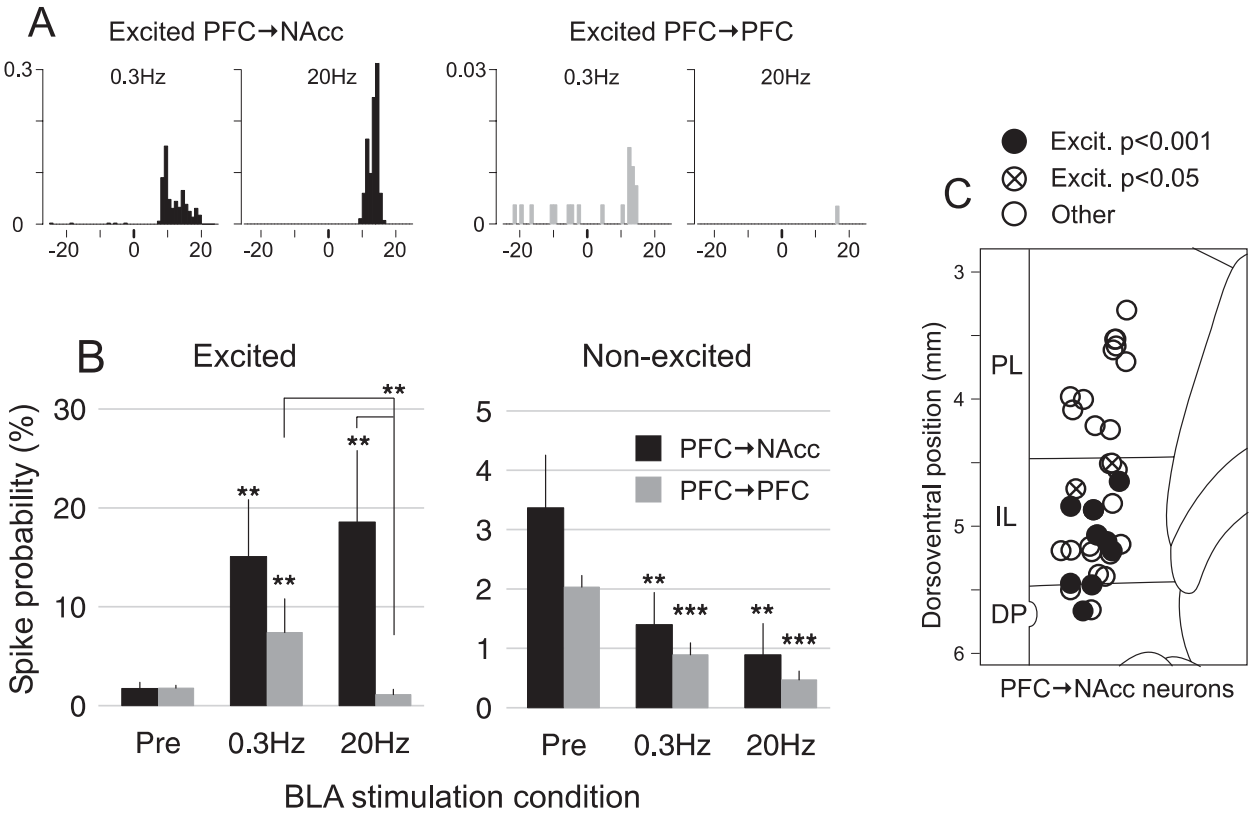

Figure 2.3 Effects of BLA electrical stimulation on mPFC projection neurons A Example peri-stimulus time histograms showing the response of an excited PFC-to-NAcc (left) and excited PFC-to-PFC (right) neuron to BLA stimulation at 0.3 and 20Hz. X-axis is post-BLA stimulus time (ms); Y-axis is response ratio per bin. In neurons with significant excitatory responses to both 0.3 and 20Hz stimuli, the onset of the response to 0.3Hz was typically 1-2ms earlier than the response to 20Hz stimulus trains. **B** 20Hz BLA stimulation elicited greater excitation in PFC-to-NAcc than in PFC-to-PFC neurons (left). For non-excited neurons with spontaneous activity of both types, BLA stimulation inhibited firing (right). ** $p<0.01$, *** $p<0.001$ (corrected) versus "Pre" condition unless noted otherwise. **C** Location of 33/66 PFC-to-NAcc neurons, including 11/12 excited neurons (see 2.3.6)). All excited PFC-to-NAcc neurons were located in IL or DP cortex.

On average, neurons that were not excited and that exhibited spontaneous spike firing showed inhibition to BLA stimulation (Figure 2.3B). There was no difference in the magnitude of inhibition when comparing PFC-to-NAcc and PFC-to-PFC neurons: -2.0±0.6% versus -1.1±0.2%, $p<0.6$ for 0.3Hz stimuli; -2.5±0.6% versus -1.6±0.3%, $p<0.5$ for 20Hz stimuli (Wilcoxon rank sum tests). However, it was difficult to obtain an accurate estimate of inhibitory responses in neurons with low baseline firing rates (Floresco and Tse 2007). Although for technical reasons (see 2.3.3.2) we were unable to quantify the significance of inhibitory responses in individual neurons, BLA stimulation (0.3 or 20Hz) reduced firing in all non-excited,

Table 2.1 PFC projection neuron locations and classification based on spontaneous activity and responses to BLA electrical stimulation.

	Response to BLA stimulation					
Projection target and location	Excited $p<0.001$	Excited $p<0.05$	Excited not signif.	Non-excited baseline ≥1%	Non-excited baseline <1%	*Total*
PFC-to-NAcc						
PL	0	0	2	6	13	21
IL	8	3	3	7	20	41
DP/MO	1	0	0	0	3	4
Total	9	3	5	13	36	66
PFC-to-PFC						
PL	0	0	4	9	11	24
IL	1	3	7	11	23	45
DP/MO	0	0	0	0	1	1
Total	1	3	11	20	35	70

spontaneously firing cells. Furthermore, stimulation induced a complete cessation of activity within the post-stimulus window in 10/14 PFC-to-NAcc neurons and 15/20 PFC-to-PFC neurons.

Neurons projecting to both NAcc and cmPFC were not frequently encountered (n=11) and exhibited little spontaneous or evoked activity. These neurons were not included in the 66 PFC-to-NAcc and 70 PFC-to-PFC neurons described above. Of the 11 neurons recorded in these experiments: 3 had spontaneous firing (at least 1% pre-stimulus spike probability) and were inhibited by BLA stimulation; 8 did not have appreciable spontaneous activity; none were significantly excited by the stimulation. In 14 non-excited projection neurons tested, very high frequency BLA stimulation (80 and 200Hz) did not evoke excitatory responses (not shown). The responses of non-excited neurons with little or no spontaneous firing is not shown.

2.4.2 Chemical stimulation of BLA

To confirm the orthodromic nature of the BLA electrical stimulation effects, the response of mPFC projection neurons to bicuculline infusion in the BLA was examined. Following bicuculline, spontaneous epileptiform discharges (EDs, measured by a field potential electrode) were recorded in the BLA; these EDs have been associated with simultaneous spike discharge in a population of neurons near the recording site (Steriade et al. 1998). The EDs were followed by spike firing in some prefrontal projection neurons, and firing within 5-26ms of the peak of the EDs (Figure 2.4A) was considered to be consistent with orthodromic transmission from BLA to mPFC (see 2.3.4).

Putative orthodromic spike discharge followed BLA EDs in 6 out of 21 PFC-to-NAcc neurons (6 rats, Figure 2.4B, top), with the following response ratios: 132, 125, 93, 40, 18, and 18% (mean 71±8%). Four of these six were located in IL or DP cortex (132, 125, 93 and 18%), and the other two were located in PL. Consistent with the electrically-evoked responses, the three neurons with the greatest response ratios were all located in IL or other ventral prefrontal regions. While most excited PFC-to-NAcc neurons (4/6) exhibited response ratios greater than 25%, there were no PFC-to-PFC neurons with an equivalently strong response. Three of 18 PFC-to-PFC neurons did exhibit post-ED spike discharge (3 rats, Figure 2.4C, top), however these responses were substantially less in magnitude (19, 4 and 1%; mean 8±6%). Two of these three neurons were located in IL cortex (19 and 1%), and the other was in PL. Excitation in all 9 of these projection neurons was significant beyond a 99.9% threshold as determined by a Poisson-based analysis.

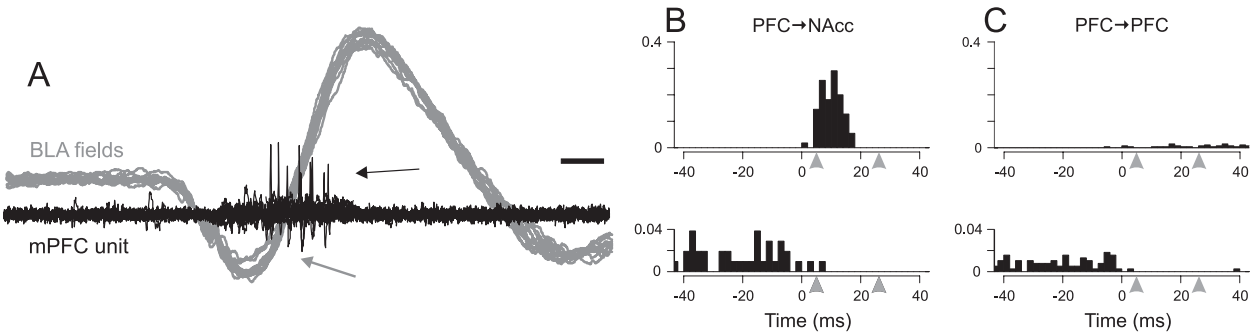

Figure 2.4 Effects of BLA chemical stimulation on mPFC projection neurons. **A** Simultaneous recording of a PFC-to-NAcc neuron discharge (black) and extracellular field potentials in the BLA (gray, 10 overlaid traces each). The large deflection in the field traces is an ED (gray arrow) caused by local infusion of bicuculline. The BLA ED occurred prior to spike discharge in the mPFC (black arrow). Scale bar: 10ms. **B** Peri-event histograms for representative responses in PFC-to-NAcc neurons: top, an excitatory response from a PFC-to-NAcc neuron (65 spikes and 55 EDs); bottom, an inhibitory response from a PFC-to-NAcc neuron (104 EDs). The arrowheads at 5 and 26ms indicate the expected range of orthodromic BLA-to-mPFC activation that would be predicted to occur from BLA afferent activation (see 2.3.4). Y-axis is response ratio per bin. **C** Peri-event histograms for representative responses in PFC-to-PFC neurons: top, an excitatory response from a PFC-to-PFC neuron (11 spikes and 287 EDs); bottom, an inhibitory response from a PFC-to-PFC neuron (384 EDs). Y-axis is response ratio per bin.

In projection neurons of both types that were not excited and that were spontaneously active, post-ED firing was typically inhibited within the 5-26 ms post-event window (Figure 2.4B,C, bottom). In three PFC-to-NAcc neurons and three PFC-to-PFC neurons, spontaneous activity was completely inhibited within the post-ED window.

2.4.3 Pavlovian odor conditioning and recording

A group of 14 rats was conditioned to odors while awake and then anesthetized for subsequent mPFC recordings. Conditioning was done by pairing a distinct odor (CS+) with a foot shock multiple times; a second, non-paired odor (CS-) was also presented during the conditioning session. After conditioning but before recording, 9 rats were exposed briefly (20sec) to the CS- and CS+ odors (with no shocks). Freezing during the CS+ odor (14.6 ±4.6%), was significantly greater than freezing during the CS- odor (8.3 ±2.5%, $p<0.02$ paired Wilcoxon rank sum test) in these rats.

To confirm the effectiveness of the conditioning procedure, a separate group of 8 rats was conditioned in the same way and then tested using longer (5 min) presentations of the CS+ and CS- odors as employed previously (Rosenkranz et al. 2003; Laviolette et al. 2005). Within the first minute of odor presentation freezing in response to the CS+ was greater than in response to the CS-, and remained greater throughout odor presentation (Figure 2.5C). The average freezing during the CS+ (36.5±5.1%) was significantly greater than during the CS- (11.7±4.1%, $p<0.008$, paired Wilcoxon rank sum test). In addition, exploratory and grooming activity scores measured during odor presentation, while not significantly different within the first minute of odor

presentation, did show a difference over minutes 2-5 of odor presentation (CS+ score 1.7±0.3; CS- score 0.8±0.6, $p<0.03$ paired Wilcoxon rank sum test).

During mPFC recordings performed under anesthesia (n=14 rats), presentation of CS+ and CS- odors caused both firing rate increases and decreases in PFC-to-NAcc (n=30) and PFC-to-PFC neurons (n=23) (Figure 2.5A), with the mean change in firing rate being approximately zero for all groups (Figure 2.5B, middle). Odor-evoked responses in rats that had been tested behaviorally did not differ from responses in untested rats (not shown), however this data set may have insufficient power to determine the effect of behavioral testing.

Population analysis showed that for excitatory odor responses (top quartile), the average response of PFC-to-NAcc neurons (n=7, 7 rats) to the CS+ was greater than the response of PFC-to-PFC neurons (n=6, 5 rats), and was also greater than PFC-to-NAcc responses to the CS- (n=7, 4 rats, Figure 2.5B, top; two-way ANOVA ($F(3,22) = 7.43$, $p < 0.002$), with significant effects of both neuron type and CS type ($F(1,22) = 6.42$ and 12.80, $p < 0.02$ and 0.002, respectively)). Although the neuron type by CS type interaction was not significant ($F(1,22) = 3.08$, $p < 0.1$), post-hoc testing revealed significant differences between groups (Figure 2.5B, top). A similar population analysis of the inhibitory responses (bottom quartile) showed a greater CS+-evoked inhibition in PFC-to-NAcc compared to PFC-to-PFC neurons (n=7 from 6 rats, n=6 from 4 rats, respectively, Figure 2.5B, bottom; two-way ANOVA ($F(3,22) = 3.66$, $p < 0.03$), with cell type as the only significant factor ($F(1,22) = 6.33$, $p < 0.02$)). In PFC-to-NAcc neurons, inhibition evoked by the CS+ was not significantly different from inhibition evoked by the CS- (n=7, 6 rats, Figure 2.5B, bottom). Unlike responses to BLA electrical stimulation, in spontaneously active neurons inhibitory responses that resulted in the total cessation of firing during the CS+ occurred in only one neuron, which was identified as a PFC-to-PFC neuron.

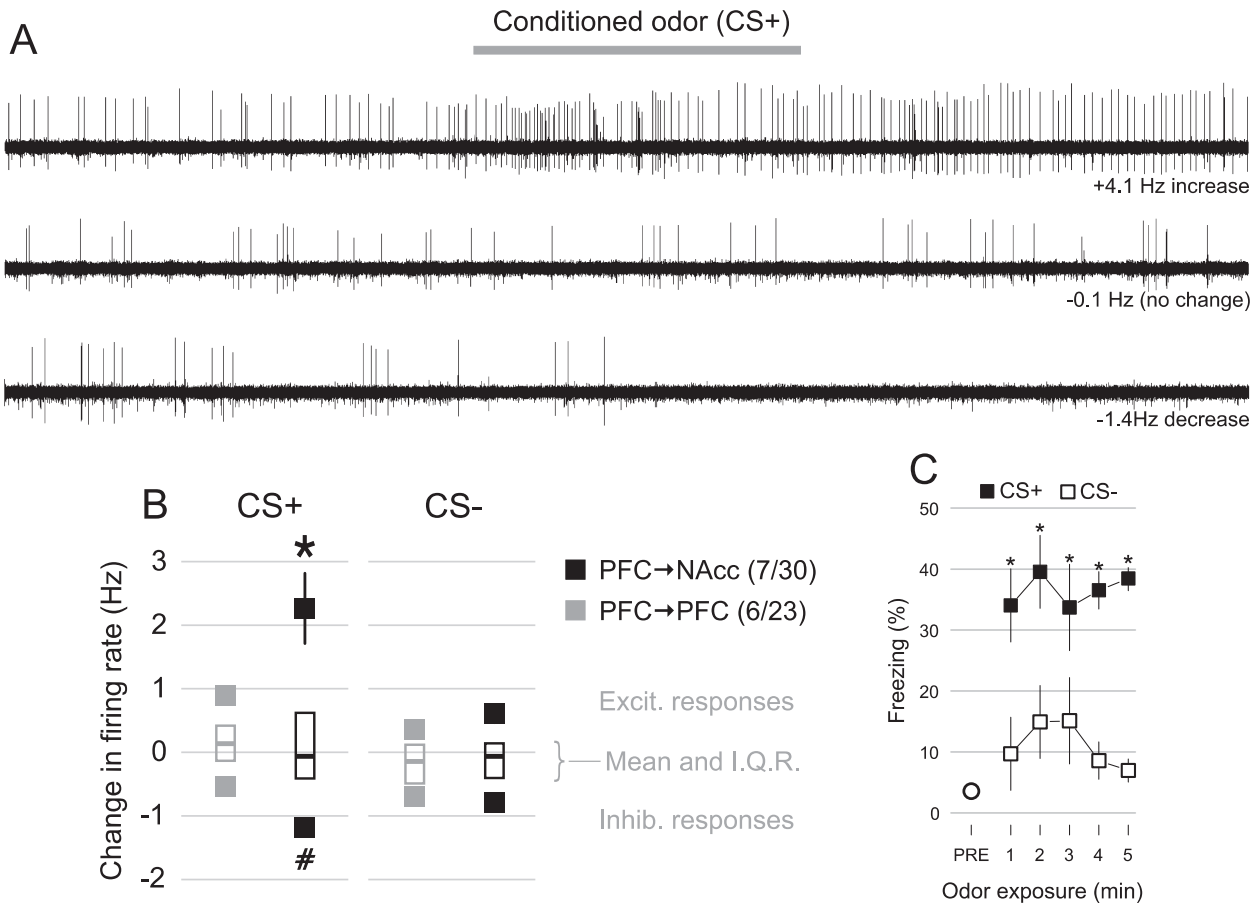

Figure 2.5 Effects of conditioned odors: population analysis. **A** Traces from three neurons show responses to the CS+ odor (gray bar, 10s): evoked excitation (top), inhibition (bottom), or no discernable response (middle). **B** Modified box-plots showing excitatory and inhibitory odor responses (change in firing rate during odor). The filled boxes show the averages of the top and bottom quartiles (greatest excitatory and greatest inhibitory responses), which were analyzed separately. 30 PFC-to-NAcc neurons were recorded, with 7 neurons each in the top and bottom quartiles; 23 PFC-to-PFC neurons were recorded, with 6 neurons in each quartile. PFC-to-NAcc neurons had greater CS+ inhibitory and excitatory responses than PFC-to-PFC neurons. Error bars = SEM. * $p<0.05$ versus all other excitatory responses. # $p<0.05$ versus the inhibitory PFC-to-PFC/CS+ response only. **C** Freezing in response to CS+ odor (black squares) and CS- odor (white squares) over a five-minute test, one day after odor conditioning in a group of 8 rats not used for electrophysiological recordings. Average freezing over a five minute period before odor exposure is indicated by the initial circle. * indicates significant difference ($p<0.04$, corrected) from CS- by paired Wilcoxon rank sum test. Error bars represent SEM.

Analysis of individual neurons revealed that 7 PFC-to-NAcc neurons (7 rats) exhibited spiking during CS+ odor presentation that was significantly greater than baseline firing during the pre-stimulus period ($p < 0.05$ for all seven; $p < 0.001$ for 5/7, see 2.3.3.3). The odor response was specific to the CS+ in 5 of the 6 neurons for which CS- data is also available, as only 1 neuron exhibited a significant excitation in response to the CS- (Figure 2.6A,B, left). As was the case for BLA stimulation, PFC-to-NAcc neurons with significant excitatory responses were found primarily in the ventral mPFC areas IL and MO (5/7) (Figure 2.6C). A similar analysis identified 7 PFC-to-PFC neurons (6 rats) with significant CS+ odor responses ($p < 0.05$ all seven; $p<0.001$ for 4/7), with 4 out of the 5 for which CS- data is available having no significant response to the CS- odor (Figure 2.6A,B, right). The difference between the CS+ and CS- response was calculated for each neuron as an index of response specificity for the CS+ over the CS-. The mean of this specificity index in PFC-to-NAcc neurons (2.4Hz, n=6) was greater than in PFC-to-PFC neurons (0.7Hz, n=5, $p<0.009$, Wilcoxon rank sum test)(Figure 2.6B). Five PFC-to-NAcc neurons exhibited significant excitation ($p<0.05$) in response to the CS- odor; however, only 2 of these 5 neurons were highly excited ($p<0.001$), and 1 of these 2 exhibited a greater excitation in response to the CS+ (Figure 2.6B, left).

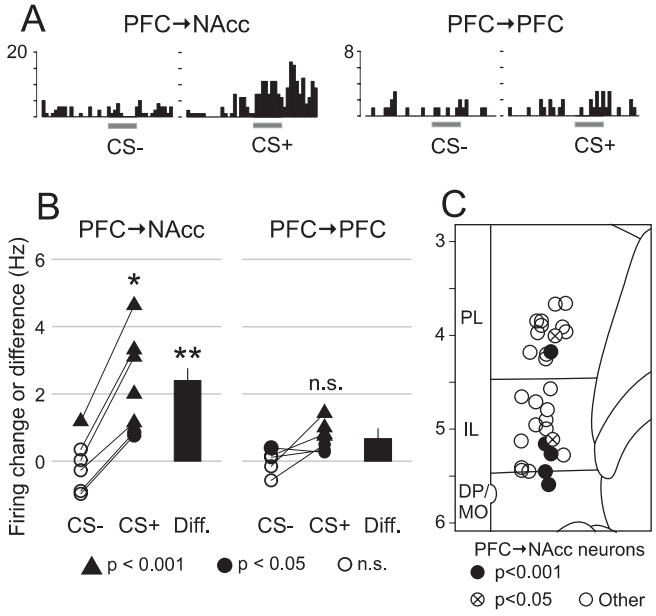

Figure 2.6 Effects of conditioned odors: single neuron analysis. A Peristimulus time histograms from a single PFC-to-NAcc neuron (left) and a single PFC-to-PFC neuron (right) during presentation of conditioned odors (1 sec bins). The gray bar indicates the time when the odor was presented (10 sec). Y-axis is number of spikes per bin. **B** Odor-evoked changes in firing rate in response to the CS+ and CS- odors for single neurons (triangles and circles); and mean differences between CS+ and CS- responses (bars). In PFC-to-NAcc neurons with significant excitatory responses to the CS+ (left), CS+ responses were greater than CS- responses (n=6, $p<0.03$ paired Wilcoxon rank sum test); but this was not the case for PFC-to-PFC neurons with significant CS+ excitation (right, n=5, $p<0.13$). The mean difference between CS+ and CS- responses was greater in PFC-to-NAcc neurons (n=6, left bar) than in PFC-to-PFC neurons (n=5, right bar; $p<0.009$, Wilcoxon rank sum test). The plotting symbols indicate the response to odor presentation: triangles for excitation exceeding a $p < 0.001$ threshold (highly excited); filled circles for excitation exceeding a $p < 0.05$ threshold; empty circles for no significant excitation. **C** The locations of all PFC-to-NAcc neurons recorded during odor testing. Most excited PFC-to-NAcc neurons (5/7) were located in IL or DP/MO cortex. Y-axis is atlas coordinates in millimeters.

2.5 DISCUSSION

A subset of mPFC neurons that project to the nucleus accumbens, located almost exclusively in the ventral mPFC, was found to be excited by BLA stimulation and by Pavlovian conditioned stimuli. These excitatory responses were greater in magnitude and more consistently evoked than those in a similar group of mPFC projection neurons that did not project to the accumbens.

The data strongly suggest that the excitatory responses were due to direct orthodromic input from the BLA, because these responses occurred at short latencies and were evoked both by electrical and cell body-specific chemical stimulation of the BLA. Even though BLA stimulation and conditioned odor responses were not measured in the same neurons, it is most likely that the odor-evoked responses in PFC-to-NAcc neurons were due to BLA input because our previous work showed that an intact BLA input is required for the induction of odor-evoked conditioned responses in mPFC neurons (Laviolette et al. 2005).

2.5.1 Behavioral responses to conditioned stimuli

In the rats that were exposed to conditioning and then tested behaviorally prior to recording (n=9 of 14), freezing responses to the CS+ odor were low compared to earlier studies (Otto et al. 1997; Laviolette et al. 2005) and were less than two-fold greater than freezing during the CS- odor. This was most likely due to the very brief odor presentations (20 sec) that were used to limit the possibility of exposure-induced extinction in the electrophysiological tests (Shipley 1974). Indeed, in a separate group of rats (n=8) that were exposed to an identical conditioning procedure, the more standard odor presentation durations (5min) elicited freezing responses that were comparable to previous reports (Otto et al. 1997), with the CS+ response more than three-fold higher than the CS- response (Laviolette et al. 2005). Therefore, the conditioning procedure employed was effective in eliciting robust fear behavior in these rats.

2.5.2 Responses to amygdala stimulation

While some previous studies in awake rats did not report excitatory responses to conditioned stimuli (Garcia et al. 1999; Milad and Quirk 2002), others have found a subset of mPFC neurons that were excited by conditioned cues (Baeg et al. 2001; Gilmartin and McEchron 2005). Studies focusing on the BLA input to mPFC have found a significant minority of mPFC neurons that are excited by BLA stimulation (Perez-Jaranay and Vives 1991; Ishikawa and Nakamura 2003), including identified projection neurons (Floresco and Tse 2007). Thus, the conflicting findings in awake rats may be due to the heterogeneity of BLA input onto mPFC neurons. We focused our current study specifically on BLA-evoked excitatory responses, which we found previously correlate best with Pavlovian conditioned responses (Laviolette et al. 2005; Laviolette and Grace 2006). The fact that BLA stimulation excites some PFC-to-NAcc neurons but produces inhibition in a substantial number of other mPFC neuron types (Floresco and Tse 2007) suggests that the amygdala input may function as a bias signal, facilitating firing of outputs to selected targets while attenuating firing in all others.

Only 18% (12/66) of PFC-to-NAcc neurons were significantly excited by BLA stimulation, with most other neurons exhibiting inhibition. Even considering only neurons in IL or other ventral mPFC regions, excitatory responses were in the minority (12/45, 27%). While this sparse excitatory response could be due to the low stimulation current or the narrow response window used, excitatory responses to chemical stimulation and conditioned odors occurred with similar frequencies (6/21 and 7/30, respectively). Furthermore, even though we only recorded from a subset of mPFC neurons, the proportions of BLA-evoked excitatory responses were comparable to those found in uncategorized (with respect to projection site)

mPFC neurons using similar methods (Ishikawa and Nakamura 2003; Floresco and Tse 2007). Finally, anesthesia is unlikely to account for the sparse excitation observed here, as fast-onset excitatory responses to conditioned stimuli were found in only 15% of uncharacterized IL neurons (Gilmartin and McEchron 2005) and in 24% of regular-spiking mPFC neurons (Baeg et al. 2001) in studies using awake rats. Thus, our results suggest that the magnitude of excitatory BLA input to PFC-to-NAcc neurons is similar to mPFC neurons in general, and that less excitation (or more inhibition) is evident in PFC-to-PFC neurons.

Similar studies of the hippocampus-to-mPFC pathway have found comparable proportions of excitatory responses in mPFC neurons (Degenetais et al. 2003; Ishikawa and Nakamura 2003). Intracellular recording from prefrontal neurons in vivo have shown that hippocampal stimulation typically evokes a complex post-synaptic response, exhibiting both excitatory and inhibitory conductances that have been attributed to monosynaptic glutamatergic input and di-synaptic GABAergic input, respectively (Degenetais et al. 2003). BLA stimulation may also evoke a similar response in mPFC projection neurons (Dilgen and O'Donnell 2004). Thus, the response of an mPFC neuron to BLA stimulation likely depends on the balance of glutamatergic and GABAergic inputs it receives. Furthermore, the typically low number of excitatory responses could be due to occlusion by fast-onset inhibitory inputs, such as those observed in somatosensory cortex pyramidal neurons in response to thalamic stimulation (Cruikshank et al. 2007).

Inhibitory responses to BLA stimulation (and conditioned odors) were detected in both populations of neurons. These two populations exhibited no differences in BLA-evoked inhibition; however, as noted above (2.3.3.2 and 2.3.3.3), low spontaneous activity did not allow for an accurate measurement of inhibition in most neurons. Thus, other methods may be

necessary to precisely determine the magnitude of BLA-evoked (and CS-evoked) inhibition. In previous studies, excitatory BLA-evoked responses were identified as being the most relevant for the role of the mPFC in conditioned fear (Laviolette et al. 2005); however, evoked inhibition may also contribute to the processing of emotional information by shaping cortical output or by entraining cortical activity to synchronized oscillations (Hasenstaub et al. 2005).

2.5.3 Prefrontal-accumbens interactions and conditioned fear

The selective activation of PFC-to-NAcc neurons by conditioned stimuli suggests that this pathway is involved in the expression of conditioned fear. Despite evidence that lesions of the mPFC or NAcc do not consistently impair conditioned fear responses (Kubos et al. 1987; Riedel et al. 1997; Quirk et al. 2000; Levita et al. 2002; Jongen-Relo et al. 2003; Cassaday et al. 2005), we and others have found that acute inactivation or pharmacological manipulations of these areas can impair conditioned fear (Laviolette et al. 2005; Resstel et al. 2006a; Schwienbacher et al. 2006; Sierra-Mercado et al. 2006; Corcoran and Quirk 2007b) This apparent discrepancy may be due to the differences in which mPFC function is altered. Thus, lesions followed by a recovery period may allow time for compensatory mechanisms to intervene (Maren et al. 1997; Anglada-Figueroa and Quirk 2005). Indeed, acute interference with neuronal activity or excitability, such as by silencing activity in the target area or by altering normal patterns of firing, often reveals the functional impact of a region that is not made apparent when permanent lesions are used (Quirk et al. 2000; Gale et al. 2001; Anglada-Figueroa and Quirk 2005). Therefore, the PFC-to-NAcc neurons may support conditioned fear in intact rats, whereas other

systems (such as outputs to the hypothalamus or brainstem (Price 1999; Petrovich et al. 2005)) may compensate for this essential survival skill in rats with permanent lesions.

Recent work by Corcoran and Quirk (2007) has shown that PL inactivation reduces conditioned, but not innate, fear. They have suggested that the specific function of the PL in conditioned fear is to integrate sensory, contextual and goal-directed information and to promote fear responses only at appropriate times and locations. The IL also receives multimodal sensory and motivational input (Conde et al. 1995), and thus the IL-to-NAcc pathway may support conditioned fear in a similar way. Indeed, we have previously proposed that the NAcc performs just such a gating function, constraining behavior based on contextual, affective and goal directed information (Grace 2000). While we and others have observed that inactivation of both IL and PL reduce several measures of conditioned fear (Laviolette et al. 2005; Laviolette and Grace 2006; Resstel et al. 2006b), there is also strong evidence that IL neurons signal safety and promote the extinction (rather than the expression) of fear behaviors (Milad and Quirk 2002; Milad et al. 2004; Burgos-Robles et al. 2007). This discrepancy may be explained by the different fear conditioning paradigms used in these studies; for example, manipulation of IL had no effect on conditioned fear in response to a tone CS (Quirk et al. 2000; Burgos-Robles et al. 2007), but abolished fear responses to a context CS (Resstel et al. 2006b) or odor CS (Laviolette et al. 2005). Therefore, considering our previous work demonstrating that IL manipulations reduce fear to an odor CS, our current results suggest that IL-to-NAcc neurons promote conditioned fear responses in this paradigm.

We tested mPFC efferent pathways to NAcc and cmPFC for their roles in encoding conditioned stimuli; however other efferent pathways may also contribute to conditioned fear. Indeed, while the PL appears to promote conditioned freezing (Corcoran and Quirk 2007b), our

results suggest that these behaviors may be mediated by PL projections to targets other than the NAcc or contralateral mPFC. However, the identity of these other projection targets is not known. Cortico-striatal neurons are thought to send collateral axons to diverse secondary targets (Levesque et al. 1996), and PFC-to-NAcc neurons in particular are known to send collaterals to cmPFC, BLA and the ventral tegmental area (Pinto and Sesack 2000). We found no significant excitation in the 11 neurons projecting to both NAcc and cmPFC; however, due to the small sample size it is unclear whether these neurons are more or less excitable than PFC-to-NAcc neurons in general. Therefore it is not known how secondary targets of PFC-to-NAcc neurons contribute to conditioned fear responses, nor whether PFC-to-NAcc neurons with different secondary targets exhibit different responses to conditioned stimuli.

2.5.4 Conclusions and implications

Our data suggest that the amygdala is capable of influencing conditioned responses at two sites: via its projections to the mPFC neurons projecting to the NAcc, and by projections to NAcc neurons receiving mPFC input. The BLA projects to the mPFC (Krettek and Price 1977b), as well as to the NAcc division that receives the strongest mPFC input, (the shell, Groenewegen et al. 1990), with many single BLA neurons projecting to both areas (Shinonaga et al. 1994). MPFC and BLA afferents target the NAcc shell cell clusters (Wright and Groenewegen 1995), and strong evidence suggests they converge and form excitatory synapses onto the same medium spiny neurons (French and Totterdell 2002, 2003). Thus, activation of the BLA alone may be sufficient to recruit both pathways that converge onto and drive NAcc neurons.

While our study has focused on the role of the mPFC in conditioned fear, there is also evidence that this amygdala-prefrontal-striatal circuit has other roles. In a study where BLA and mPFC were disconnected, rats failed to seek larger rewards that required greater effort to obtain, suggesting that the influence of reward value on decision making is diminished by this lesion. In mPFC/NAcc disconnection studies, rats exhibit deficits that suggest this pathway is necessary for switching strategies (Block et al. 2007) or modifying behavior based on task feedback (Christakou et al. 2004). Therefore, the amygdala activation of IL-to-NAcc neurons may represent a mechanism by which reward value informs behavioral choice (Cardinal et al. 2002). Indeed, in humans with focal lesions of the amygdala, choice-related signals in the anterior cinglulate cortex (comparable to rodent mPFC (Ongur and Price 2000)) are far weaker than in non-lesioned individuals (Hampton et al. 2007). Furthermore, a similar function has been attributed to the BLA-to-orbitofrontal cortex pathway in reversal learning tasks in rodents (Schoenbaum et al. 1999; Schoenbaum et al. 2003). Amygdala-evoked excitation in mPFC can be modulated by dopamine and by hippocampal inputs (Ishikawa and Nakamura 2003; Floresco and Tse 2007), suggesting that the affective drive of a strategy or behavioral set is plastic, and subject to being modified by other salient cues or task constraints.

CHAPTER 3 : REGULATION OF EVOKED SPIKING IN NUCLEUS ACCUMBENS NEURONS: INTEGRATION OF AMYGDALA AND PREFRONTAL CORTICAL INPUTS

3.1 ABSTRACT

Single nucleus accumbens (NAcc) neurons receive excitatory synaptic input from cortical and subcortical sources, and how they integrate these inputs critically determines NAcc neuron output. While synaptic input summation has been characterized at subthreshold intensities, no measurements have been made of multi-input evoked spiking. We recorded single NAcc neurons in urethane-anesthetized rats, and measured spiking elicited by coincident stimulation of two major NAcc afferent regions: the basolateral amygdala and medial prefrontal cortex (BLA and mPFC). BLA input increased the spike output elicited by mPFC stimulation. This facilitation was dependent on the timing of the stimulation pulses, consistent with the summation of monosynaptically evoked excitatory activity. When mPFC input intensity was below spiking threshold, the addition of BLA input produced the largest facilitation of evoked spiking, and the latency of the evoked spikes reflected the latency of the individual inputs. When mPFC inputs were stimulated at higher intensities, BLA-mediated facilitation was weaker, and the spike latency reflected only the mPFC input. Thus, NAcc neurons appear to integrate both the magnitude and timing of afferent synaptic activity. Because the latency of evoked spikes

depended on the input stimulation intensity, NAcc neuron output – and NAcc-mediated behaviors – may be influenced by the balance or imbalance of synaptic activity in its afferent structures.

3.2 INTRODUCTION

As a ventral extension of the striatum, the NAcc receives its primary glutamatergic inputs from cortical and subcortical structures including the mPFC and the BLA. As such, the NAcc is an interface for several potential sources of motivational and goal-directed information (O'Donnell et al. 1999; Grace 2000). While this cortical/limbic integration is thought to be among the most important features of the NAcc, how this integration gives rise to firing in NAcc neurons is not well characterized.

Single NAcc medium spiny neurons (the primary output neurons of the NAcc) receive convergent excitatory synaptic input from multiple afferent structures (French and Totterdell 2002, 2003), and there is electrophysiological evidence that this convergence occurs in the majority of NAcc neurons (O'Donnell and Grace 1995; Goto and O'Donnell 2002). Because a barrage of excitatory synaptic activity is needed to drive firing in NAcc neurons (Blackwell et al. 2003; Wolf et al. 2005), this convergence is crucial for the functional output of the NAcc. The integration and interaction of excitatory inputs have been characterized in adjacent spines of NAcc neurons recorded in vitro (Carter et al. 2007), in terms of subthreshold input summation in vivo (Goto and O'Donnell 2002), and in computational neuronal models (Wolf et al. 2005). Although these studies help explain synaptic summation at subthreshold levels of stimulation,

subthreshold observation may not be sufficient to explain the complex process of action potential generation, which in medium spiny neurons is governed by periodic membrane potential shifts and outward-rectifying potassium channels activated near spiking threshold (O'Donnell and Grace 1995; Wilson and Kawaguchi 1996; Wickens and Wilson 1998). Thus, it is necessary to investigate directly how the interactions among inputs give rise to suprathreshold spiking activity. While several studies have observed evoked spiking due to converging input (O'Donnell and Grace 1995; Finch 1996; Mulder et al. 1998; Floresco et al. 2001b), the specific features of this evoked activity (e.g. response rate, latency, timing dependence) are not known.

To study spike firing evoked by the integration of synaptic activity, the extracellular responses to stimulation of cortical and sub-cortical afferent regions were measured in single NAcc neurons. Two regions were stimulated: the medial prefrontal cortex (mPFC) and the basolateral amygdala (BLA). These structures both project densely to the NAcc, where their terminals converge within the same subregions (Wright and Groenewegen 1995) and likely synapse upon single medium spiny neurons (O'Donnell and Grace 1995; French and Totterdell 2002, 2003). The BLA is known to encode the value of reward-associated cues (Schoenbaum et al. 1998; Paton et al. 2006), and the mPFC is implicated in goal-directed behavior (Floresco et al. 1999; Ostlund and Balleine 2005; Block et al. 2007). Therefore in order to show how affective information can influence goal-related encoding the NAcc, this study specifically focused on the ability of BLA inputs to modulate firing evoked by activation of the mPFC. Furthermore, both BLA neurons and mPFC-to-NAcc projecting neurons are activated by odors that have been paired with a foot shock (Rosenkranz and Grace 2002; Laviolette et al. 2005; McGinty and Grace 2007). Thus the interaction of these inputs may also be relevant to the expression of Pavlovian conditioned fear.

Recordings were made from NAcc neurons in urethane-anesthetized rats. Neurons were identified as receiving both BLA and mPFC input on the basis of short-latency spike discharge evoked by single stimulation pulses delivered to each structure. The response rate and latency of spikes evoked by mPFC stimulation alone were measured, and compared with spikes evoked by paired stimulation of the BLA and mPFC at different current intensities and inter-stimulus intervals. BLA input facilitated and shifted the latency of mPFC-evoked spikes in a manner consistent with the summation of monosynaptic excitation. Furthermore, the effects of BLA input were greatest when modulating a weak mPFC input, suggesting that input integration leading to spike discharge depends on both the timing and relative intensity of the component inputs.

3.3 METHODS

Extracellular recordings were obtained from 210 NAcc neurons in 132 rats. All neurons were identified as receiving excitatory input from the mPFC, and all but 19 neurons were also identified as receiving excitatory input from the BLA. The interaction of BLA and mPFC inputs was tested with several different protocols designed to measure different features of evoked spike responses (see 3.3.3); single neurons were typically tested in more than one protocol. All experiments were performed in accordance with the National Institutes of Health *Guide for the Care and Use of Laboratory Animals* and were approved by the University of Pittsburgh Animal Care and Use Committee.

3.3.1 Subjects and Surgery

Male Sprague-Dawley rats (mean 310g, range 270-430g) were anesthetized with a single injection of urethane (1.4-1.5mg/kg in distilled water), providing stable anesthesia for the duration of the experiment, which did not exceed 8 hours. For experiments in which drugs were administered, the rats were implanted with a femoral vein catheter after the onset of anesthesia (loss of reflexive withdrawal in response to a foot pinch, 20-60 minutes after injection). After anesthesia onset, rats were placed in a stereotaxic apparatus (David Kopf Instruments, Tujunga, CA). An incision was made in the skin, the skull was cleaned, small holes were drilled overlying the electrode target regions, and the dura was resected. The electrode target coordinates were determined using the atlases of Paxinos and Watson (1998; 2005); coordinates are given in mm relative to the bregma suture landmark: AP for the anterior-posterior distance, ML for medial-lateral, DV for dorsoventral.

Bipolar stimulating electrodes (side-by-side with 1mm tip separation) were lowered into the BLA (AP -3.6, ML 4.8, DV -9.0, negative pole) and mPFC (AP +3.0, ML 0.8, DV 5.5, negative pole), and a recording electrode was lowered to the dorsal border of the NAcc near the core/shell border (AP +1.2, ML 0.8 to 1.0, DV 6.0-8.0). The mPFC stimulating electrodes were coupled to a 30g cannula guide tube to allow simultaneous electrical stimulation and drug infusion in the same region (Plastics One "chemotrodes", C232G-MS303/2). Infusions were only performed in a small number of experiments (see 3.3.4). The electrode leads were exposed for 0.8mm from the tip, allowing for current spread to areas dorsal to the tip placement (Figure 3.1B). The poles of the BLA electrode were placed in the same sagittal plane, and the poles of the mPFC electrode were placed in approximately the same coronal plane. Stimulation was

controlled through the Master-8 stimulator and Isoflex stimulus isolation units (A.M.P.I., Jerusalem, Israel).

Extracellular recording electrodes were pulled from 2mm outside diameter, filamented borosilicate glass (World Precision Instruments, Sarasota, FL). The tips were broken under microscopic control to achieve an impedance of 8-12 MΩ (measured in situ) and filled with 2M NaCl with 2% Pontamine Sky Blue dye. Signals from neurons in the NAcc were amplified and band pass filtered at 200-4000Hz (Fintronics WDR-420, Orange, CT). The amplified signals were passed to a speaker and oscilloscope for real-time monitoring, and to a data acquisition board and PC (Microstar Laboratories, Bellevue, WA) for storage and analysis. Offline analysis was performed using custom software (Neuroscope, Brian Lowry) and scripts for the R programming environment (The R Development Core Team 2005).

3.3.2 Neuron identification and selection

Neurons were recorded only if they received excitatory input from the mPFC and (for 191/210 neurons) from the BLA as well. Similar to previous studies (Floresco and Grace 2003; McGinty and Grace 2007), a cell searching procedure was used to identify NAcc neurons receiving BLA and mPFC input: single, alternating stimulation pulses were delivered to the BLA and mPFC at an overall rate of 0.5Hz. as the recording electrode was slowly advanced through the NAcc (DV 6.0-8.0), NAcc neurons were identified by the presence of biphasic action potentials occurring shortly after the stimulus artifacts (Figure 3.2B).

To determine the timing of orthodromic inputs to NAcc, the conduction times of the mPFC-to-NAcc and BLA-to-NAcc pathways were measured in preliminary experiments. The

NAcc was stimulated while recording from antidromically activated projection neurons in mPFC and BLA (see 2.3.2). The mean and distribution of the antidromic latencies (conduction times) of 141 mPFC-to-NAcc projecting neurons (which include 66 neurons recorded in McGinty & Grace, 2007) are illustrated in Figure 3.3A (top). The conduction times of 41 BLA-to-NAcc projecting neurons were also measured, and the mean and distribution are shown in Figure 3.3B (top). These conduction time distributions were used to establish criteria for selecting NAcc neurons.

Neurons were judged to be suitable for recording if the mean spike latency for both inputs was 20ms or less, corresponding to the maximum BLA-to-NAcc and mPFC-to-NAcc conduction times (Figure 3.3). Although the source of all evoked spikes could not be definitively determined, by selecting responses within this short range, the likelihood of recording responses due to monosynaptic, orthodromic input from the BLA and mPFC was maximized. In addition, neurons were only judged acceptable for recording if they exhibited at least a 50% evoked response rate to 400μA stimulation of the BLA and 500μA stimulation of the mPFC, with each input tested separately at 0.3Hz. Because approximately 95% of striatal neurons are medium spiny neurons (Kemp and Powell 1971; Jiang and North 1991b), this cell type is likely to comprise the great majority of the neurons recorded in this study. Neurons with steady spontaneous firing, typical of tonically active striatal interneurons (Wilson et al. 1990), were rarely encountered, and were not recorded.

3.3.3 Tests of mPFC/BLA input interactions

The object of these experiments was to test the effects of excitatory BLA inputs on spiking responses evoked by the mPFC in single NAcc. Upon isolation of a neuron responding to both inputs, up to four distinct tests were performed to investigate the mPFC/BLA interactions in that neuron. Two of these tests were designed to measure the influence of the BLA on mPFC-evoked spike *rate* (3.3.3.1 and 3.3.3.2). The other two tests were designed to measure the BLA influence on spike *latency* (3.3.3.3 and 3.3.3.4). In all of these tests, the BLA was activated with electrical stimulation; BLA inactivation effects were *not* tested because BLA principal neurons exhibit very low spontaneous activity and thus are unlikely to provide a tonic excitatory influence to the NAcc (Rosenkranz and Grace 1999; Buffalari and Grace 2007).

The stimulation current intensities used for each neuron were based on evoked spiking probability. "Subthreshold" stimulation currents were defined as eliciting a 1-4% response rate (spikes per 100 stimuli). This intensity of stimulation provided adequate activation of BLA inputs to the neuron (indicated by its modulation mPFC-evoked spiking, see 3.4.2) but by itself contributed a negligible number of evoked spikes. Although the membrane potential could not be observed, based on previous studies it is expected that subthreshold stimulation should consistently evoke depolarizing post-synaptic potentials (EPSPs) in the recorded neuron (O'Donnell and Grace 1995; Goto and O'Donnell 2002). In almost all experiments, the BLA was stimulated at subthreshold current intensities. For mPFC, stimulation current was varied according to the test protocol being performed (see below). All stimulation pulses were 0.25ms in duration.

3.3.3.1 BLA input effect on mPFC-evoked spike rate The mPFC was stimulated at "threshold" current intensities, defined here as evoking spikes at a ~50% response rate. BLA stimulation current was subthreshold, as defined above. The mPFC was stimulated alone for 20 trials at a rate of 0.3Hz (baseline period); then a single BLA stimulation pulse was introduced in each trial. The inter-stimulus interval (ISI) of the mPFC/ BLA pulse pair varied; in most experiments, the BLA pulse preceded the mPFC pulse at ISIs of 1ms, 11ms, 21ms, and 31ms, which covered an adequate response range based on initial experiments (i.e. Figure 3.5D). The ISIs were typically rotated from one trial to the next, and trials with no BLA stimulation ("mPFC alone" trials) were added to the rotation in order to monitor baseline responsivity during the test. To test the symmetry of these BLA/mPFC interactions, in a small number of experiments (n=21 neurons, Figure 3.5D, right), the current intensities were reversed – i.e. BLA at threshold (~50% response), and mPFC at subthreshold. Finally, the specificity of the BLA stimulation effects was tested in 19 neurons identified as receiving only mPFC (but not BLA) excitatory input; for these tests, BLA stimulation current was fixed at 400μA. At least 10 trials at each ISI were tested. The responses were grouped by ISI, and the spike rates (spikes/100 stimuli expressed as %) were calculated. Because the spiking due to subthreshold BLA stimulation was negligible, any changes in mPFC-evoked firing were attributed entirely to the summation of mPFC-evoked responses and subthreshold BLA-evoked events.

In a subset of neurons these tests were performed after IV injection of receptor antagonists or channel blockers: dopamine D1 antagonist SCH23390, 0.5mk/kg, n=14 neurons; dopamine D2 antagonists eticlopride or raclopride, 0.2 or 0.1 mg/kg, respectively, n=15 neurons; NMDA channel blocker MK801, 0.05 or 0.1 mg/kg, n=11 neurons. These doses have been shown previously to have potent activity at the target receptors and to be effective in relevant

behavioral tasks (Caine and Koob 1994; Nicola and Deadwyler 2000; Floresco et al. 2001b; Cervo et al. 2003; Biondo et al. 2005).

3.3.3.2 BLA input effect on the mPFC current input/spike output curve At non-spike evoking input intensities, the summation of BLA and mPFC inputs is dependent on the amplitude of the component EPSPs (Goto and O'Donnell 2002). Therefore, we tested whether spike-evoking mPFC/BLA interactions were also amplitude dependent. In addition to the criteria outlined above (3.3.2), neurons were recorded only if they exhibited a 100% spike rate to 700μA mPFC stimulation. Similar to the first test (3.3.3.1), the mPFC was stimulated alone or with the BLA at ISIs of 1ms, 11ms, and 31ms, rotated from trial-to-trial (0.3Hz trial rate). BLA current was kept at subthreshold intensities, whereas the mPFC current was varied from 0% to 100% spike rate intensities in increments of 10-20μA. At least 10 trials were performed per ISI at a given current intensity. To cover the entire current/response range, stimulation current began at 60-80% spike rate to mPFC alone, and then was adjusted above and below this value in alternating steps until 0% and 100% rates were observed for all ISIs.

For analysis, the trials were grouped by ISI, and the evoked spike rate at each current increment was plotted. Thus, each neuron produced four current/response curves (mPFC alone, 1ms, 11ms, and 31ms ISIs). The responses between 0% and 100% were fit to linear equations, which were used to perform two calculations of the BLA stimulation effects. (Linear fits were preferred over sigmoid fits in order to accommodate partial curves.) First, the slopes of the fitted lines were calculated in order to measure the effect of BLA stimulation of the mPFC current input/spike output relationship. Second, the fitted lines were used to calculate the increase in spike rate due to BLA input at low and high mPFC current intensities; this calculation provided a

concrete, quantitative estimate of how BLA input efficacy varied over a physiologically relevant range of mPFC-evoked activity. For each neuron the maximum current eliciting a 0% spike rate for the mPFC input alone was calculated (termed "low current"). Then, the response rate at this low current for the 1ms, 11ms, and 31ms ISI conditions was calculated, yielding values that represented the increase in evoked spiking due to BLA input. Similarly, for each of the three ISI curves, the minimum current eliciting a 100% spike rate was calculated (termed "high current"). The mPFC alone spike rate was calculated at these high currents, and the difference between these values and 100% represented the increase in evoked spike rate due to BLA stimulation. Thus, the estimated increase in spiking due to BLA input was calculated at a low and high current value for each ISI. The effects at low current were then compared to the effects at high current at each ISI.

Neurons were accepted for analysis if all four current/response curves spanned at least a 70% change in response ratio. The linear equations were well-fit to the data, with a mean *r* value of 0.88 ± 0.06, and p-values of less than 0.01 for all fits. Estimated spike rates below 0% or above 100% were rectified to 0 and 100%, respectively.

3.3.3.3 BLA input effect on mPFC-evoked spike latency In order to measure BLA input effects on mPFC-evoked spike latency, the mPFC was stimulated alone or with the BLA in pulse pairs. Unlike the tests meant to measure spike rate changes (3.3.3.1 and 3.3.3.2), for these tests evoked spiking was maintained at ~50% in all conditions by adjusting the mPFC current (BLA current was always subthreshold). Thus, differences in spike latency were not confounded by differences in spike rate at different ISIs. In addition, the mPFC/BLA ISIs (1ms, 11ms, 31ms and "mPFC alone") were tested in blocks of 50-200 trials to provide an accurate estimate of the

spike latency and variance (rather than in rotated trials as above). Finally, in a subset of neurons (n=18/41), the latency of spikes evoked by BLA stimulation alone was also measured.

In addition to the mean change in spike latency for all neurons, the latency changes in individual neurons were also calculated. For each neuron, the "latency shift" was calculated by subtracting the mPFC alone-evoked latency from paired mPFC/BLA-evoked latency. We hypothesized that spikes evoked by mPFC/BLA stimulation at 1ms ISI would occur at latencies that were in between the individual mPFC input latency and BLA input latency. If this were the case, the magnitude and direction of the latency shift at 1ms ISI would be explained by the discrepancy between the two component input latencies. Thus, in the neurons where both mPFC alone and BLA alone spike latency data were available (n=18), an "expected latency shift" was calculated, defined as half the difference between the BLA- and mPFC-evoked spike latencies. This was calculated for the 1ms ISI only, and as such the BLA-evoked latency was adjusted by 1ms to account for the timing difference between the two stimulation pulses; thus, the equation for expected latency shift was

$$\text{Expected latency shift} = \frac{L_{\text{mPFC}} - (L_{\text{BLA}} - 1)}{2},$$

where L_{mPFC} and L_{BLA} are the mean single input spike latencies for mPFC and BLA, respectively. The expected latency shift was compared to the actual latency shift in these 18 neurons, quantifying the influence of the BLA input upon the timing of mPFC/BLA-evoked responses.

3.3.3.4 Effect of subthreshold BLA and subthreshold mPFC stimulation To extend our investigation of synaptic integration and spike timing, we measured spiking evoked by paired mPFC/BLA stimulation using subthreshold current intensities for both inputs. The mPFC-evoked spike latency was measured over 20 trials at ~50% response rate, and the same measurement was

made for BLA-evoked spikes. Then, the BLA and mPFC currents were both adjusted to subthreshold intensities (as defined in 3.3.3) and stimulated concurrently at a 1ms ISI for 20-100 trials (0.3Hz). Subthreshold mPFC current was on average 10% less than the current needed to elicit a 50% response rate during paired pulse stimulation at 1ms ISI (n=14, not shown). The rate and latency of the coincidentally-evoked spikes were measured. For analysis, the mean response rate and latency were calculated. The individual input latencies and paired pulse-evoked latency were used to calculate the "latency shift" and "expected latency shift" for the 1ms ISI as described above (3.3.3.3); these two values were compared to determine the influence of the component latencies on the paired-pulse-evoked spike timing.

3.3.4 Effect of mPFC inactivation on BLA-evoked spiking

In neurons excited by both BLA and mPFC, the BLA was stimulated at a current amplitude evoking a ~50% spike rate for 200 trials (0.3Hz trial rate). Then, tetrodotoxin (TTX, 1μM) or sterile Dulbecco's phosphate buffered saline vehicle was infused into the mPFC (0.5μL over 2-6 minutes via 33g cannula and syringe pump). The post-infusion BLA-evoked spike rate was measured for up to 800 trials (~44.5 minutes). The mean spike rate and latency for the 200 pre-infusion trials was compared to the final 200 post-infusion trials (taking place at least 20 minutes post-infusion).

3.3.5 Analysis

Statistical comparisons were performed using paired t-tests (within neuron) or repeated measure ANOVA with Tukey's Honest Significant Difference post-hoc testing (Norman and Streiner 2000). For non-normally distributed data, paired Wilcoxon Rank Sum tests were performed, with multiple significant p-values corrected with Holm's stepwise Bonferroni method. Thus, unless otherwise stated, all statistical comparisons are within-neuron, and all p-values are corrected or are derived from group-level post-hoc tests. Mean values are expressed as "mean ± standard error of the mean", and all error bars on graphs show the standard error of the mean.

For the experiments in which evoked spike latencies were recorded for BLA stimulation alone, mPFC stimulation alone, and paired pulse BLA/mPFC stimulation (3.3.3.3 and 3.3.3.4), we performed multiple linear regression analyses relating the paired pulse spike latency to the individual input spike latencies. Thus, the model approximation was:

$$L_{MB} \sim L_{mPFC} + L_{BLA}$$

Where L_{MB} is the mean latency of paired pulse evoked spikes. The effect of the component latencies on the paired pulse latencies were determined using marginal t-tests on the partial slopes (regression coefficients) for each input. In addition, we created reduced linear models,

$$L_{MB} \sim L_{mPFC}$$

and

$$L_{MB} \sim L_{BLA},$$

and compared the adjusted coefficient of determination (R^2) from these models to the complete model above. The model that produced the greatest adjusted R^2 was considered to provide the more complete and efficient fit of the data (Neter et al. 1990). Although there was a positive

correlation between and L_{mPFC} and L_{BLA} in the data used for the model in Table 3.1, the effect of this co-linearity was negligible (variance inflation factor ~2.3 (Neter et al. 1990)), and analysis of a subset of the data exhibiting less co-linearity (variance inflation factor ~1.2) produced the same results (not shown).

3.3.6 Histology

At the end of the experiment, the stimulating electrode placements were marked by electrolytic lesion (100μA for 10 seconds). The final position of the recording electrode was marked by iontophoretic ejection of the Pontamine Sky Blue dye (-20μA for 60 minutes). The rats were decapitated, and their brains were fixed in 8% paraformaldehyde with 1% potassium ferricyanide. After 48 hours, the brains were transferred to a cryoprotectant solution of 25% sucrose. They were sliced on a freezing microtome and mounted onto slides for subsequent Nissl staining using standard histological procedures.

The location of the recording and stimulating electrodes was determined using the atlases of Paxinos and Watson (1998; 2005). Neuron locations were reconstructed from the location of the dye deposit and electrode positions noted in the experimental log. Neurons were recorded in both the shell and core subregions of the NAcc. Only neurons that were clearly contained within the core or shell were assigned to a subregion; if a neuron's actual or reconstructed location was within 0.1mm of the core/shell border, it was not assigned to either subregion. Of 210 neurons, 197 were plotted onto atlas sections (Figure 3.1A); the remaining 13 were determined to be in the NAcc, but could not be precisely plotted due to section damage or inadequate staining.

3.4 RESULTS

3.4.1 Properties of BLA- and mPFC-evoked spiking

Extracellular activity was recorded from NAcc neurons in anesthetized rats. Of 210 neurons recorded, 115 were confirmed to be in the medial shell, and 38 were confirmed to be in the medial core (Figure 3.1A). The remaining cells were located too close to the core/shell border to confirm their location. Unless otherwise reported, there were no significant differences between core and shell neuronal responses, or there were too few core neurons to perform a statistical comparison; thus, core and shell responses were grouped together.

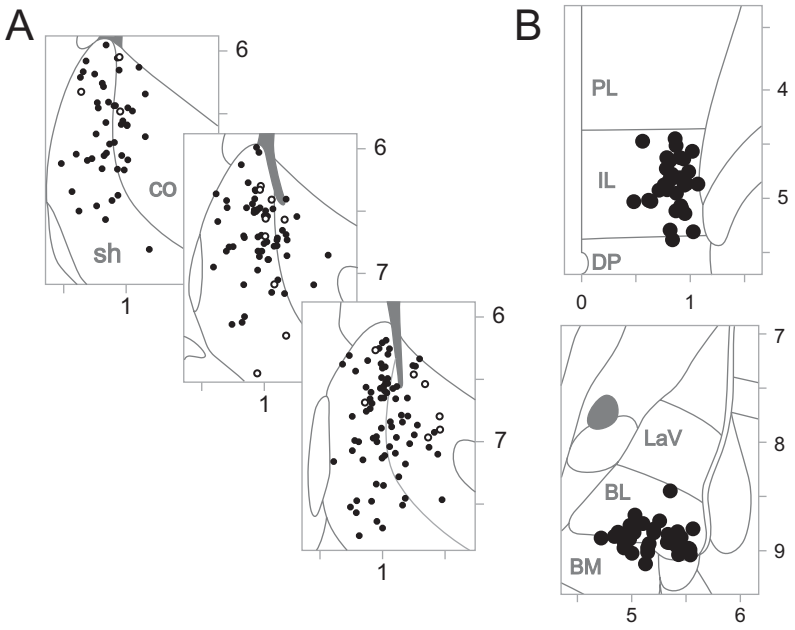

Figure 3.1 The locations of recorded neurons and stimulating electrodes. **A** Neurons were recorded from the medial shell (sh) and medial core (co) of the NAcc. The locations of 197/210 neurons recorded in this study are shown in three representative atlas sections (Paxinos and Watson 2005). Filled dots represent neurons receiving both BLA and mPFC inputs, and empty circles represent neurons receiving input only from mPFC. **B** The location of 33 representative stimulating electrode placements in the mPFC (top) and BLA (bottom). The electrodes leads were exposed for ~0.8mm dorsal from the tip; thus, for dorsal IL placements, current spread to PL was likely, and for BM placements, current spread to BL was likely. Abbreviations: prelimbic cortex (PL), infralimbic cortex (IL), dorsal peduncular cortex (DP); lateral amygdala subnucleus (LaV), basolateral amygdala subnucleus (BL), basomedial amygdala subnucleus (BM). The numbers and tick marks indicate atlas coordinates in mm.

We selected neurons that received excitatory input from both mPFC and BLA (Figure 3.2). The mean latency of mPFC-evoked spikes was 13.7 ± 0.3ms (n=69 from 41 rats) and of BLA-evoked spikes was 14.3 ± 0.4 ms (n=69, 45 rats)(Figure 3.3). For 46 neurons in which both were measured, BLA and mPFC input latencies differed on average by 0.8 ± 0.5ms ($p<0.08$), and exhibited a positive correlation ($r = 0.421$, $p<0.004$). The distributions of these orthodromically evoked responses were consistent with conduction times for BLA-to-NAcc and mPFC-to-NAcc projecting neurons, which were determined by antidromic activation (Figure 3.3). In the neurons where latency variance was also measured (n=62/69 for BLA, n=62/69 for mPFC), variance was typically less than 5ms (Figure 3.4A1); however for 10/62 mPFC inputs and 18/62 BLA inputs, the variance was greater. These high variance responses appeared as widely spread evoked action potential latencies (Figure 3.4A2) or in some neurons as a multimodal latency distribution (Figure 3.4A3). The variance of both BLA and mPFC inputs was measured in 39 neurons (22 rats). These cells exhibited high and low latency variance spiking; however there was no correlation between the input variances in individual neurons (Figure 3.4B). BLA-evoked spiking exhibited greater variance than mPFC-evoked spiking when measured in all 39 neurons (difference 1.9 ± 1.2ms, $p<0.04$, paired Wilcoxon Rank Sum test), and there was a trend towards a greater BLA-evoked variance among the 26/39 neurons with low variance responses (<5ms) to both inputs (0.6 ± 0.3ms, $p<0.053$)(Figure 3.4B).

Mean mPFC-evoked spike latencies were faster for shell neurons than core neurons: for 33 shell neurons, 12.9 ± 0.4ms; for 11 core neurons, 14.8 ± 0.7ms ($p<0.031$ by two sample t-test). BLA-evoked responses also exhibited faster latencies in shell neurons (shell 13.4 ± 0.5ms, n=34; core 16.0 ± 0.8ms, n=13, $p<0.018$).

Figure 3.2 Experimental schematic and examples of extracellular action potentials. A Stimulating electrodes were placed in BLA and mPFC, and extracellular signals were recorded from neurons in the NAcc. **B** Neurons excited by BLA and mPFC were identified by action potentials following stimulation of these regions. The traces show five examples of action potentials (thin arrows) evoked by stimulation of mPFC (left) or BLA (right) in the same NAcc neuron. The large arrow heads indicate the stimulation artifacts, which in this and following figures have been cropped for clarity. Scale bar: 5ms.

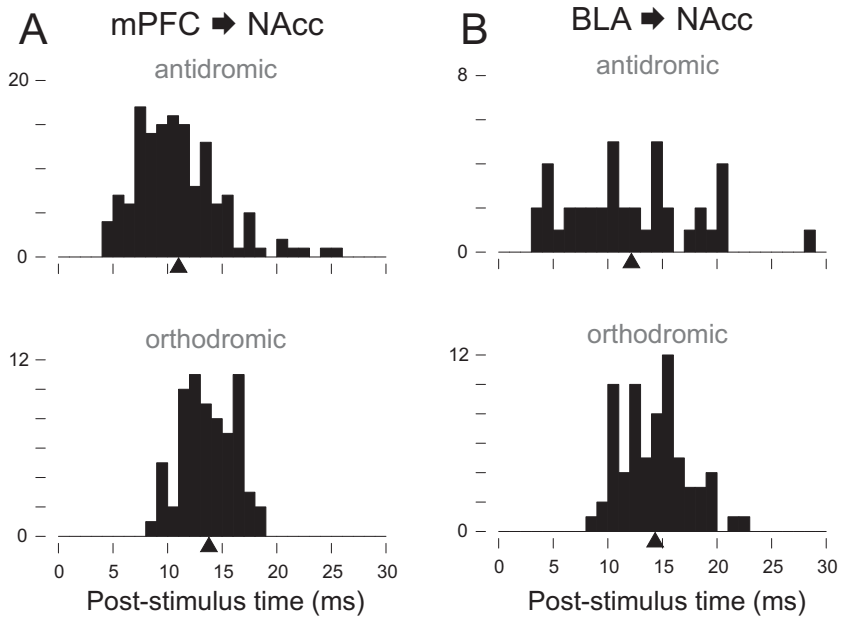

Figure 3.3 Spikes evoked by stimulation of BLA and mPFC are consistent with orthodromic, monosynaptic transmission. The conduction times of neurons projecting from mPFC to NAcc (**A**, top) and BLA to NAcc (**B**, top) were determined by antidromic stimulation of NAcc and recordings from mPFC and BLA; mPFC-to-NAcc antidromic mean 11.0 ± 0.3ms, n=141 neurons; BLA-to-NAcc antidromic mean 12.1 ± 0.9, n=41. Orthodromically-evoked spike latencies in the NAcc were measured in response to mPFC stimulation (**A**, bottom), and BLA stimulation (**B**, bottom) (see text for orthodromic means). The black arrow heads indicate the mean value for each histogram. The mean orthodromic latencies were significantly longer than the mean antidromic conduction times: for mPFC-to-NAcc, orthodromic was 2.7 ± 0.3ms longer ($p<10^{-8}$); for BLA-to-NAcc, 2.2 ± 0.4ms longer ($p<0.03$) by two-sample t-test. This small difference is consistent with the synaptic delay due to orthodromic transmission.

3.4.2 BLA input increased the mPFC-evoked spike rate

The convergence of excitatory BLA and mPFC responses in single NAcc neurons suggests that simultaneous activation of these inputs will facilitate spike firing. Therefore, in neurons receiving both mPFC and BLA inputs, the effect of BLA stimulation on mPFC-evoked spiking was measured. The mPFC was stimulated at threshold current intensities (~50% evoked spike rate), and the BLA was stimulated at subthreshold current (no evoked spiking) at different inter-stimulus intervals relative to the mPFC pulse (Figure 3.5A,B). In an initial sample of 18

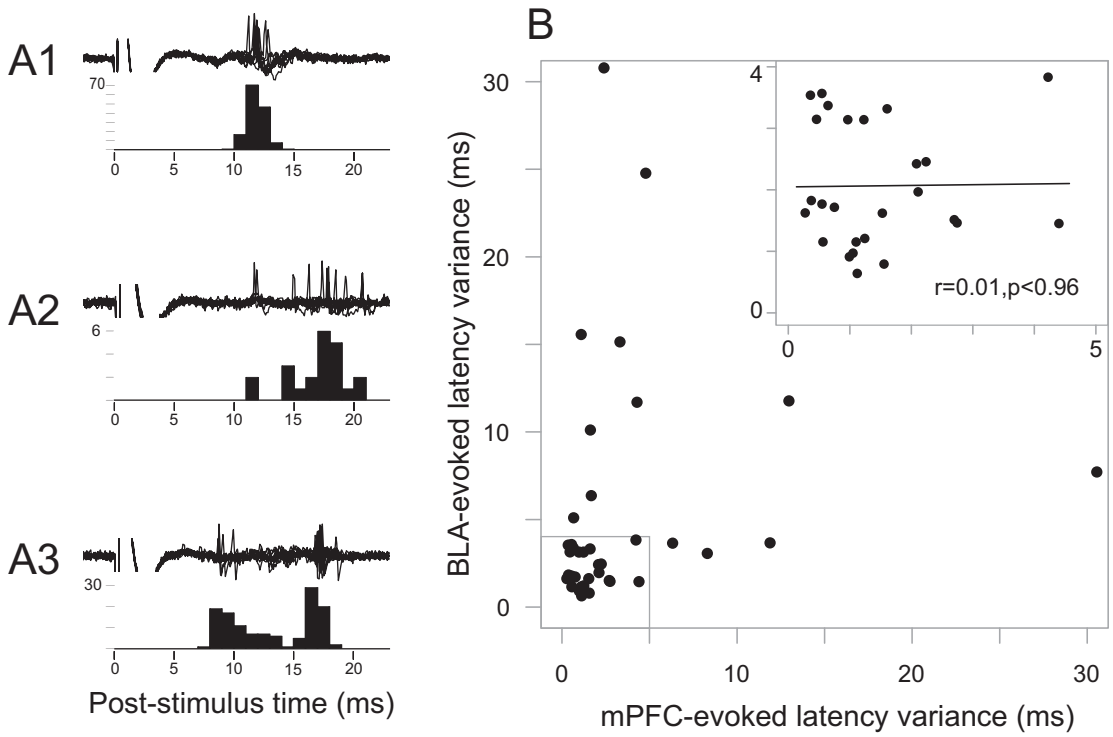

Figure 3.4 Evoked spikes exhibited variable latencies. The latency variance of evoked spikes was typically less than 5ms (**A1**). However, a minority of neurons exhibited highly variable spike latencies; these neurons fired over a wide range of latencies (**A2**), and approximately half of these high variance neurons exhibited a multimodal latency distribution (**A3**). The three examples in **A** show mPFC-evoked spikes in three different neurons, each with 10 overlaid traces and PSTH for 50-200 trials. **B** The scatter plot shows the latency variances for the BLA- and mPFC-evoked spikes in 39 neurons for which both were measured; the inset shows those neurons with input latency variances less than 5ms (n=26). There was no relationship between the variances of the BLA and mPFC input latencies (inset, fit line and statistics).

neurons (15 rats), evoked spiking was measured using mPFC/BLA ISIs in increments of 5-10ms. The mPFC-evoked spike rate was increased when BLA pulses were 3ms prior to or 2ms after mPFC pulses ($p<0.01$) (Figure 3.5C); evoked spiking exhibited smaller increases at longer ISIs, and was indistinguishable from baseline when BLA preceded mPFC at ISIs of 18ms or greater (ANOVA, effect of ISI, $F(4,64) = 4.47$, $p<0.003$) (Figure 3.5C). In a sample of 54 neurons (37 rats), mPFC/BLA paired pulses were tested at 1ms, 11ms, 21ms, and 31 ms ISIs (BLA pulse prior to mPFC). BLA input increased the mPFC-evoked spike rate at both 1ms and 11ms ISIs by $32.3 \pm 3.6\%$ ($p<10^{-7}$) and $16.7 \pm 4.4\%$ ($p<0.001$), respectively; the increase at 1ms was greater than at 11ms ($p<0.001$) (effect of ISI, $F(5,265) = 20.7$, $p<10^{-15}$) (Figure 3.5D). The symmetry of this mPFC/BLA interaction was tested in 21 additional neurons (14 rats), where *sub*threshold mPFC pulses were paired with threshold (~50%) stimulation of BLA (mPFC prior to BLA). The rate of BLA-evoked spiking was increased at 1ms ISI by $45.3 \pm 4.8\%$ ($p<10^{-8}$), but not at 11ms ($12.4 \pm 7.4\%$, $p<0.30$) (effect of ISI, $F(5,100) = 17.4$, $p<10^{-11}$)(Figure 3.5D). Neurons lacking spike-evoking BLA input may nonetheless receive excitatory BLA synaptic activity (O'Donnell and Grace 1995) that can modify mPFC-evoked spiking. However, in 19 neurons identified as receiving mPFC input but not BLA input (16 rats), BLA stimulation (400μA) did not facilitate mPFC-evoked spiking at any ISI (effect of ISI $F(5,90) = 2.5$, $p<0.04$) (Figure 3.5D). All significance values above were derived from ANOVA and group-wise post-hoc tests.

To test whether dopamine or NMDA-dependent mechanisms contributed to the BLA facilitation of mPFC-evoked spiking, these experiments were repeated in a separate population of neurons after systemic administration of dopamine D1, D2, or NMDA receptor blocking drugs. Drug administration had no effect on the facilitatory influence of BLA input (Figure 3.6).

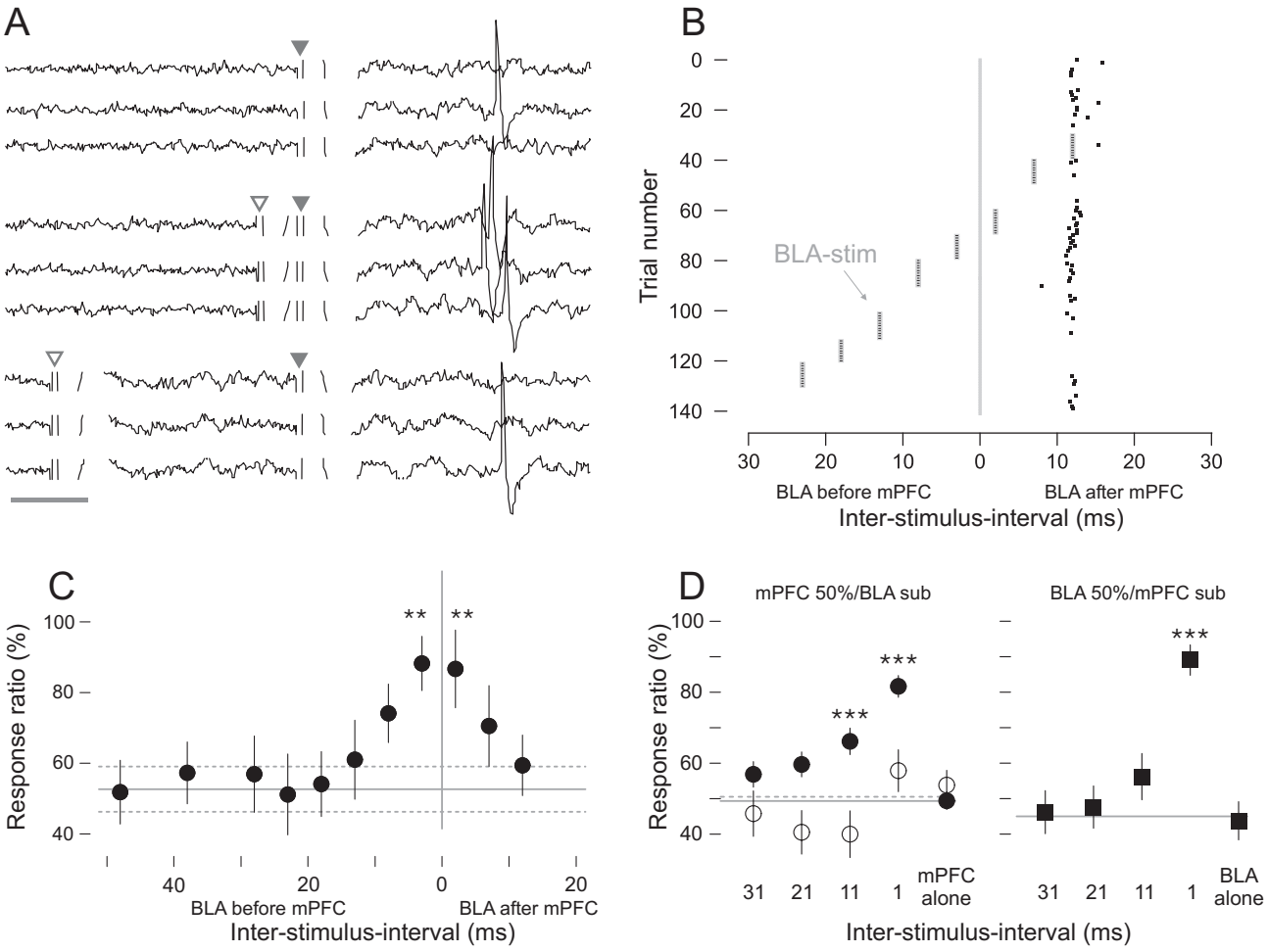

Figure 3.5 Subthreshold BLA stimulation increased mPFC-evoked spiking at short inter-stimulus intervals. A Nine traces from a single neuron; the top three show evoked responses (1 spike) to mPFC stimulation (filled arrowheads); the middle show evoked responses (3 spikes) to mPFC stimulation with subthreshold BLA stimulation (open arrowheads) at a 3ms ISI; the bottom three show mPFC with BLA at 18ms ISI (1 evoked spike). Scale bar: 5ms. **B** A raster plot showing a sequence of mPFC and BLA stimulation at different ISIs: mPFC stimulation occurred at t=0 in each trial, BLA stimulation (stippled bars) occurred at variable ISIs, and spikes are shown as black dots. mPFC stimulation alone produced a ~50% response (trials 1-30), and BLA stimulation alone did not evoke spikes. At short ISIs (trials 61-80), the response rate was greater compared to mPFC stimulation alone or mPFC with BLA at longer ISIs. **C** In a sample of 18 neurons where mPFC/BLA ISIs were varied in increments of 5-10ms, mPFC-evoked spike rate were greatest at near-coincident ISIs. ** indicates significant difference from baseline. The gray lines shows the mean and SEM of the baseline mPFC-evoked spike rate measured before BLA stimulation. **D** In a sample of 54 neurons (left, filled circles, solid baseline), BLA stimulation increased mPFC-evoked spiking at 1ms and 11ms ISIs (BLA prior to mPFC). There was no effect on mPFC stimulation alone, presented in interleaved trials. BLA stimulation had no effect in 19 neurons that received only mPFC input (left, empty circles, dotted baseline). In 21 neurons, the reciprocal experiment was performed (right, black squares): subthreshold mPFC stimulation increased BLA-evoked spiking at 1ms ISIs. *** indicates significant difference from both baseline and "mPFC alone" or "BLA alone" as appropriate, by ANOVA and post-hoc tests.

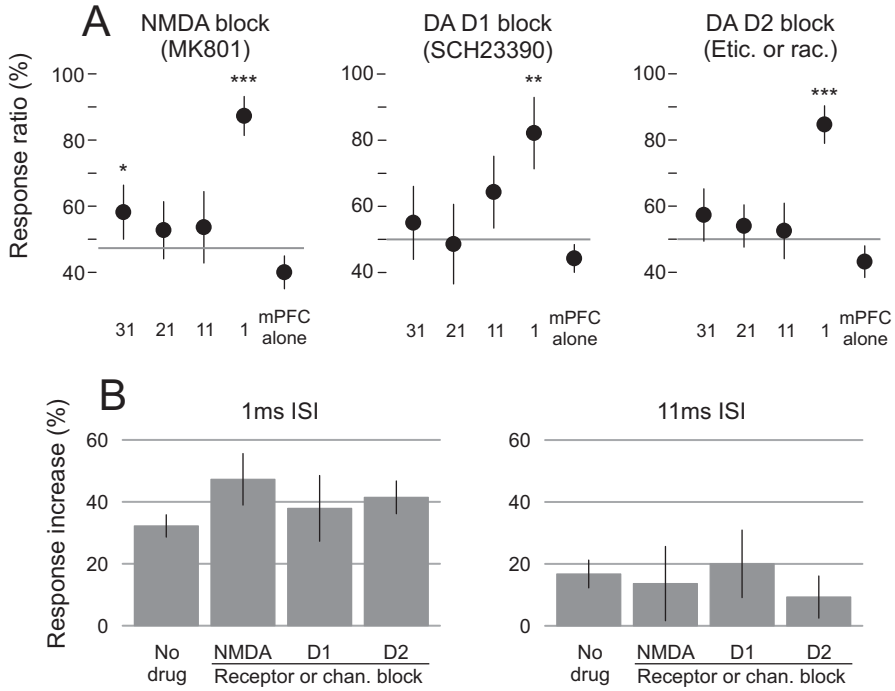

Figure 3.6 NMDA channel or dopamine receptor blockade did not change the BLA-mediated facilitation of mPFC-evoked spiking. A Subthreshold BLA stimulation was paired with threshold mPFC stimulation at different ISIs (BLA prior to mPFC, as in Figure 3.5D) after systemic administration of the NMDA blocker MK801 (n=11, 7 rats), the D1 antagonist SCH23390 (n=14, 12 rats) or the D2 antagonists eticlopride or raclopride (n=15, 13 rats). See 3.3.3.1 for dose information. *, **, and *** indicate significant difference from "mPFC alone" within drug treatments. **B** The increase in evoked spiking compared to "mPFC alone" at 1ms (left) and 11ms ISIs (right). The "No drug" data is from Figure 3.5D; NMDA, D1 and D2 data are from part **A** of this figure. There were no significant differences between "No drug" and any of the drug conditions for either 1ms or 11ms ISI responses.

3.4.3 BLA facilitation of mPFC-evoked spiking depended on the mPFC-evoked spike rate

The summation of subthreshold BLA- and mPFC-evoked EPSPs has been shown to depend on the amplitude of the evoked potentials (Goto and O'Donnell 2002). Therefore, we tested whether the BLA facilitation of mPFC-evoked spiking was dependent on the evoked spike rate. The BLA and mPFC were stimulated with paired pulses at different ISIs. The BLA stimulation current amplitude was maintained at subthreshold intensities (similar to the experiment above),

while the mPFC current was varied from 0 to 100% response intensities in small increments. Thus for each neuron, the mPFC input current vs. spiking response curve was constructed for mPFC stimulation alone, and for mPFC preceded by a BLA pulse at 1ms, 11ms, and 31ms ISIs (Figure 3.7A). The current/response curves were fit to linear equations, and these fit lines were used to compare the responses at different current amplitudes and ISIs (Figure 3.7B).

In 19 neurons receiving BLA and mPFC inputs (15 rats), the slope of the current/response curve for mPFC/BLA at 1ms ISI was less than the slope for mPFC alone by 12 ± 5% (spike rate) per 100μA; and the slope at the 11ms ISI was less than the slope for mPFC alone by 10 ± 5% per 100μA ($p<0.041$ for both ISIs) (Figure 3.7C, left). Next, the linear fit equations were used to quantify the difference in BLA input efficacy at high and low mPFC currents. The spike rate increases due to concurrent BLA stimulation were calculated for each ISI at two different mPFC current intensities: low current (the 0% response for mPFC alone) and high current (the 100% response for paired mPFC/BLA input) (see 3.3.3.2, Figure 3.7B). For mPFC/BLA at 1ms compared to mPFC alone, the spike rate increase at low current was 14.1 ± 5.1% greater than at high current ($p<0.025$); a similar difference was evident for mPFC/BLA at 11ms compared to mPFC alone (low current 9.5 ± 4.2% greater than high current, $p<0.040$). In contrast, there was no significant difference between the effects of low and high current for mPFC/BLA at 31ms (-6.6 ± 3.8, $p<0.08$) (Figure 3.7C, right). These effects were similar in the subset of neurons for which the latency variance of both inputs was less than 5ms (n=13), except that the difference between low and high currents for mPFC/BLA at 11ms was not statistically significant (not shown). All comparisons above were performed with paired Wilcoxon rank sum tests, and multiple significant p-values were corrected within groups.

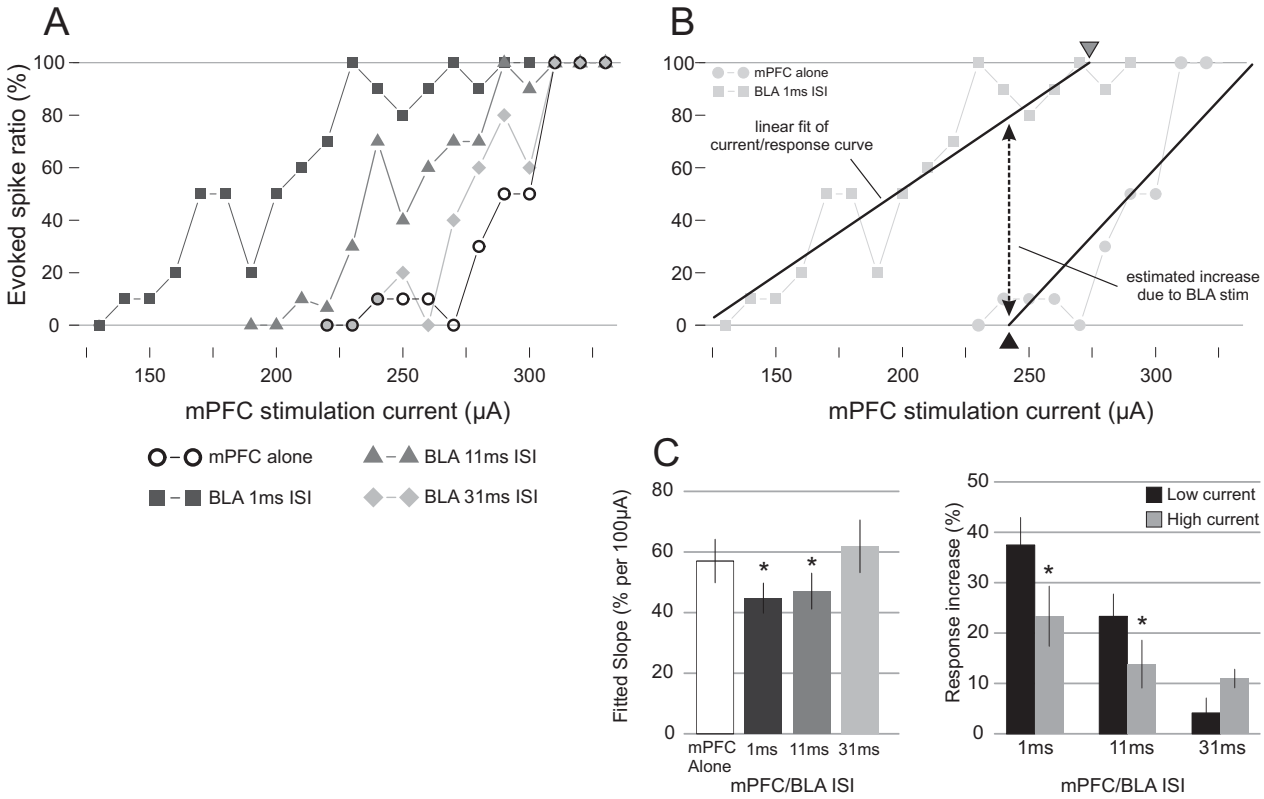

Figure 3.7 BLA-mediated facilitation of mPFC-evoked spiking was greatest for subthreshold mPFC input. A The mPFC-evoked spike rate was measured at a range of current intensities; mPFC was stimulated alone or with subthreshold BLA pulses at 1ms, 11ms, and 31ms ISIs. The resulting current/response curves are shown for a single neuron. **B** The current/response curves for mPFC with BLA were compared to the curve for mPFC alone. The linear portions of the curves were used to calculate the slopes of the current/response relationship in each condition (solid fit lines). From these fit lines, the effect of BLA stimulation at a given ISI (dotted double arrow) was estimated at two current intensities: a low current value (black triangle, bottom), and a high current value (gray triangle, top). See 3.3.3.2 for details. **C** The slope of the current/response curve was reduced by BLA stimulation at 1ms and 11ms ISIs (left, * indicates significant difference from mPFC alone). At these two ISIs, the estimated effect of BLA stimulation (spike rate increase due to BLA) was greater at low current than at high current (right, * indicates significant difference from "low current" within ISI). There was no change in slope or effect of BLA stimulation at 31ms ISI.

3.4.4 BLA input shifted the latency of mPFC-evoked spikes

In addition to the effects on spike rate, we also tested the effects of BLA input on mPFC-evoked spike timing. The latency and latency variance of spikes evoked by mPFC alone compared to the spikes evoked by BLA and mPFC paired pulses at different ISIs. The evoked spike rate was maintained at ~50% in all conditions (by adjusting the mPFC current) so that changes in spike

latency would not be confounded by changes in spike rate. 18 neurons were tested at 1ms, 11ms, and 31ms ISIs (8 rats); an additional 23 neurons were tested at 1ms ISI only (12 rats).

Paired pulse mPFC/BLA stimulation at 1ms ISI evoked spikes with slightly but consistently shorter latencies than did mPFC stimulation alone (-0.6 ± 0.2ms, n=41, $p<0.01$ by t-test). A similar latency decrease was observed at the 11ms ISI (-1.2 ± 0.4ms, n=18, $p<0.002$ by ANOVA; effect of ISI, $F(3,51) = 9.2$, $p<10^{-4}$) (Figure 3.8A). The latency decrease with mPFC/BLA at 11ms ISI was accompanied by a nearly twofold increase in spike latency variance (3.0 ± 1.3ms, n=18, $p<0.018$ by Wilcoxon Rank Sum test) (Figure 3.8B). There was no change in latency variance with mPFC/BLA at 1ms or 31ms. These results were the same for neurons with low latency variance (<5ms) in the mPFC input (n=33 for 1ms, n=15 for 11ms and 31ms ISI) (Figure 3.8B). BLA input had no effect on the binomial tendency (runs statistic) of mPFC-evoked spiking at any ISI (not shown).

The latency changes due to BLA input were also examined at the single neuron level. Although the average latency decreases at 1ms and 11ms ISIs were small, some single neurons exhibited large changes in spike latency due to BLA input ("latency shifts") that were dependent on the spike latency evoked by mPFC input alone. Neurons with long-latency mPFC alone-evoked spiking exhibited shorter latencies during paired pulse BLA/mPFC stimulation at 1ms (Figure 3.9A1), and a few neurons with short mPFC alone-evoked spike latencies exhibited longer latencies with concurrent BLA input (Figure 3.9A2). Overall, there was a positive correlation between latency shift and mPFC alone-evoked spike latency ($r = 0.426$, n=41, $p<0.006$); this correlation was particularly strong among neurons with mPFC input latency variances less than 5ms ($r = 0.695$, $p<10^{-5}$, n=33) (Figure 3.9B). Weaker correlations were evident for responses to BLA/mPFC stimulation at 11ms and 31ms ISIs (Figure 3.9C,D).

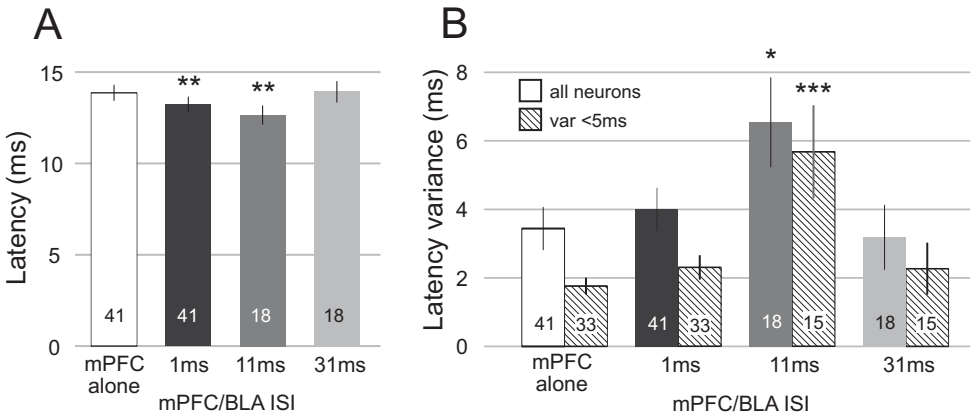

Figure 3.8 BLA input altered the latency and variance of mPFC evoked spikes. 41 neurons were tested at 1ms ISI, 18 were tested at 1ms, 11ms, and 31ms ISIs (BLA prior to mPFC). **A** mPFC-evoked spike latency was slightly, but significantly reduced by subthreshold BLA stimulation at 1ms and 11ms (** indicates significant difference from mPFC alone). Differences were assessed with paired t-test (mPFC alone vs. 1ms) or ANOVA and post-hoc tests (mPFC alone vs. 11ms). **B** The latency variance was unchanged by 1ms BLA stimulation (n=41), but was increased at 11ms (n=18). The data for all neurons are shown in the solid bar of the pair, and the data from only low latency variance neurons (<5ms, n=33 and n=15) are shown in the hatched bar. * and *** indicate significant difference from "mPFC alone" for all neurons and low latency variance neurons, respectively, by paired Wilcoxon Rank Sum tests. The numbers within the bars indicate the number of neurons.

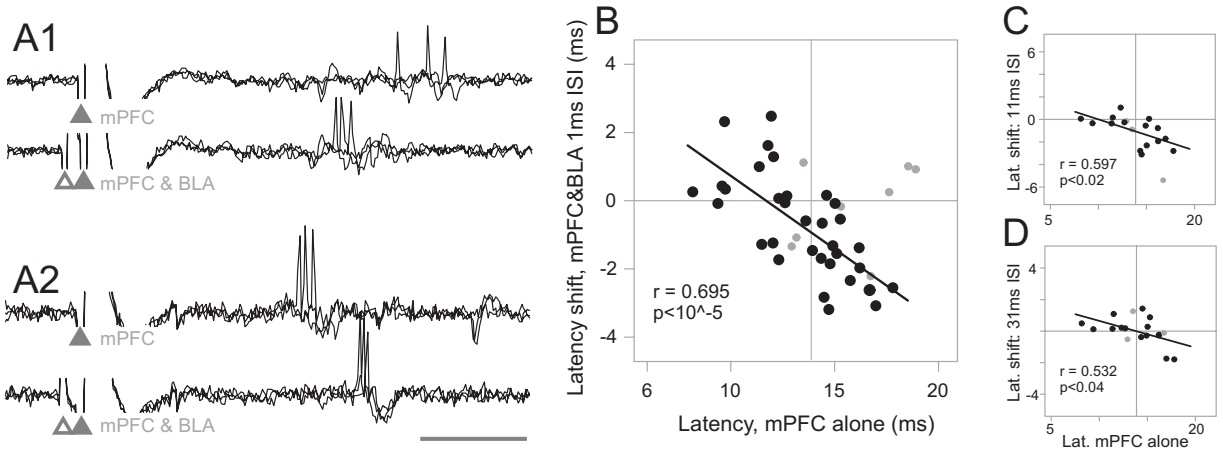

Figure 3.9 A change in the spike latency occurring with BLA stimulation was correlated with the spike latency evoked by mPFC input alone. A1 Long latency responses were typically shortened by BLA input. The latency of mPFC evoked spiking for this neuron (top, three overlaid traces) was reduced when subthreshold BLA stimulation was applied at 1ms (bottom, three overlaid traces). **A2** In a few neurons, short spike latencies were lengthened by concurrent BLA input. In this neuron, the mPFC evoked spike latency (top, three traces) was increased during mPFC/BLA stimulation at 1ms ISI (bottom, three traces). MPFC and BLA stimulation artifacts are at the solid and empty arrow heads, respectively. Scale bar: 5ms. **B** The change in spike latency during 1ms mPFC/BLA stimulation (y-axis) was correlated with the latency of spikes evoked mPFC stimulation alone (x-axis). The black dots correspond to neurons with low latency variance (n=33/41); the gray dots show neurons with high latency variance (n=8/41). The fit line and statistics are for the low variance neurons only. A weaker correlation between latency change and mPFC input latency was found at 11ms (**C**) and 31ms ISIs (**D**) (n=15/18 with low latency variance). The axes use the same units as **B**.

We hypothesized that the magnitude and direction of the latency shifts could be explained by the individual BLA-evoked spike latency. Thus, in a subset of neurons (n=18), the latency of BLA-evoked spiking was measured in addition to the mPFC-evoked and paired-pulse evoked spike latencies. The latency shift due to mPFC/BLA at 1ms was compared to the timing discrepancy between the BLA and mPFC inputs ("expected latency shift", see 3.3.3.3). The observed latency shift due to paired pulse stimulation at 1ms was not correlated with the expected latency shift ($r = 0.387$, $p < 0.11$ for all neurons; $r = 0.280$ $p<0.31$ for 15/18 low latency variance neurons) (Figure 3.10).

This result suggested that the BLA-evoked spike latency had little influence on the paired pulse-evoked latency. To explicitly test this, a multiple linear regression was performed that related the paired pulse evoked latency at 1ms ISI (dependent variable) to the individual BLA- and mPFC-evoked latencies for each neuron (independent variables) (see 3.3.5). In 18 neurons, mPFC input latency but not BLA input latency contributed significantly to the regression (Table

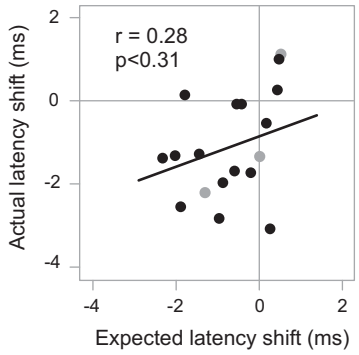

Figure 3.10 The expected latency shift did not predict the actual change in latency. The discrepancy between the BLA and mPFC input latencies ("expected latency shift", see 3.3.3.3) was compared to the change in latency during paired pulse mPFC/BLA stimulation at 1ms ISI. While 1ms BLA stimulation changed the mPFC-evoked response latency (Figure 3.9), there was no correlation between this shift, and the expected latency shift. Black dots show low latency variance neurons (n=15/18), and gray dots show high variance neurons (n=3/18). Fit line and statistics refer to the low variance neurons.

3.1). Furthermore, exploratory step-wise modeling revealed that a model with mPFC input latency as the sole independent variable produced a better fit (greater adjusted R^2) than the full model containing both input latencies (Table 3.1). Thus, the BLA input latency contributed negligibly to the model fit.

Table 3.1: Multiple linear regression relating paired pulse-evoked latency to individual BLA and mPFC input latencies when mPFC current is tuned to evoke a 50% response rate (see 3.3.5)

Full Model	Adjusted R^2	Regressor	Slope	Std. err.	T	P
$L_{MB} \sim L_{mPFC} + L_{BLA}$	0.758	L_{mPFC}	0.625	0.141	4.44	**0.0005**
		L_{BLA}	0.106	0.147	0.72	**0.4835**
Reduced models						
$L_{MB} \sim L_{mPFC}$	**0.766**	L_{mPFC}	0.700	0.093	7.52	$1x10^{-06}$
$L_{MB} \sim L_{BLA}$	0.476	L_{BLA}	0.589	0.145	4.06	0.0009

3.4.5 Subthreshold paired stimulation evoked spikes at latencies that reflected both BLA and mPFC inputs

Activation of two subthreshold excitatory inputs can elicit suprathreshold spiking responses in NAcc neurons (Finch 1996); however, the response rate and latencies of jointly-evoked spikes have not been characterized. Therefore, we measured the rate and timing of spikes evoked by paired mPFC/BLA pulses at 1ms ISI using subthreshold current intensities for both inputs (Figure 3.11A). The spike rate evoked by paired subthreshold stimulation was variable across neurons (range 6.7 to 90%) and averaged 37.1 ± 3.8% (n=38, 28 rats). For 32/38 neurons, the individual BLA input and mPFC input latencies were measured in addition to the paired pulse spike latency. The mean of the BLA and mPFC input latencies was highly correlated with the

latency of the paired pulse evoked spikes ($r = 0.764$, $p<10^{-6}$) (Figure 3.11C). In addition, the expected shift in latency was correlated with the actual shift in latency due to paired mPFC/BLA stimulation ($r = 0.569$ $p<0.001$). Three neurons exhibited large expected and actual latency shifts (>5ms); excluding their influence ($r = 0.527$, $p<0.004$; Figure 3.11D). Thus, when both current amplitudes were subthreshold, the timing difference between mPFC and BLA inputs predicted the change in latency due to paired pulse stimulation; this was substantially different

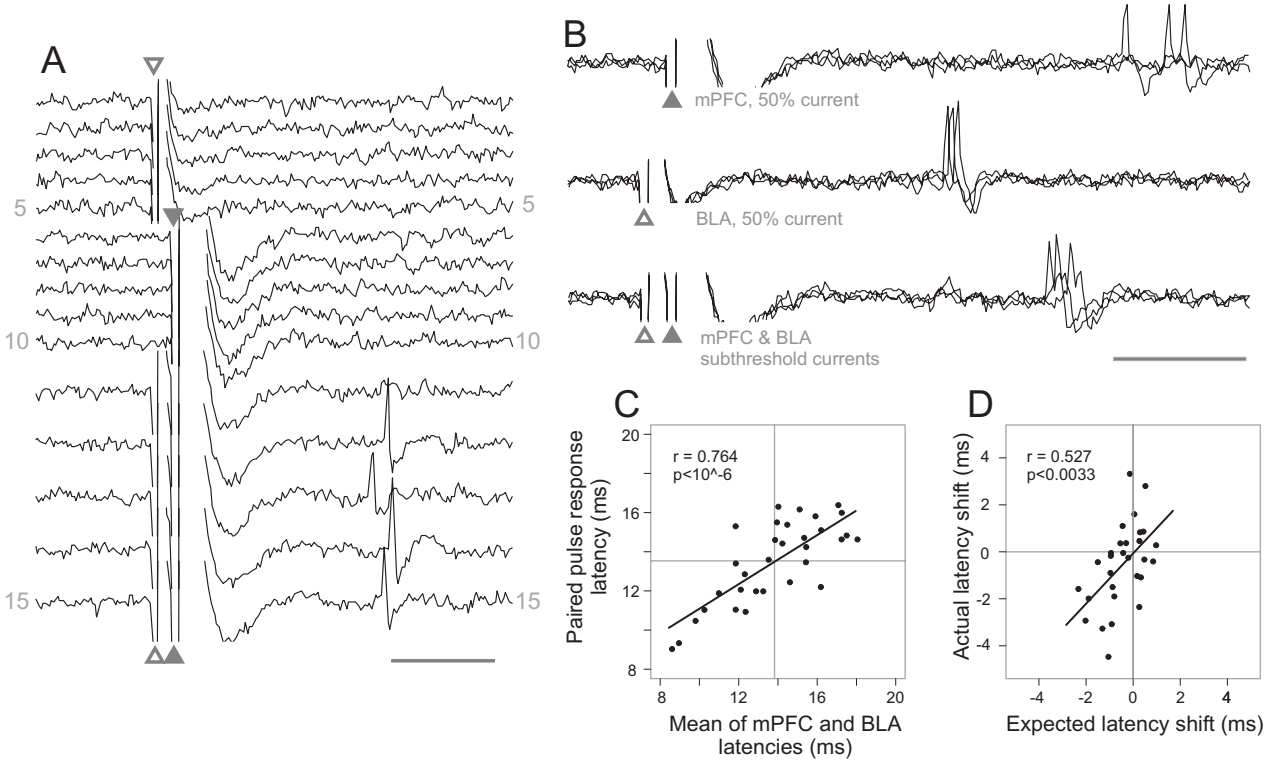

Figure 3.11 Subthreshold stimulation of BLA and mPFC evoked spikes at latencies that were dependent on the latencies of both inputs. **A** Traces from a single neuron where subthreshold, coincident stimulation of BLA and mPFC evoked spikes. Stimulation of the BLA (traces 1-5) or mPFC (6-10) did not evoke firing, but both inputs stimulated at 1ms ISI (11-15) evoked spikes. **B** When stimulated at threshold for each input, this neuron exhibited mPFC-evoked spikes at mean latency of 16.2ms (top, three traces), and BLA-evoked spikes at 12.5ms (middle, three traces). When both inputs were stimulated at subthreshold currents at 1ms ISIs, the resulting spikes were at an intermediate latency of 14.6ms (bottom, three traces). Scale bar: 5ms. **C** The latency of coincidentally-evoked spikes was correlated with the mean of the individual BLA and mPFC input latencies (fit line and statistics). **D** The expected latency shift (based on the mPFC/BLA input latency difference) was correlated with the actual latency shift (fit lines, statistics, excluding three outlying points not shown). Thus when both BLA and mPFC inputs were at subthreshold intensities, the mPFC/BLA input latency difference predicted the change in latency due to coincident stimulation. This was not observed when mPFC current was tuned to evoke a 50% response rate (Figure 3.10).

than the relationship observed when mPFC current was tuned to a 50% response (Figure 3.10). This suggested that both BLA and mPFC inputs influence the latency of paired pulse-evoked spikes. To explicitly test this, the latency of the jointly evoked spikes was fitted to the latencies of the individual mPFC- and BLA-evoked inputs in a multiple linear regression model. Both input latencies contributed significantly to the model (Table 3.2). Furthermore, step-wise exploratory modeling showed that the best fit was achieved when both mPFC and BLA input latencies were used as regressors, suggesting that both inputs contributed to the model fit (Table 3.2). Thus, both inputs predicted the paired pulse response timing when they were stimulated at subthreshold currents.

Table 3.2: Multiple linear regression relating paired pulse-evoked latency to the component input latencies when using subthreshold stimulation of both inputs.

Full Model	Adjusted R^2	Regressor	Slope	Std. err.	T	P
$L_{MB} \sim L_{mPFC} + L_{BLA}$	**0.576**	L_{mPFC}	0.420	0.102	4.12	**0.0003**
		L_{BLA}	0.232	0.084	2.78	**0.0095**
Reduced models						
$L_{MB} \sim L_{mPFC}$	0.481	L_{mPFC}	0.548	0.101	5.45	$7x10^{-6}$
$L_{MB} \sim L_{BLA}$	0.350	L_{BLA}	0.389	0.092	4.21	0.0002

3.4.6 TTX infusion in mPFC did not change BLA-evoked responses

Stimulation of BLA excites mPFC neurons projecting to NAcc (Chapter 2); thus, the mPFC may contribute to BLA-evoked spiking in NAcc neurons. To test this contribution, recordings were made from NAcc neurons receiving BLA and mPFC inputs, and BLA-evoked spiking was measured before and after inactivation of mPFC with TTX. In 8/8 neurons tested (8 rats), the

BLA-evoked spike rate decreased after mPFC TTX infusion (mean decrease -11.0 ± 3.0%). However, similar effects were evident after infusion of vehicle (n=9 neurons, 9 rats), where the BLA-evoked spike rate decreased by 7.0 ± 4.5%. The decrease due to TTX was not larger than the decrease due to vehicle infusion ($p<0.82$, Wilcoxon rank sum test). Thus, while TTX infusion in the mPFC decreased BLA-evoked spiking, these effects may be attributable to the infusion, rather than the specific effects of the drug. Neither TTX infusion nor vehicle had an effect on latency, latency variance, or binomial tendency (runs statistic) of the BLA-evoked firing (not shown).

3.5 DISCUSSION

The convergence of limbic and cortical afferents is a key feature of the NAcc that distinguishes it from other striatal regions. Synaptic input summation within single NAcc medium spiny neurons is thought to be a substrate for the integration of emotional, contextual and goal-directed drives (O'Donnell and Grace 1995; Grace 2000). While this integration has been characterized at subthreshold intensities (Goto and O'Donnell 2002; Carter et al. 2007), the present study shows in detail the effects of coincident cortical and subcortical activation on NAcc neuron spike output. In neurons receiving converging excitation from BLA and mPFC, BLA input facilitated mPFC-evoked spiking, and this facilitation was greatest when the mPFC-evoked spike rate was near 0%. When BLA and mPFC were both stimulated at subthreshold intensities, the timing of spikes elicited by coincident stimulation reflected the timing of the two component inputs. Thus, BLA input both augmented and shifted the latency of mPFC-evoked spikes.

The BLA and mPFC projections to NAcc are glutamatergic, and these inputs can be modulated by many non-glutamatergic neurotransmitter systems (Meredith 1999; Sesack et al. 2003; Tepper and Bolam 2004). However, BLA stimulation was most effective at short latency ISIs, consistent with monosynaptic conduction times from the BLA and mPFC to the NAcc. This timing-dependence suggests that BLA stimulation effects are mediated by glutamatergic fast synaptic transmission. In addition to their direct projections, there may be multi-synaptic pathways through which the BLA and mPFC could excite NAcc neurons (Groenewegen et al. 1990). To minimize multi-synaptic excitation, recordings were limited to neurons with spike latencies consistent with mPFC- and BLA-to-NAcc projection conduction times. In some experiments, recordings were further limited to exclude neurons with highly variable spike latencies. Thus, while the origin of all evoked spikes cannot be determined precisely, the selection criteria employed here maximized the measurement of monosynaptic inputs. Given that the mean latency of orthodromically evoked spikes was consistent with the mean antidromic conduction times (taking into account a synaptic delay), it is likely that monosynaptic excitation represents the primary mode of excitation examined in these results.

Neurons were selected based on their evoked spiking responses to BLA and mPFC. Because afferent stimulation does not typically evoke action potentials in NAcc neurons (O'Donnell and Grace 1995; Brady and O'Donnell 2004), the cells we recorded likely make up a fraction of NAcc neurons. This evoked spiking may be attributable to especially dense or potent innervation from the target regions, or to the patterns of afferent fibers activated by electrical stimulation – reflecting synaptic input rather than the intrinsic properties of the neurons (Wickens and Wilson 1998). Furthermore, the latency variances of BLA-evoked and mPFC-evoked spikes showed no evidence of correlation in single neurons, suggesting that evoked

spiking was dependent on the properties of the individual synaptic inputs rather than the intrinsic properties of the neuron. Most NAcc medium spiny neurons exhibit EPSPs evoked from several sites (O'Donnell and Grace 1995) (consistent with anatomical evidence (French and Totterdell 2003)), suggesting that converging excitatory inputs are common in these neurons. Thus, although a comparatively narrowly defined selection of neurons was recorded, the results should be applicable to NAcc medium spiny neurons in general.

In previous reports, mPFC stimulation only evoked action potentials during periodic membrane depolarizations ("up-states") (O'Donnell and Grace 1995). In the current study mPFC-evoked spike rates were observed that varied linearly with the applied current between 0 and 100%. Thus, in a subset of neurons, the mPFC input alone was clearly sufficient to evoke spikes. Bistable membrane states in NAcc neurons impact the integration of afferent inputs (O'Donnell and Grace 1995; Wilson and Kawaguchi 1996; Kerr and Plenz 2002); however, the extracellular recording approach used in the current study could not take such transitions into account. Responses were sampled over many regularly spaced trials, so that the data almost certainly include spikes elicited from both depolarized and hyperpolarized membrane potentials (i.e. "up" and "down" states). Because mPFC/BLA input integration may depend on the membrane potential from which the responses are evoked (Goto and O'Donnell 2002), the effects we report here may reflect the average influence of postsynaptic active properties.

3.5.1 Mechanisms of integration

The BLA-mediated increase in mPFC-evoked spike rate was critically dependent on the timing of the two inputs. Facilitation was maximal at ISIs of 1ms, of intermediate value at 11ms, and

was non-existent at 21ms or longer. This narrow window for integration corresponds closely to the latency distributions of spikes orthodromically evoked from the two structures. While NDMA channels contribute to excitatory synaptic currents in NAcc neurons (Carter et al. 2007), blockade of these channels with MK801 did not attenuate the BLA-mediated increase in spike firing – consistent with previous reports that hippocampal-evoked spiking is unchanged by systemic NMDA receptor antagonists (Floresco et al. 2001b). Thus, our results suggest that non-NMDA excitatory synaptic activity provides the primary drive for evoked spiking due to low frequency afferent electrical stimulation. NMDA channels may have other important roles in medium spiny neurons, such as governing activity-dependent long term potentiation (Charpier and Deniau 1997). Furthermore, other effects of BLA input (such as decreased mPFC current input/spike output slope) were not tested in the presence of NMDA- (or DA-) blocking drugs; thus it is not known of these receptors participate in other aspects of limbic/cortical synaptic input integration.

Interestingly, the influence of the BLA on the current/response *slope* was not as narrowly timing-dependent as its influence on spike rate, suggesting that other mechanisms may contribute to this effect. BLA input attenuated the slope of the mPFC current/spike output curve at 1ms and 11ms ISIs, but not at 31ms; however (unlike the change in spike rate) the changes in slopes at 1ms and 11ms were approximately equal (-12% and -10% per 100μA, respectively). Although more data are necessary to determine the precise duration, our findings suggest that the effect of BLA stimulation on a neuron's input/output relationship persists for at least 11ms after the activation of BLA. It is possible that the depolarizing influence of the BLA could open voltage-dependent, slowly inactivating conductances, and that the long lasting decrease in input resistance that results could attenuate the current/response relationship. NAcc neurons exhibit

several voltage-sensitive conductances (Surmeier et al. 1989; Nisenbaum et al. 1994); however with out direct evidence it is difficult to hypothesize which specific conductances might contribute to this effect. Furthermore, other mechanisms could also account for or contribute to these observations, such as spike threshold changes related to EPSP kinetics (Wickens and Wilson 1998), EPSP interactions with bistable states (O'Donnell and Grace 1995; Wilson and Kawaguchi 1996), and passive properties of dendrites. Intracellular observations of BLA- and mPFC-evoked EPSPs would be necessary to determine the specific mechanisms underlying activity-dependent input summation, as well as the role of bistable membrane fluctuations.

In addition to facilitating mPFC-evoked spiking, BLA input shifted the latency of mPFC-evoked spikes. This shift was maximal at a 1ms ISI, and also appeared to depend on the strength of mPFC input. At the 11ms ISI, the latency shift was accompanied by an increased latency variance, possibly reflecting a prolonged post-stimulus excitation due to asynchronous synaptic activity. When mPFC and BLA inputs were both stimulated at subthreshold intensity at a 1ms ISI, the change in latency due to coincident stimulation was well-predicted by the timing discrepancy between the BLA and mPFC inputs. Furthermore, the coincidentally-evoked response latency was optimally described by a regression model that included both component input latencies. Thus, in response to two similar subthreshold inputs, evoked spiking reflected the timing of both excitatory synaptic components. In contrast, when mPFC current was tuned to produce a 50% response during coincident stimulation (requiring greater mPFC current), the latency shift was not well-predicted by the mPFC/BLA input timing difference, and the mPFC input latency alone was the best predictor of the coincidentally-evoked spike latency. Thus, in response to unequal excitatory inputs, the evoked spike timing was most influenced by the stronger component. These results suggest that spikes elicited by two summated EPSPs reflect

both the timing and intensity of the component inputs, with stronger inputs determining the spike latency when input intensities are unequal.

In neurons where only mPFC stimulation could evoke spikes, BLA stimulation had no effect on mPFC-evoked firing. Although subthreshold evoked events were not measured, it is likely that in these neurons BLA stimulation evoked at least a nominal EPSP – given the large proportion of neurons exhibiting BLA-evoked EPSPs in previous intracellular recordings (O'Donnell and Grace 1995; Goto and O'Donnell 2002) and the dense innervation of this region by BLA afferent terminals (Wright and Groenewegen 1995). The lack of BLA-mediated facilitation in these mPFC-responsive neurons may suggest that small BLA-evoked EPSPs have little effect on evoked spiking responses.

3.5.2 Functional implications

Taken together, these data show that NAcc neurons are able to integrate limbic and cortical synaptic activity in two dimensions: input intensity and input timing. In both cases, integration was most evident when the BLA and mPFC inputs were at similar subthreshold intensities. Extrapolated to a population of NAcc neurons, these results suggest that weak, coincident activation of two afferent structures may generate activity in a larger ensemble of neurons than activation of either structure alone. Reflecting the timing of both afferent systems, neurons in an ensemble would exhibit firing within the same specific temporal window. Thus, ensembles of NAcc neurons may be able to distinguish themselves within the dynamic milieu of NAcc activity by sharing a common timing signature that reflects their common inputs. Because single NAcc neurons receive many inputs that could influence firing, the control of spike timing may be a

critical mechanism by which the different afferent structures control the output of NAcc neurons. Higher intensity mPFC stimulation elicited responses that reflected the mPFC timing alone, suggesting that evoked spike timing reflects the component inputs only when those inputs are of equivalent magnitude. Thus, strong activation of one afferent structure may be sufficient to disrupt ongoing ensemble activity, or create new ensembles based on changing affective, contextual or cognitive demands. In behaviors that rely on the mPFC-to-NAcc projection such as memory-guided navigation (Floresco et al. 1999), behavior may be optimal when mPFC-to-NAcc inputs are coordinated with other inputs, but may be disrupted by imbalanced or uncoordinated afferent activity (Grace 2000). For example, a salient emotional stimulus may be capable of interrupting ongoing goal-directed behavior by intensely activating BLA-to-NAcc neurons and interfering with mPFC-to-NAcc or hippocampal-to-NAcc transmission. In psychiatric disorders such as schizophrenia and post-traumatic stress disorder, cognitive ability may be impaired by just such a mechanism, as sufferers of these diseases exhibit elevated basal and evoked amygdala activity (Shin et al. 2005; Hall et al. 2008). In Pavlovian conditioned fear, which activates the BLA and the mPFC-to-NAcc projection (Rosenkranz and Grace 2002; McGinty and Grace 2007), adequate input to NAcc from both structures may be necessary to interrupt or re-direct ongoing behavior to permit the expression of defensive fear reactions (Laviolette et al. 2005). Thus, the balance or imbalance of afferent inputs to NAcc neurons may have consequences for normal and pathological cognitive function.

CHAPTER 4: THE EFFECTS OF PAVLOVIAN CONDITIONED ODORS IN NUCLEUS ACCUMBENS NEURONS

4.1 ABSTRACT

Projection neurons of the BLA and mPFC fire actions potentials in response to conditioned stimuli, as do neurons in the NAcc. Excitatory BLA and mPFC afferents converge upon single neurons in the NAcc, and mutually facilitate evoked firing in these cells. Therefore, we hypothesized that NAcc neuronal responses to conditioned stimuli depend on BLA and mPFC afferent input. In chloral-hydrate anesthetized rats, we recorded from NAcc neurons receiving BLA and mPFC inputs, and measured their responses to Pavlovian conditioned odors. Rather than increasing evoked firing, conditioned odors typically caused inhibition. These responses were neither specific to the conditioned odor, nor were they distinguishable from responses to odors presented before conditioning. Given the strong evidence for the facilitatory effects of BLA and mPFC on the NAcc, we conclude that different recording conditions or neuron selection criteria may be necessary to observe excitatory responses to conditioned stimuli.

4.2 INTRODUCTION

The NAcc supports reward-directed behavior, and NAcc neurons encode many aspects of reward-related tasks. Sensory events, motor activity, upcoming rewards, and task contingencies have all been associated with changes in NAcc neuron firing (Carelli 2002; Setlow et al. 2003; Nicola et al. 2004; Wilson and Bowman 2005; Wan and Peoples 2006). Among the many functions attributed to NAcc neurons, the encoding of stimuli that predict future reward or punishment is thought to be critical for reward-directed behavior. In situations where rats are rewarded for responding to a discrete cue, cue presentation increases the firing of a substantial portion of NAcc neurons (Setlow et al. 2003; Nicola et al. 2004). The magnitude of this increase predicts the behavioral response (Nicola et al. 2004), and manipulations that attenuate this activity also attenuate the behavior (Yun et al. 2004). Although the NAcc receives afferent input from several subcortical and cortical structures that could encode information about conditioned stimuli (French and Totterdell 2002, 2003), the specific inputs that mediate cue responses in the NAcc are unknown.

In Chapter 2, we showed that the BLA activates a subpopulation of mPFC neurons that project to the NAcc, and that a similar portion of these neurons is activated by Pavlovian conditioned cues. Therefore, the cue-evoked responses of NAcc neurons may be dependent on input from the mPFC. Projection neurons in the BLA also encode conditioned cues (Rosenkranz and Grace 2002; Maren and Quirk 2004), and the BLA projection to the NAcc is necessary for conditioned cues to activate behaviors such as drug seeking (Di Ciano and Everitt 2004), and second-order conditioned responses (Setlow et al. 2002). Thus, both the BLA and mPFC could potentially relay conditioned stimulus-related information to the NAcc.

In Chapter 3, we showed that the NAcc contains neurons that receive excitatory input from both BLA and mPFC. Simultaneous activation of both structures increased the magnitude of evoked spiking in these neurons, compared to activation of one input alone. Because conditioned stimuli activate BLA and mPFC efferent neurons, we reasoned that conditioned stimuli would also excite NAcc neurons receiving input from these two structures. To test this hypothesis, we recorded such NAcc neurons during odor-based Pavlovian conditioning in chloral hydrate-anesthetized rats. Because most NAcc neurons are silent under anesthesia, we tested the effects of conditioned odors by measuring changes in mPFC-evoked spiking. Unexpectedly, conditioned odors had no effect, eliciting a non-significant, non-selective decrease in the evoked response. These results suggest that other afferent inputs or recording conditions may be necessary for NAcc neurons to express conditioned responses.

4.3 METHODS

4.3.1 Subjects and surgery

Twenty-six NAcc neurons were recorded from 20 male Sprague-Dawley rats, weighing 300g on average (range 280-330g). Eighteen neurons were recorded after Pavlovian odor conditioning, 14 were recorded before conditioning, and 6 were recorded both before and after conditioning. The rats were anesthetized with an initial intraperitoneal injection of chloral hydrate (400 mg/kg, 8% solution in 0.9% saline). After the rats no longer displayed a reflexive withdrawal in response to a foot pinch, they were implanted with a femoral vein catheter. Anesthesia was

maintained with supplemental doses of 8% chloral hydrate (0.1-0.3ml I.V. through the catheter, every 15 minutes) to ensure stable neuronal responses throughout the experiment, which was not longer than 8 hours. Supplemental anesthesia was not administered during the conditioning or testing procedures.

The rats were placed in a stereotaxic apparatus (David Kopf Instruments, Tujunga, CA) and fitted with an anesthesia mask (Kopf model 906) that held the head stable while allowing odorized air to be passed in front of the rat's nose. The skull was exposed and cleaned, and holes were drilled overlying the electrode target regions. Target coordinates were determined using the atlases of Paxinos and Watson (1998; 2005), and are given relative to the Bregma suture landmark: AP for the anterior-posterior coordinate, ML for medial-lateral, DV for dorsal-ventral.

Bipolar stimulating electrodes (Plastics1 C212G-MS303/2) were lowered into the BLA (AP -3.6, ML 4.8, DV 9.0) and the mPFC (AP 3.0, ML 0.7, DV 5.5); the coordinates refer to the negative pole. The BLA electrodes were placed in the basolateral, basomedial and lateral subnuclei of the BLA; the mPFC electrodes were placed in the infralimbic and prelimbic cortical areas. In addition to these cranial electrodes, a pair of 23G needles were inserted into the plantar region of the left hind limb to deliver foot shocks during the odor conditioning protocol. The BLA, mPFC and foot electrodes were connected to a Master-8 stimulator and stimulus isolation units (A.M.P.I., Jerusalem, Israel).

A recording electrode was lowered to the dorsal border of the NAcc (AP 1.2, ML 0.8, DV 6.0). These electrodes were pulled from 2mm outside-diameter, filamented borosilicate glass tubing (World Precision Instruments, Sarasota, FL). The tips were broken under microscopic control to achieve an impedance of 8-12 MΩ (measured in situ through the amplifier), and the electrodes were filled with the recording solution (2M NaCl with 2% Pontamine Sky Blue dye).

Neuronal signals were amplified and band pass filtered at 200-4000Hz (Fintronics WDR-420, Orange, CT), monitored with an oscilloscope and speaker, and passed to a data acquisition board and PC (Microstar Laboratories, Bellevue, WA) for storage and analysis. Offline analysis was performed using custom software (Neuroscope, Brian Lowry) and routines for the R programming environment (The R Development Core Team 2005).

4.3.2 Neuron selection and odor conditioning

Only NAcc neurons receiving excitatory input from BLA and mPFC were recorded. Because NAcc neurons are typically silent under anesthesia, a cell searching procedure was used to identify these neurons. The recording electrode was lowered slowly through the NAcc (DV 6.0-8.0) while alternating stimulation pulses were applied to the BLA and mPFC at an overall rate of 0.5Hz. Action potential discharge that followed within 20ms of the BLA and mPFC stimulation pulses indicated the presence of a NAcc neuron with putatively monosynaptic, orthodromically evoked responses (see Figure 3.2 and Figure 3.3). Neurons were suitable for use in this experiment if the evoked spike rate was at least 50% in response to both 400μA BLA stimulation and 500μA mPFC stimulation, with each input tested separately at a rate of 0.3Hz.

The equipment used for the odor-based Pavlovian conditioning is similar to that used previously by our group (Rosenkranz and Grace 1999; Laviolette et al. 2005): A mixture of O2/CO2 (95/5%) was passed through the anesthesia mask at ~5psi. Through a custom-built series of air lines, odor-containing bottles, and solenoid pinch valves, the odor content of the O2 could be rapidly switched from no odor to one of two distinct odorants. The exit port of the anesthesia mask was directed to an activated charcoal scavenging system to keep the odors

contained within the apparatus. The apparatus was sealed to prevent escape of odor-bearing air, and all air lines were checked daily for cross-contamination and deodorized or replaced if necessary. The two odorants used in this experiment were liquid extracts of almond and peppermint (McCormick, Hunt Valley, MD), with distilled water added to reduce ethanol content to ~10%.

When a suitable neuron was identified, the O2/CO2 gas flow was turned on for five minutes (with no odor), after which the anesthesia level was checked and adjusted if necessary. Then, the conditioning procedure began: the two odors were presented six times each in alternating fashion; presentations were 10 seconds each, and inter-presentation intervals were 60 seconds. For the first presentation of each odor, no shock was given. For the next five presentations, one odor (designated CS+) was accompanied by a 5 second foot shock during the last 5 seconds of odor presentation (100 pulses at 20Hz, 3-5mA). The other odor (CS-) was presented without foot shock. Thus, five CS+/foot shock pairings were performed. The CS+ was always presented first, and the CS-, second. The odor designated as CS+ was randomized, so that in 15/26 neurons the CS+ was almond, and in 11/26 it was peppermint. As in previous studies (Rosenkranz and Grace 2002; Laviolette et al. 2005), odor identity did not affect the results, and the data were grouped and analyzed together. No stimulation was applied to the BLA or mPFC during conditioning.

After the conditioning protocol ended, a 5 minute "cool down" period followed during which the (non-odorized) O2/CO2 flow was maintained and no stimuli or shocks were administered. The anesthesia level was adjusted if necessary, and then the testing protocol began. In pilot experiments, NAcc neurons were typically silent throughout conditioning, and did not fire in response to odors presented after conditioning (not shown). Thus, to test the

effects of conditioned odors on NAcc neurons, we measured the facilitation or depression of mPFC stimulation-evoked spike firing during conditioned odor presentation. The mPFC was stimulated at 0.3Hz at a current sufficient to produce ~50% evoked spike ratio. After 40 baseline stimulation trials (with no odor), the CS+ or CS- was presented for 20 trials, followed by 40 trials with no odor; the sequence was then repeated (40 trial baseline, 20 trials with odor, 40 trials with no odor), using the odor which had not been presented before. In 13/18 neurons, the CS+ was tested first, and in 5/18 it was tested second; presentation order had no effect on the results, and the data were combined and analyzed together. The conditioned odor responses of 18 neurons were measured in 17 rats; thus, in all but one experiment, only one neuron was tested post-conditioning per rat.

In addition to the 18 neurons tested after odor conditioning, in 14 neurons the effects of odors on mPFC-evoked spiking were tested before odor conditioning – i.e. before the odors had become associated with foot shock. The testing procedure was the same as described above, and the odors were designated nominally as CS+ and CS- according to the conditioning that would occur later during the experiment. In 6 of these 14 neurons, odor responses were tested both before and after odor conditioning.

4.3.3 Analysis and histology

The mPFC-evoked response ratios (expressed as % of spikes per 100 stimuli) were measured before, during and after CS+ and CS- presentation. Because CS+ and CS- odors were both tested in each neuron, within-cell comparisons of the odor-evoked spike rates were made. All

statistical comparisons and p-values refer to paired t-tests (within neuron) unless noted otherwise.

At the end of the experiment, the recording electrode placement was marked by iontophoretic dye ejection (-20μA for 60 minutes), and the stimulating electrode placements were marked by electrolytic lesion (100μA for 10 sec). The rats were given an overdose of anesthetic and decapitated, and their brains were removed, fixed in 8% paraformaldehyde with 1% potassium ferricyanide, and then later transferred to a cryoprotectant solution (25% sucrose). The brains were sliced on a freezing microtome and stained with Cresyl Violet using standard histological procedures. The electrode placements were determined using the atlases of Paxinos and Watson (1998; 2005).

4.4 RESULTS

A total of 18 NAcc neurons that received excitatory input from BLA and mPFC were recorded. Spiking evoked by mPFC stimulation was measured before and during presentation of a distinct odor (CS+) that had been paired with a foot shock earlier in the recording session. The spike rate evoked by mPFC stimulation was unchanged during CS+ presentation, exhibiting a decrease of 8.3 ± 4.3% (mean ± SEM, spikes/100 stimuli) that did not reach statistical significance ($p<0.069$). Presentation of a non-paired odor (CS-, n=17) in the same neurons also had no effect on mPFC-evoked spike firing (increase of 2.1 ± 6.0%, $p<0.74$) (Figure 4.1).

To compare the CS- and CS+ -evoked responses in each cell, the change in spike rate due to CS- was subtracted from the change due to CS+ (Figure 4.2A). On average, this response index was -9.3 ± 5.7%, the negative value indicating greater inhibition or less excitation due to the CS+. This index was not significantly different from zero ($p<0.12$). Excluding one cell with a 70% increase in firing during the CS- (more than 2 standard deviations above the mean), the response index mean was -5.7 ± 4.6% (not different than zero, $p<0.24$). Similar to previous studies (Nicola et al. 2004; Roitman et al. 2005), a subset of neurons was inhibited by the CS+; the average response index among these neurons was -10.8 ± 5.4% ($n=11$, $p<0.074$). The CS+ and CS- responses were further compared by linear regression (Figure 4.2B). There was a weak positive relationship between the CS- and CS+ -evoked responses ($r = 0.45$, $p<0.069$ for all data; $r = 0.50$, $p<0.048$ excluding the one outlier); however this relationship was not evident in CS+ -inhibited neurons ($n=11$, $r = 0.006$, $p<0.99$).

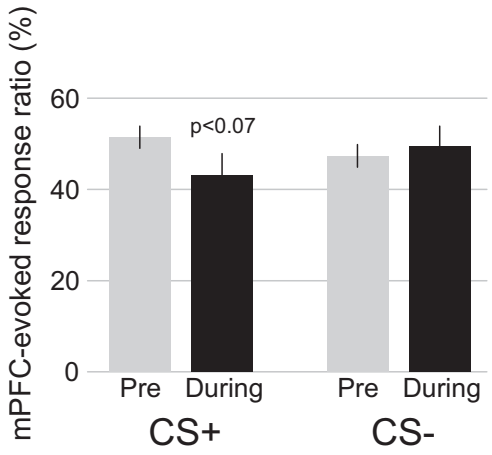

Figure 4.1 Presentation of conditioned odors did not change mPFC-evoked spiking in NAcc neurons. However, there was a weak trend towards a decrease in response to the CS+. "Pre" indicates 40 trials before odor presentation; "During" indicates 20 trials over which odors were presented. n=18 for CS+, n=17 for CS-.

In the prefrontal cortex neurons recorded in Chapter 2, CS+ presentation evoked a larger range of excitatory and inhibitory changes in firing, producing a wider distribution of responses compared to the CS-. However, in the current study, the variance of CS+ -evoked responses was not different than that for CS- -evoked responses, (CS+ 3.4%, CS- 6.2%, $p<0.85$ by Fligner test for homogeneity of variances (Conover et al. 1981)). We also tested the effects of odors in neurons recorded before the conditioning protocol had been performed (n=14). While the variances of responses to the nominal CS+ and CS- presented before conditioning were only 1.6 and 2.4%, respectively, the variances were not significantly less than for the post-conditioning CS+ and CS- responses described above ($p<0.16$ and $p<0.42$, respectively, by Fligner test). The distributions of both pre- and post-conditioning odor responses are shown in Figure 4.3.

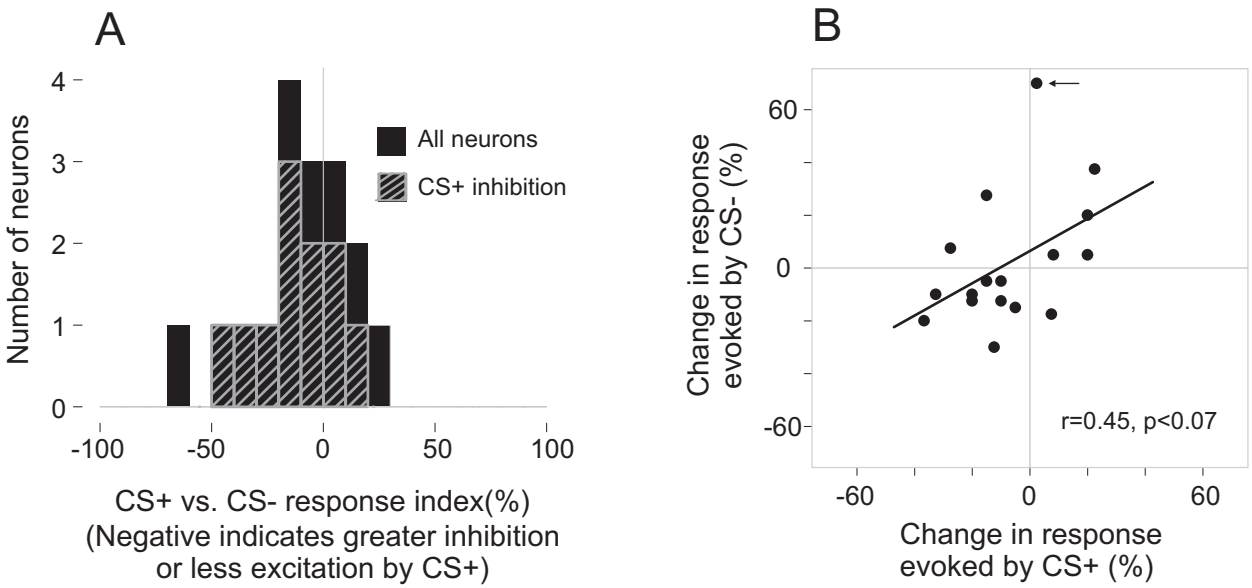

Figure 4.2 The effects of odor presentation were similar for the CS+ and CS-. **A** This histogram shows the distribution of the odor response index (CS- response subtracted from CS+ response) for all neurons (black bars, n=17) and for those neurons for which the CS+ caused inhibition (black with gray hatching, n=11). The mean of this index was not significantly different from zero for either all neurons or for CS+ -inhibited neurons. **B** This scatter plot shows that CS+ response plotted against the CS- response for each neuron (n=17). There was a weak positive relationship between the CS+ and CS- responses (fit line and statistics), which reached statistical significance when one neuron with strong CS- -evoked excitation (arrow) was omitted ($r= 0.50$, $p<0.048$).

Six neurons were tested for odor responses both before and after conditioning. For the CS+: three neurons had responses that were less after conditioning (-30, -30 and -40% change in spike rate, indicating more inhibition or less excitation), one neuron had greater responses after conditioning (40% increase), and two neurons had virtually unchanged responses after

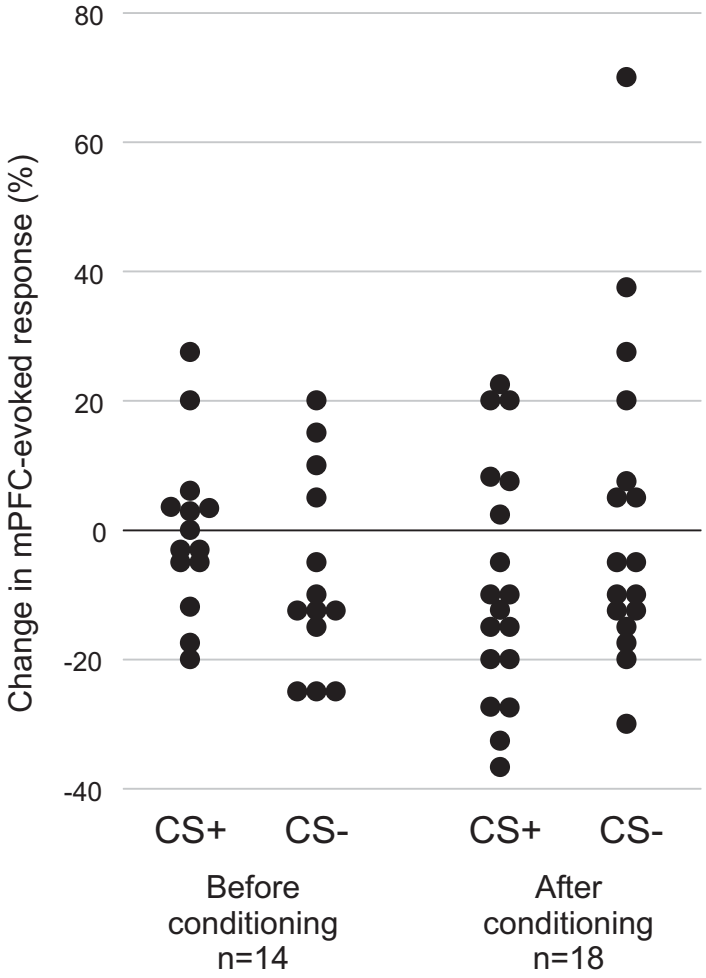

Figure 4.3 The distribution of odor-evoked responses both before and after Pavlovian conditioning. The effects of odor presentation on mPFC-evoked firing were tested before Pavlovian conditioning was performed. The change in firing for 14 neurons (one dot per neuron) is shown in response to presentation of the nominal CS+ and CS- (left columns). Overlapping responses are shown adjacent to one another. For comparison, the right columns show the distribution of responses from the 18 neurons recorded after conditioning (the same data is shown in Figure 4.1 and Figure 4.2). There was no significant difference in variance between the post-conditioning CS+ and CS- effects, or between the pre- and post- conditioning odor effects.

conditioning (0 and 2% increase). For the 5 neurons for which CS- responses were available: one had lesser responses (-8%), three had greater responses (15, 18 and 50%), and one had virtually unchanged responses (-2%).

4.5 DISCUSSION

Given that both BLA and mPFC projection neurons are activated by conditioned cues (Chapter 2, Rosenkranz and Grace 1999), we hypothesized that a subpopulation of NAcc neurons that receives both mPFC and BLA input would be excited by presentation of a Pavlovian conditioned odor. In contrast, we found no significant change in evoked firing during conditioned odor presentation. Furthermore, although conditioned stimuli cause both firing rate increases and decreases in NAcc neurons (Roitman et al. 2005; Day et al. 2006a; Wan and Peoples 2006) and in the mPFC afferents to the NAcc (Chapter 2), the distribution of odor-evoked responses did not differ for the CS+ and CS-, nor did the distribution of post-conditioning odor responses differ from responses to pre-conditioning odor presentation.

The average response to the CS+ was not statistically different from the response to the CS-, even when considering the subset of neurons (n=11) for which the CS+ was inhibitory. Furthermore, there was a weak positive correlation between the CS+ and CS- responses – indicating that single neurons responded in similar ways to both the foot shock-paired and un-paired odors. While the CS- may have been imbued with some emotional salience during conditioning, in previous studies (and in Chapter 2) such cross-sensitization was minimal, and the odor-evoked responses (both neuronal and behavioral) were robust and CS+ -specific

(Rosenkranz and Grace 2003; Laviolette et al. 2005). Thus, the low magnitude and lack of odor specificity in the responses we observed in the NAcc suggests that they do not reflect the emotional salience of the conditioned stimuli.

Although the inhibitory responses we observed in a subset of neurons were weak and non-specific on average, in a small number of these the responses may have been potent and specific (Figure 4.2A). In freely behaving rodents, Pavlovian conditioned stimuli evoke inhibitory responses in a subpopulation of NAcc neurons (Roitman et al. 2005; Day et al. 2006a; Wan and Peoples 2006), and we have observed BLA-mediated inhibition of mPFC input to the NAcc (see Chapter 5). Thus, some neurons in our sample may have been encoding the presence of the conditioned odor cue. Whether they are a distinct subpopulation, or lie within a continuum of responsive neurons is not clear.

Despite the weak inhibitory trend in CS+ responses, we maintain that the BLA and mPFC afferents to the NAcc are critical sources of excitatory input. There is strong evidence to support this claim. First, a substantial subpopulation of NAcc neurons is excited by cues that predict rewarding or punishing outcomes (Setlow et al. 2003; Roitman et al. 2005; Wilson and Bowman 2005); indeed, negative reinforcers and their predictors appear to elicit more excitatory responses than positive reinforcers (Setlow et al. 2003; Roitman et al. 2005). Second, approximately 25% of mPFC-to-NAcc projection neurons are excited by conditioned odors (Chapter 2), as are many BLA projection neurons (Rosenkranz and Grace 2002; Maren and Quirk 2004). Furthermore, up to 50% of BLA neurons that project to mPFC (conveying emotional information (Laviolette et al. 2005)) also send collateral axons to the NAcc (Shinonaga et al. 1994). Finally, preliminary reports suggest that conditioned-cue excitatory responses in NAcc neurons can be abolished by inactivation of the BLA (Ambroggi et al. 2007; Jones et al. 2007). All of this evidence suggests

that a significant portion of the neurons we recorded, specifically selected as those receiving excitatory inputs from the BLA and mPFC, would have been activated by conditioned cues. Indeed, even in a non input-specific sample of NAcc neurons, a subset would be expected to exhibit selective CS+ excitation (Roitman et al. 2005); in contrast, presentation of the CS+ elicited inhibition in most neurons. Therefore, we conclude that different experimental conditions may be necessary to reveal excitation in NAcc neurons recipient of those inputs.

There are several possible explanations for the lack of conditioned excitation in our sample of NAcc neurons. First, it is possible that the NAcc neurons were depressed due to anesthesia, and thus were unable to express suprathreshold excitatory responses. For example, NAcc neurons in awake rats are activated by positive and negative primary reinforcers (Barrot et al. 2002; Setlow et al. 2003; Roitman et al. 2005), yet we observed no excitation during the foot shock. While an anesthetic-induced depression is possible, it does not explain why mPFC-evoked spiking showed no appreciable increase due to the CS+, as we have shown that mPFC inputs can be enhanced by subthreshold BLA stimulation (Chapter 3). Intracellular recording may be necessary to determine whether odor presentation elicits subthreshold changes in NAcc neuron activity under anesthesia. A second possibility is that inputs other than mPFC and BLA are necessary to drive conditioned responses. For example, conditioned response behaviors can depend on context (Holt and Maren 1999), and spatial and contextual information is conveyed to the NAcc through the ventral hippocampus (Goto and Grace 2005b; Burhans and Gabriel 2007). Furthermore, the hippocampus gates incoming activity from other afferents by promoting depolarizing “up-state” transitions in NAcc neurons (O'Donnell and Grace 1995). Thus, NAcc neurons may be unresponsive to conditioned cues without substantial hippocampal input (in addition to BLA and/or mPFC). Finally, recent studies have shown that NAcc dopamine is

necessary for behavioral responses to conditioned cues (Nicola et al. 2005) and behaviorally predictive, cue-evoked spiking in the NAcc is abolished by inactivation of the ventral tegmental area (Yun et al. 2004). If NAcc dopamine release or neuronal responses to dopamine release were attenuated in our experiments (possibly due to anesthesia, see Kiyatkin and Brown 2007), then the effects of conditioned cues may have been similarly attenuated.

In summary, depression of neuronal activity due to anesthesia may be responsible for the lack of excitatory responses to conditioned stimuli, and afferent inputs from the hippocampus or dopamine neurons may also provide a critical excitatory or modulatory drive that was absent in our experiments. Therefore, it may be possible to unmask the excitatory influence of Pavlovian conditioned odors by activating hippocampal or dopaminergic afferents to the NAcc, or by selecting NAcc neurons recipient of hippocampal inputs. Because we have also observed activity dependent, BLA-mediated depression of NAcc neuron responses (Chapter 5), further experiments may also show specific inhibitory effects of conditioned cues.

CHAPTER 5: ACTIVITY-DEPENDENT DEPRESSION OF MEDIAL PREFRONTAL CORTEX INPUTS IN ACCUMBENS NEURONS BY THE BASOLATERAL AMYGDALA

5.1 ABSTRACT

The NAcc integrates motivational information from the BLA with goal-related information from mPFC. Phasic activation of the BLA occurs in response to salient conditioned stimuli, which may lead to NAcc dopamine (DA) release and the depression of other afferent inputs. While we have previously shown that BLA facilitates mPFC inputs in the NAcc, the effects of strong, phasic BLA activation are not known. In urethane-anesthetized rats, we recorded from NAcc neurons receiving excitatory input from both mPFC and BLA. BLA train stimulation depressed mPFC-evoked spiking. While we hypothesized that DA or NMDA receptors might mediate this depression, blockade of these receptors was without effect. BLA-mediated depression was only evident when the BLA stimulation evoked spikes in the recorded neuron; thus depolarization of the recorded neuron may be critical for this effect. The ability of the BLA to suppress mPFC-to-NAcc signaling may be a mechanism by which normal or pathologically heightened emotional states disrupt goal-directed behavior in favor of emotionally-driven responses.

5.2 INTRODUCTION

In the presence of salient conditioned cues, normally quiescent BLA neurons exhibit dramatic increases in firing rate (Pratt and Mizumori 1998; Schoenbaum et al. 1999). This phasic BLA activity is thought to be critical for emotional stimuli to influence behavioral responding (LeDoux et al. 1990; Schoenbaum et al. 2003), and preliminary evidence suggests that the direct activation of NAcc neurons by the BLA mediates cued reward seeking (Ambroggi et al. 2007). We have shown that BLA activation can facilitate mPFC-evoked spiking in NAcc neurons where these inputs converge (Chapter 3); however, these results were obtained using only low frequency, non-spike-evoking BLA stimulation. The effects of higher intensity BLA activation on mPFC-to-NAcc transmission are not known. Given that robust cue-evoked firing in BLA neurons appears to be essential for some motivated behaviors, the effects of phasic BLA activity in the NAcc may be an important mechanism by which motivational information influences action selection (Nicola 2007).

Although the BLA projection to the NAcc is glutamatergic, high frequency BLA stimulation or salient emotional cues may activate other neurotransmitter systems. Specifically, extracellular NAcc dopamine (DA) is increased by primary or conditioned emotional stimuli (Kalivas and Duffy 1995; Young et al. 1998), and this DA signal may be necessary for both behavioral and neuronal responses to those stimuli (Yun et al. 2004; Nicola et al. 2005). High frequency BLA stimulation has also been reported to increase extracellular DA in the NAcc, and induce NMDA- and DA D1-dependent plasticity of BLA inputs (Floresco et al. 1998; Floresco et al. 2001b). DA modulates corticostriatal transmission through both D1 and D2 receptor subtypes (West and Grace 2002; Goto and Grace 2005b); thus, high frequency BLA stimulation could

potentially modulate mPFC inputs onto NAcc neurons through both NMDA- and DA-dependent mechanisms.

To test this hypothesis, we recorded from NAcc neurons receiving both BLA and mPFC input, and observed the effects of 20Hz BLA stimulation on mPFC-evoked spiking. The evoked responses were depressed both during and after BLA activation. Interestingly, while the post-activation depression of mPFC inputs was dependent on DA D1-receptors, the depression observed *during* BLA activation was unchanged by DA receptor or NMDA channel blockade.

5.3 METHODS

5.3.1 Subjects and Surgery

A total of 80 NAcc neurons were recorded from male Sprague-Dawley rats with an average weight of 310g (range 270-360g). The rats were anesthetized with a single injection of urethane (1.4-1.5g/kg in distilled water); this provided stable anesthesia for the duration of the experiment, which did not exceed 8 hours. Surgery was initiated when the rat no longer displayed a reflexive withdrawal in response to a foot pinch (20-60 min after injection). For experiments where antagonist drugs were delivered, the rats were first implanted with a femoral vein catheter. The rats were placed in a stereotaxic apparatus (David Kopf Instruments, Tujunga, CA), and the skull was exposed and cleaned. Burr holes were drilled in the skull overlying the electrode targets, and the overlying dura mater was carefully resected. The coordinates of the target regions are

given relative to the Bregma suture: AP for anterior-posterior distance; ML for medial-lateral; DV for dorsal-ventral.

Stimulating electrodes were lowered into the BLA (AP -3.6, ML 4.8, DV -9.0) and the mPFC (AP +3.0, ML 0.8, DV 5.5). The electrodes were Plastics One model C232G-MS303/2 bipolar electrodes with 0.8mm of wire exposed at the tip of each pole. The two poles of the BLA electrode were oriented in the same sagittal plane, and the two poles of the mPFC electrode were in approximately the same coronal plane. The stereotaxic coordinates and stimulating electrode locations all refer to the negative pole. A recording electrode was lowered to the dorsal border of the NAcc, near the border of the shell and core subregions (AP +1.2, ML 0.8 to 1.0, DV 6.0). The recording electrodes were pulled from 2mm outside diameter, filamented borosilicate glass (World Precision Instruments, Sarasota, FL). The tips were broken back under microscopic control to achieve an impedance of 8-12 MΩ as measured in situ through the amplifier (Fintronics WDR-420, Orange, CT), and filled with 2M NaCl with Pontamine Sky Blue dye.

5.3.2 Electrophysiological recordings and neuron selection

Signals from neurons in the NAcc were amplified and band pass filtered at 200-4000Hz (Fintronics WDR-420, Orange, CT). The amplified signals were passed to an oscilloscope and speaker for real-time monitoring, as well as to a data acquisition board and PC (Microstar Laboratories, Bellevue, WA) for storage and analysis. Offline analysis was performed using custom software (Neuroscope, Brian Lowry) and scripts for the R programming environment (The R Development Core Team 2005). Electrical stimulation pulses were delivered through the Master 8 Stimulator (A.M.P.I., Jerusalem, Israel) and stimulus isolation units.

The neurons of interest were those NAcc neurons that were excited by stimulation of both mPFC and BLA, indicating converging excitatory inputs from both afferent structures. These neurons were isolated by slowly advancing the recording electrode through the NAcc while single electrical stimulation pulses were delivered to the mPFC and BLA at an overall rate of 0.5Hz. NAcc neurons (typically not spontaneously active) were identified by the presence of action potentials following the stimulation pulses (see Figure 3.2). In this experiment, NAcc neurons were considered suitable for recording if they met two criteria: they produced at least a 50% spike ratio to 400μA stimulation of the BLA and 500μA stimulation of the mPFC; and the evoked spike latency was 20ms or less, consistent with monosynaptic, orthodromic transmission (see 3.3.2 and Figure 3.3).

5.3.3 BLA train stimulation and drug administration

Once a suitable neuron was found, the effect of BLA train stimulation on mPFC-evoked spiking was tested. MPFC stimulation current was adjusted to produce a 40-60% evoked spike rate; thus, the currents used were different for each neuron. The mPFC was first stimulated for 40 trials at a rate of 0.3Hz (baseline, 2.2 min). Then, as the mPFC stimulation continued, BLA train stimulation was introduced for 80 trials (4.4 min); in these trials, a single BLA stimulus train (5 pulses at 20Hz) was delivered 2.8s before the mPFC stimulation pulse. This interval was determined by the overall trial rate of 0.3Hz (3.3s interval), and the 0.5s gap between the mPFC pulse at the end of one trial, and the beginning of the BLA train in the next trial. After these 80 trials, mPFC stimulation continued for as long as the recording conditions remained stable (i.e. consistent signal-to-noise ratio, background noise and action potential shape). Because some

recordings became unstable before sufficient post-train responses could be observed, fewer post-train neurons are reported compared to the number reported during BLA trains.

In most experiments, the BLA stimulation current was adjusted to threshold intensities, such that the 5 pulse BLA stimulation train evoked spikes at about a ~50% response ratio (mean current 330μA). To test the role of BLA-evoked spiking, in a few experiments (n=7), the BLA current was adjusted below spike threshold for the first 40 train stimulation trials (subthreshold, mean 200μA), and then increased to produce a 50% spike rate in the next 40 train stimulation trials (threshold, mean 320μA). In 18 additional neurons for which data is not shown, only subthreshold BLA current was applied (mean 170μA).

The effects of BLA train stimulation were tested after systemic injection of the DA D1 antagonist SCH23390, DA D2 antagonists eticlopride or raclopride, or the NMDA channel blocker MK801. All drugs (acquired from Sigma, St Louis, MO) were dissolved in sterile 0.9% saline. The drug doses were (in mg/kg I.V.): SCH23390 0.5, eticlopride 0.2, raclopride 0.1, MK801 0.05 or 0.1. These doses have been shown previously to have potent activity at the target receptors and to be effective in relevant behavioral tasks (Caine and Koob 1994; Nicola and Deadwyler 2000; Floresco et al. 2001b; Cervo et al. 2003; Biondo et al. 2005).

The drugs were injected into the femoral vein 5-15 minutes prior to testing the effects of BLA train stimulation. Typically, only a single injection was administered and only one neuron was recorded per rat, with the following exceptions: In seven rats (1 SCH23390, 6 MK801), the drug was administered, and the BLA train effects tested on one neuron; then, at least 2 hours later, a second dose of the same drug was given and the BLA train effects tested in a second neuron. In three rats (all SCH23390), two neurons were tested within 2 hours of the same injection. These 10 neurons recorded after a second injection or after a delay did not have

different responses from the majority of neurons that were recorded immediately after the first injection (not shown). Furthermore, the D1 antagonist effects of SCH23390 have an extended period of activity well beyond two hours after systemic administration (Schulz et al. 1985; McQuade et al. 1988; Canini and Bourdon 1998; O'Neill and Shaw 1999).

5.3.4 Analysis and histology

The mPFC-evoked spike rate was measured before, during and after BLA train stimulation, as was the BLA-evoked spike rate during the train. The responses were grouped into bins of 10 trials each and the spike rates (spikes/100 stimuli, expressed as a percentage) were compared across stimulation conditions. The differences between treatment conditions were assessed with paired t-tests (within neuron) with Holm's modified Bonferroni correction for multiple comparisons. All mean values are expressed as "mean ± standard error of the mean"; all error bars on graphs show the standard error of the mean. Unless otherwise stated all p-values described in the text refer to the results of within-neuron paired t-tests, corrected for multiple comparisons if appropriate.

At the end of the experiment, the stimulating electrodes were marked by passing 100μA of current through them for 10 seconds. The final position of the recording electrode was marked by iontophoretic ejection of the Pontamine Sky Blue dye (-20μA for 60 minutes). The rats were decapitated, and their brains were fixed in 8% paraformaldehyde with 1% potassium ferricyanide. After 48 hours, they were transferred to a cryoprotectant solution of 25% sucrose. The brains were sliced on a freezing microtome and mounted onto slides for later Nissl staining using standard histological procedures. The location of the recording and stimulating electrodes

was determined using the atlases of Paxinos and Watson (1998; 2005). Neurons were recorded in both the shell and core subregions of the NAcc. For analysis purposes, only neurons that were certain to be within the core or shell were assigned to a subregion; if a neuron's actual or reconstructed location was within 0.1mm of the core/shell border, it was not assigned to either subregion.

5.4 RESULTS

A total of 80 NAcc neurons that were excited by stimulation of both the mPFC and BLA were recorded. The neurons were located in the medial shell or in the medial core near the shell border (Figure 5.1A). Because medium spiny neurons compose approximately 95% of striatal neurons (Kemp and Powell 1971; Jiang and North 1991a), almost all of the neurons recorded in this study were likely to be the medium spiny subtype. The stimulating electrode tips were

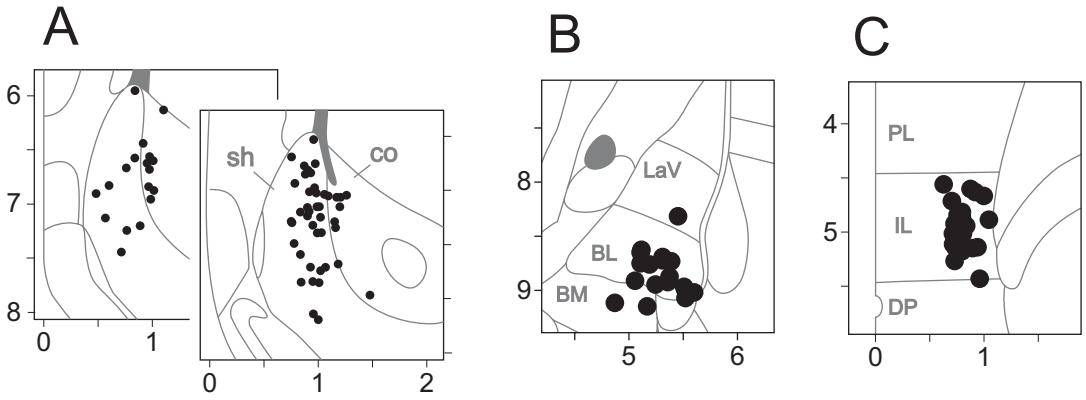

Figure 5.1 The locations of recorded cells and stimulating electrodes. **A** Two coronal atlas sections show the locations of 76/80 recorded cells in the NAcc. Most neurons were recorded in the shell (sh), and a smaller number were recorded in the core (co). **B** The BLA stimulating electrode tips were placed in the basolateral (BL), lateral (LaV) and basomedial (BM) subnuclei. Placements in BM were acceptable because the exposed lead extended 0.8mm dorsal of the tip, into the BL subnucleus. **C** The mPFC stimulating electrode tips were placed in the deep layers of infralimbic cortex (IL), with the exposed lead extending into the prelimbic cortex (PL) for placements in dorsal IL. For clarity, only 20 representative placements are shown each in **B** and **C**. The numbers indicate stereotaxic coordinates in mm. DP: dorsal peduncular cortex.

placed in the basolateral, lateral and basomedial subnuclei of the BLA and in the deep layers of the infralimbic subregion of the mPFC (Figure 5.1B).

5.4.1 BLA train stimulation depressed mPFC-evoked spiking

MPFC-evoked spiking was measured before, during and after train stimulation of the BLA (Figure 5.2). In 7 neurons from 4 rats, BLA stimulation was tested at both subthreshold (evoking no spikes) and threshold current amplitudes (evoking a ~50% response) (Figure 5.3).

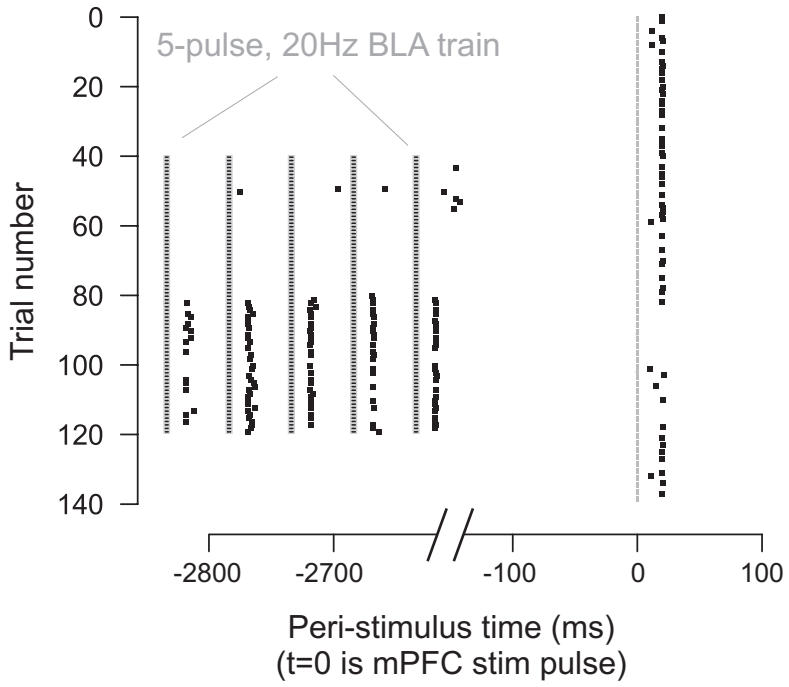

Figure 5.2 Raster showing mPFC- and BLA-evoked spiking in a single NAcc neuron over 140 trials. Each row shows the stimulation and evoked spiking during one trial. The black dots are spikes; the gray line at t=0 indicates the mPFC stimulation time in each trial; the black and gray stippled lines show BLA stimulation pulses. The mPFC was stimulated alone over trials 1-40. Subthreshold train stimulation of BLA applied 2833ms before mPFC stimulation (trials 41-80) had no effect on the mPFC-evoked spike rate; however threshold BLA stimulation (trials 81-120, ~50% average BLA-evoked response) reduced mPFC-evoked spiking.

Subthreshold BLA trains did not change the mPFC-evoked firing (decrease in spike rate of 2.1 ± 3.6%); however mPFC-evoked spiking was decreased during threshold BLA trains by 19.2 ± 4.7% compared to the spike rate before trains, and by 17.0 ± 3.7% compared to the spike rate during subthreshold train stimulation ($p<0.008$ for both comparisons) (Figure 5.3).

Nine additional neurons were tested with only threshold BLA stimulation (5 rats); their responses were similar, and thus these data were combined with the 7 neurons described above. In these 16 neurons, threshold BLA trains decreased the mPFC-evoked spike rate by 19.9 ± 3.6% ($p<0.001$). In a subset of neurons with stable post-train recording conditions (n=9/16), evoked spiking was recorded for 350 trials after the end of BLA trains. In these neurons the mPFC-evoked spike rate remained depressed after BLA stimulation by 17.0 ± 5.1% ($p<0.01$) (Figure 5.4). Although threshold stimulation of the BLA appeared to be necessary to decrease mPFC-evoked spiking, there was no correlation between the spiking evoked by the BLA stimuli and the resulting decrease in mPFC-evoked spiking (not shown; $r = 0.06$, $p<0.83$ for entire BLA train; $r = 0.02$, $p<0.94$ for the first BLA stimulus). Train stimulation had no effect on the latency, latency variance or binomial tendency (runs statistic) of the mPFC-evoked response (not shown).

To confirm that only threshold intensity BLA stimulation decreases mPFC-evoked firing, 18 additional neurons (12 rats) were tested using only subthreshold BLA trains. The mPFC-evoked spike rate was unchanged during train stimulation in these neurons (not shown; increase of 0.3 ± 3.7%, $p<0.94$), and was unchanged within 100 trials following the end of the trains (-3.8 ± 5.1%, n=16, $p<0.47$). In addition, there was no relationship between the amplitude of the BLA stimulation current and the change in mPFC-evoked spike rate during trains (not shown; $r = 0.14$, $p<0.58$).

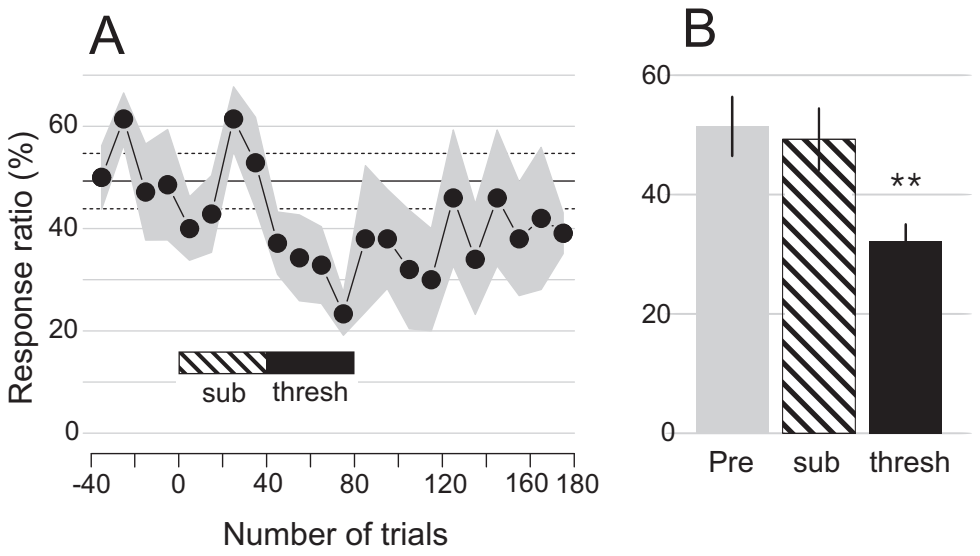

Figure 5.3 In 7 NAcc neurons, mPFC-evoked spiking was reduced during threshold BLA train stimulation. A This time series shows the mPFC-evoked spike ratio before BLA stimulation (trials -40 to 0), and during subthreshold ("sub", 1 to 40), and threshold ("thresh", 41 to 80) BLA train stimulation. The gray shaded area shows the SEM of the response. The black horizontal lines show the mean and SEM for trials -40 to 0. **B** MPFC-evoked firing decreased only during threshold BLA train stimulation (trials 41 to 80). ** indicates significant difference from "Pre" (trials -40 to 0) and "sub" (trials 1 to 40).

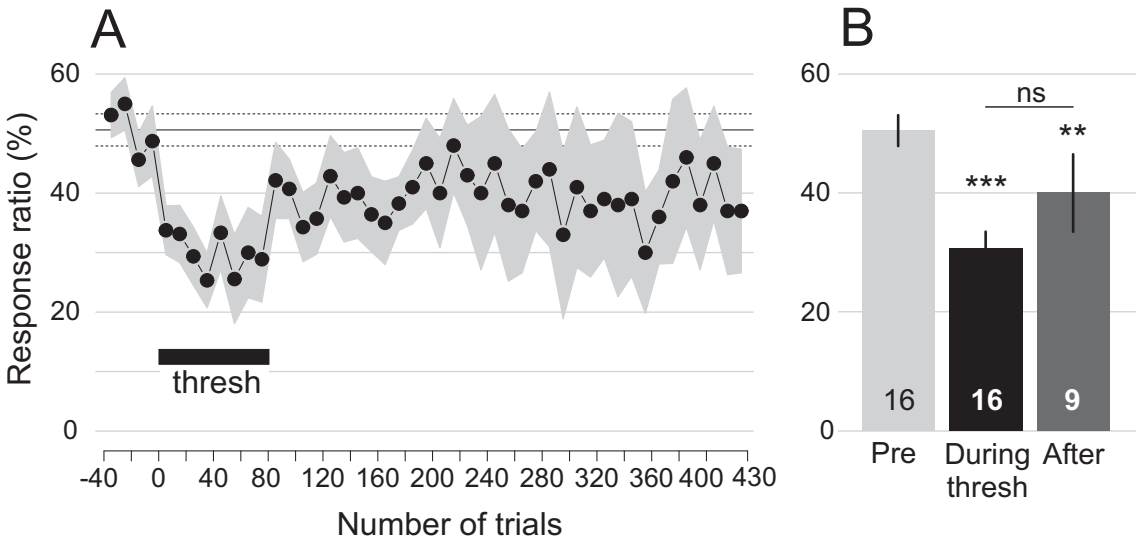

Figure 5.4 In 16 neurons, mPFC-evoked spiking was depressed during and after threshold BLA trains. A This time series shows mPFC-evoked firing before BLA stimulation (-40 to 0), during threshold BLA trains ("thresh", 1-80), and up to 350 trials post-BLA stimulation (for neurons with stable recording conditions). The gray area shows the SEM of the response, and the black horizontal lines show the mean and SEM over trials -40 to 0. This sample includes the seven neurons shown in Figure 5.3; to integrate their data into this figure, the 40 trials of subthreshold train stimulation were omitted from the time series. **B** mPFC-evoked firing not only decreased during threshold BLA stimulation (trials 0 to 80), but remained depressed after BLA trains ended (trials 100 to 430) in the 9/16 neurons for which data was available. *** and ** indicates significant difference from "Pre" (trials -40 to 0). There was no significant difference (ns) between spiking during and after trains. The numbers within the bars indicate the number of neurons.

5.4.2 DA or NMDA receptor blockade did not attenuate BLA train effects

To assess the roles of DA and NMDA receptors in the BLA-mediated depression of mPFC-evoked spiking, the effects of BLA train stimulation were measured in the presence of antagonists for DA D1 receptors (SCH23390), DA D2 receptors (eticlopride or raclopride), or NMDA receptors (MK801) (Figure 5.5). Typically, only one injection was performed and only one cell recorded per rat (see 5.3.3). In 14/14 neurons recorded after systemic injection of MK801, BLA train stimulation decreased mPFC-evoked spiking 17.1 ± 6.3% ($p<0.017$) during the train. Although the post-train spike rate appeared to be less than the pre-train response (-13.5 ± 6.5%, n=9/14), the difference did not reach statistical significance ($p<0.072$). In 17/17 neurons recorded after injection of SCH23390, mPFC-evoked firing decreased during the train by 17.6 ± 5.5% ($p<0.006$). Unlike the other antagonist drugs tested, SCH23390 treatment attenuated the post-train depression of mPFC-evoked firing; post-train spiking was only 6.0 ± 5.4% less than pre-train responses (n=11/17, $p<0.30$) and was 22.7 ± 4.7% greater than responses during the train (n=11/17, $p<0.002$). Finally, in 15/15 neurons recorded after injection of either eticlopride or raclopride (the data are similar and are pooled), mPFC-evoked firing was reduced both during (-17.1 ± 6.3%, $p<0.004$) and after BLA train stimulation (-13.5 ± 6.5%, n=11/15, $p<0.03$)).

In some neurons, the mPFC-evoked spike rate (with no BLA stimulation) was measured during administration of DA- or NMDA-receptor blocking drugs. Consistent with previous observations (West and Grace 2002), injection of SCH23390 reduced the mPFC-evoked spike rate by 26.4 ± 6.5% (not shown, n=8, $p<0.003$, paired t-test). However, as noted above, this decrease did not occlude spike rate depression due to BLA train stimulation. Neither MK801 (n=8) nor the DA D2 antagonist drugs (n=13) altered mPFC-evoked firing (not shown).

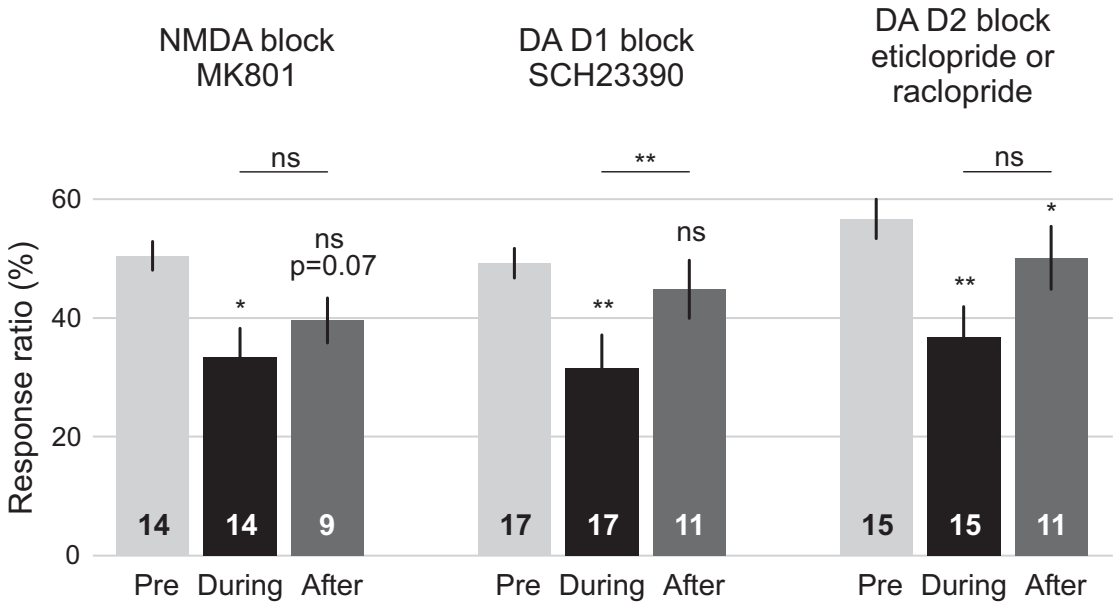

Figure 5.5 The effects of BLA train stimulation were not reversed by NMDA channel or DA receptor blockade. In neurons recorded after systemic injection of MK801 (n=14), SCH23390 (n=17), or eticlopride /raclopride (n=15), mPFC-evoked firing was reduced during threshold BLA trains (black bars). In neurons recorded with eticlopride or raclopride (n=11/15), post-train firing was also depressed (dark gray bars). In the presence of MK801 (n=9/14), post-train spiking was not significantly depressed, but showed no significant change from spiking during the train. In contrast, SCH23390 (n=11/17) blocked the post-train depression. ** and * indicate significant difference from "Pre" within each treatment, unless otherwise indicated. "ns" indicates no significant difference. The numbers within the bars indicate the number of neurons.

5.4.3 Shell and core neurons were depressed by BLA train stimulation

Among the 16 neurons recorded with no drug, 8 were definitively localized to the NAcc shell. BLA train stimulation significantly decreased mPFC-evoked firing in these 8 neurons (-21.6 ± 4.9%, $p<0.004$). BLA trains also decreased spiking in shell neurons recorded in the presence of MK801 (-27.7 ± 9.7%, n=6, $p<0.04$) or in the presence of DA D2 antagonists (-20.8 ± 7.0%, n=10, $p<0.016$). There was no significant change in the presence of SCH23390 (-16.2 ± 8.6%, n=9, $p<0.10$); however, the value was not different than that observed in the absence of drug

($p<0.6$, two sample t-test), and was well within the 95% confidence interval of the non-drug response (-10.0 to -33.2%).

In the experiments performed with no drug, 4 neurons were recorded in the core, and all 4 exhibited a decrease in mPFC-evoked spiking during BLA train stimulation. In the presence of MK801, 2 out of 3 confirmed core neurons exhibited a decrease; and in the presence of SCH23390, 1 out of 2 core neurons showed a decrease during train stimulation. There were no core neurons recorded in the D2 antagonist experiments. Because very few core neurons were recorded, no statistical comparisons between core and shell neurons were made.

5.5 DISCUSSION

NAcc neurons integrating BLA and mPFC inputs are an interface between affective and goal-related motor information. While these inputs can facilitate one another (Chapter 3), we hypothesized that strong BLA activation may depress mPFC-driven spiking, representing a second mechanism by which affect can influence behavior. Here, we show evidence for an activity-dependent, heterosynaptic depression of mPFC-to-NAcc input by the BLA at a cellular level. In neurons receiving excitatory input from both mPFC and BLA, spiking evoked by mPFC stimulation was reduced when the BLA was repetitively stimulated with trains; this reduction persisted for more than 300 trials (15 minutes) after the BLA train stimulation ended. BLA stimulation was only effective when the BLA current was at threshold, causing evoked spiking (~50% response rate) in the NAcc neuron being recorded. Not only did subthreshold BLA stimulation have no effect on mPFC-evoked responses on average, but there was also no

relationship between the subthreshold current amplitude and the change in mPFC-evoked firing. Thus, the effects of high frequency BLA stimulation appear to depend on BLA-evoked spiking activity in the recorded neuron, rather than the absolute intensity of BLA stimulation.

5.5.1 Mechanisms for amygdala-mediated response depression

While we hypothesized that BLA train stimulation would activate NMDA and DA receptors (Floresco et al. 2001b, a), blockade of these receptors did not reverse the robust depression of mPFC inputs during BLA trains. BLA stimulation was only effective when it evoked spikes in the recorded neuron, which is strong evidence that sufficient post-synaptic depolarization is necessary for depression of evoked spiking.

During action potential firing, the entire soma and dendritic arbor of medium spiny neurons are invaded by calcium (Kerr and Plenz 2002; Wolf et al. 2005), an important signaling molecule for synaptic plasticity (Charpier and Deniau 1997). Thus, repetitive BLA-evoked firing may increase calcium concentrations within the recorded neuron, leading to reduced synaptic excitability through calcium-activated second messengers. In addition to NMDA-receptors, medium spiny neurons express L-type calcium channels (Day et al. 2006b) and calcium-permeable AMPA receptors (Carter and Sabatini 2004). If intracellular calcium is involved in activity-dependent depression of mPFC inputs, non-NMDA channel types may provide sufficient calcium influx, as BLA train stimulation still depressed firing in the presence of MK801.

Activity-dependent depression could also be mediated by changes in the intrinsic excitability of the recorded neuron. Medium spiny neurons exhibit potassium conductances that

are activated (and inactivated) at near-threshold membrane potentials (Surmeier et al. 1989; Nisenbaum et al. 1994; Mahon et al. 2000). The depolarization-dependent opening of these channels during BLA train stimulation could lead to increased membrane conductance and decreased excitability, reducing the spike output evoked by mPFC stimulation (but see Mahon (2000)). Because the extracellular recordings we performed did not allow measurement of intrinsic membrane properties, intracellular recording will be necessary to determine whether and on what time scale BLA train stimulation engages active conductances.

While BLA-evoked spiking in the recorded neuron was necessary for the depression of mPFC inputs, the amount of spiking elicited by the BLA trains did not predict the magnitude of the depression. Thus, an activity-dependent mechanism may be necessary to initiate input depression, while other mechanisms may determine its magnitude. Apart from DA (which has been ruled out by the antagonist experiments), the NAcc is innervated by local and exogenous peptides, local interneurons and other neuromodulatory inputs that could be recruited during BLA stimulation (Delfs et al. 1998; Meredith 1999; Tepper and Bolam 2004).

The mechanisms underlying NAcc response depression following high frequency stimulation have been addressed in two in vitro studies. Pennartz and Lopez da Silva (1994) found that the excitatory response to mPFC afferent fibers decreased as the frequency of stimulation increased up to 12Hz, and Lape and Dani (2004) showed that 10Hz local stimulation decreased excitatory post-synaptic potentials and currents. However, these effects were attributable to pre-synaptic vesicle depletion (Lape and Dani 2004), and persisted in the presence of receptor antagonists for GABA, DA, NMDA, acetylcholine and opiates (Pennartz and Lopes da Silva 1994; Lape and Dani 2004). Because the response depression we have observed was measured in the non-train-stimulated mPFC input, pre-synaptic vesicle depletion is not a likely

mechanism. Of course, physiological conditions in vitro differ from those in vivo; therefore, the results obtained in these two different preparations may not be directly comparable.

5.5.2 mPFC input interactions with dopamine

High frequency stimulation of afferents to the NAcc (including BLA) can increase extracellular DA (Floresco et al. 1998; Jackson and Moghaddam 2001; Howland et al. 2002) and induce DA-dependent synaptic plasticity in the NAcc (Floresco et al. 2001a). Therefore, we hypothesized that BLA-mediated depression of mPFC inputs may also be dependent on these receptor systems. However, systemic blockade of DA receptors did not attenuate these effects. Interestingly, blockade of D1 receptors with SCH23390 did attenuate the response depression observed in the minutes after train stimulation ended. This is consistent with previous studies of the hippocampus-to-NAcc pathway, where a DA D1-dependent depression of BLA inputs was measured minutes after 20Hz hippocampal train stimulation (Floresco et al. 2001b). Thus, our results suggest that the afferent input arising from the BLA may also mediate a long-duration, DA D1-mediated depression of NAcc responses, and that this may represent a common consequence of intense afferent activation in this region.

Several studies have reported that both DA D1 and D2 receptors modulate cortically evoked responses in the NAcc and striatum (West and Grace 2002; Goto and Grace 2005b); however, we only found effects of D1 receptor blockade. This discrepancy may be due to the different ways in which evoked responses were measured or the different locations of the recorded responses: subthreshold EPSPs in dorsal striatum (West and Grace 2002) and field potentials in NAcc core (Goto and Grace 2005b) compared to extracellular spike activity in

NAcc shell and core in the current study. Brady & O'Donnell (2004) found that D2 receptor antagonists facilitated mPFC-evoked EPSPs in NAcc core and shell neurons, but only relative to responses evoked during the up-state, and only when NAcc DA was increased by ventral tegmental area stimulation. They reported no effect of D2 antagonists on responses evoked by mPFC stimulation alone (their figure 7C, D). Thus, the effects of D2 antagonists may depend on the method of measuring cortically evoked responses, the specific recording site, and the amount of synaptically released dopamine.

5.5.3 Implications for normal and pathological accumbens function

The reduction in mPFC-evoked firing by activation of the amygdala suggests that glutamatergic afferents to the NAcc interact in different ways that depend on input timing and activity state. We have previously shown that low frequency, subthreshold BLA stimulation can increase the mPFC-evoked spike rate in NAcc neurons, depending on the precise timing of the two inputs (Chapter 3). We now show that strong activation of the BLA at a long ISI reduces the efficacy of mPFC input. Thus, the BLA can facilitate or depress the mPFC drive of the NAcc depending on the timing and intensity of the activity in that afferent.

This dual-nature interaction between the BLA and mPFC inputs has implications for the transition from healthy cognitive function to pathological mental states. The NAcc has been posited as a structure where emotional and goal-related motor information directly interface: the NAcc integrates signals from the BLA, mPFC and other inputs, activating an appropriate motor plan (Nicola 2007). We have proposed that in healthy individuals, no single afferent system dominates NAcc activity, and behavior reflects the balanced influences of affective, goal-

oriented, and contextual constraints (Grace 2000). In several psychiatric disorders, the amygdala is persistently active or hyper-excitable. In individuals with schizophrenia, amygdala activation is greater than in healthy subjects in response to both neutral and fearful faces (Hall et al. 2008), and similar high levels of amygdala activation occur in both addicted individuals (Kilts et al. 2001) and sufferers of posttraumatic stress (Shin et al. 2005). The hyper-responsivity of the amygdala in these disorders may lead to an unusually elevated BLA drive of the NAcc and thus a decreased responsivity of NAcc neurons to prefrontal input. Unbalanced BLA/mPFC afferent interactions in the NAcc may lead to impaired motivation and cognitive function, as prefrontal signals (e.g. relating to learned safety (Milad and Quirk 2002) or non-drug goals (Kaufman et al. 2003)) become less effective in driving NAcc neurons and guiding behavior. Such a reduction in corticostriatal throughput could be a particularly devastating insult in schizophrenia and drug addiction, where the capability of prefrontal cortex itself is diminished during the course of the disease (Lewis et al. 2001; Kalivas and Volkow 2005). Although the mechanism underlying the amygdala-mediated depression of cortical inputs is unknown, this phenomenon has the potential to be a target for pharmacological intervention in the treatment of these disorders.

CHAPTER 6: GENERAL DISCUSSION

We have proposed that the BLA can influence mPFC-to-NAcc transmission, constituting an interface between motivation and action. Here we have shown evidence for this interface, and characterized the functional connectivity within this circuit. Stimulation of the BLA and Pavlovian conditioned cues elicited excitatory responses in a subset of mPFC neurons that projected to the NAcc, and BLA input facilitated mPFC-evoked spiking in NAcc neurons where BLA and mPFC afferents converged. Taken together, these results suggest a synergy of BLA effects: promoting firing in the mPFC-to-NAcc pathway and facilitating this cortically-evoked excitation in the NAcc. Interestingly, non-excited mPFC-to-NAcc neurons were often inhibited by the BLA, and response facilitation in NAcc neurons only occurred in cells receiving sufficient BLA input. Thus, the influence of the BLA may be selective for only certain mPFC-to-NAcc channels, biasing the choice of an appropriate motor plan (Nicola 2007). When BLA input strongly activated NAcc neurons, mPFC-evoked spiking was depressed, suggesting that the BLA gates mPFC-to-NAcc transmission through multiple mechanisms depending on activity state. We have previously theorized that affective input to NAcc constrains action selection (Grace 2000); our current findings are consistent with this hypothesis, and demonstrate specific cellular interactions – in both NAcc and mPFC – that may underlie this interface.

6.1 THE FUNCTIONAL BLA-MPFC-NACC CIRCUIT

6.1.1 Activity timing and input integration in the NAcc

The facilitation of mPFC inputs in NAcc neurons by the BLA was dependent on the relative timing of the stimulation pulses. With nearly synchronous stimulation of BLA and mPFC, facilitation was maximal; at ~10ms ISI, facilitation was minimal, and was accompanied by increased spike time variability; at 20ms ISI or more, no facilitation was apparent (Chapter 3). Such a narrow window for integration suggests that only temporally coordinated BLA and mPFC activity could give rise to facilitatory interactions (and promote ensemble formation) in NAcc neurons.

The BLA-mediated excitation of mPFC-to-NAcc neurons (Chapter 2) suggests that BLA activation can elicit excitatory drive in both the BLA-to-NAcc and mPFC-to-NAcc pathways; however, given the conduction times within this circuit (Figure 2.1 and Figure 3.3), converging synaptic activity would be likely to arrive in the NAcc at different times. A volley of action potentials arising simultaneously in BLA efferent neurons would reach terminals in the NAcc within 12ms (average) via the monosynaptic pathway, and would activate mPFC-to-NAcc afferent terminals within 25ms via the di-synaptic pathway (16ms BLA-to-mPFC + 9ms for IL-to-NAcc, on average). Thus, a 13ms gap would separate the two barrages of synaptic activity – comparable to the 11ms inter-stimulus interval that produced minimal facilitation of BLA and mPFC inputs. Although the shortest latency BLA-to-mPFC and mPFC-to-NAcc pathways (~5ms each) could give rise to nearly synchronous converging inputs, these represent only a

small fraction of fibers in the circuit; furthermore, the BLA activates both short and long latency mPFC-to-NAcc projections (see page 32).

Thus, our data suggest that simultaneous activation of BLA efferents should produce a non-synchronous pattern of BLA and mPFC afferent activity in the NAcc, resulting in negligible facilitation of these inputs. This hypothesis is consistent with our observation that the effects of mPFC inactivation on BLA-evoked spiking were indistinguishable from mPFC vehicle infusion (see 3.4.6). Our previous studies have emphasized that serial transmission of affective information from BLA to mPFC supports the expression of conditioned behaviors (Laviolette et al. 2005); however, purely serial transmission in this circuit appears to be incompatible with the timing-dependent facilitatory mechanisms in the NAcc that may be important for NAcc neuron output. If this is the case, what circumstances would give rise to facilitation of BLA/mPFC afferent activity? Activation of the BLA and mPFC by a third structure that projects to both (such as hippocampus (Ishikawa and Nakamura 2006)) could of course drive synchronous activity in both regions, resulting in facilitatory synaptic integration in the NAcc. However, we propose that BLA and mPFC neurons may be able to fire synchronously without an external influence, by entraining their activity to rhythmic oscillations.

In the awake brain, cortical output can be influenced by fast synchronized oscillatory activity. Although fast synchronization between BLA and mPFC has not yet been observed, the anatomy and physiology of these regions appear capable of supporting it: First, both the mPFC and BLA contain networks of GABAergic interneurons (Kawaguchi and Kubota 1997; Muller et al. 2005) that are essential for oscillatory activity (Bragin et al. 1995; Wang and Buzsaki 1996). Second, they are connected by relatively short latency direct projections that (in part) target interneurons (Brinley-Reed et al. 1995; Gabbott et al. 2006), an arrangement thought to be

essential for synchronization (Traub et al. 1996; Bibbig et al. 2002). Third, both the BLA and mPFC can generate gamma band oscillations (~40Hz) (Collins et al. 2001; Bauer et al. 2007; Izaki and Akema 2008, DJ Lodge, AA Grace, M Behrens, in preparation). Indeed, BLA and mPFC also synchronize their activity with other regions to which they are connected (Bauer et al. 2007). These oscillations are most evident in response to behaviorally relevant stimuli, and appear to occur when information transfer between the two regions is necessary for learning or behavior – such as between BLA and perirhinal cortex during trace conditioning (Bauer et al. 2007), and the mPFC and hippocampus during context learning (Jones and Wilson 2005). BLA/mPFC interactions appear to be essential for behavioral responses to conditioned stimuli (Laviolette et al. 2005) and for rewards to guide decision-making (Floresco and Ghods-Sharifi 2007). Given the anatomy and connectivity of these two regions, it is plausible that these interactions include synchronized fast oscillations, as well as serial transmission.

Synchronized, rhythmic BLA and mPFC firing would result in synchronous converging synaptic excitation in the NAcc, given the average conduction times of these pathways. Gamma-range synchronization (~40Hz) could restrict efferent firing to within <10ms (Bauer et al. 2007), which is well within the window for facilitatory interactions in NAcc neurons. As a result, gamma band synchronization may allow BLA and mPFC to exploit the integrative properties of NAcc neurons, activate specific neuronal ensembles, and dictate action selection. As in cortical systems, such coordination would not be tonically present, but would arise transiently depending on sensory input or cognitive demands (Gray et al. 1990; Engel and Singer 2001). Thus, while important behavioral functions may be mediated by serial transmission from the BLA to the mPFC (Laviolette et al. 2005; Floresco and Tse 2007) and from the mPFC to the BLA (Rosenkranz et al. 2003; Likhtik et al. 2005), synchronized BLA and mPFC firing (though

speculative) could be yet another mode of interaction – one particularly relevant to the drive of NAcc neurons.

6.1.2 BLA input effects in the NAcc: response facilitation or response depression?

Stimulation of the BLA either facilitated or depressed mPFC-evoked firing in NAcc neurons depending on the timing and intensity of the BLA input. Facilitation occurred when BLA input was below spike threshold and was coincident with mPFC inputs; depression occurred with high frequency BLA input that was suprathreshold at long ISIs. While these results suggest two distinct mechanisms for the BLA gating of mPFC inputs, it is unclear whether they occur independently or concurrently in the awake brain. If BLA afferent synaptic activity were bistable – varying between low and high intensity drive of NAcc neurons – then facilitation and depression could occur independently. BLA neurons do transition from low to high frequency firing in response to a conditioned stimulus (Schoenbaum et al. 1999; Maren and Quirk 2004), but the specific responses of BLA-to-NAcc neurons are not known. Furthermore, while rhythmic bistable synaptic inputs are conspicuous in medium spiny neurons recorded under anesthesia (Wilson and Kawaguchi 1996), desynchronized inputs dominate in the awake state (Steriade et al. 2001; Mahon et al. 2006).

Conversely, if BLA synaptic activity varied continuously from low to high intensity, then both mechanisms could be engaged simultaneously within the same neuron. We observed that facilitation between BLA and mPFC inputs was greatest for low intensity mPFC stimulation, and attenuated as input current increased. This suggests that as synaptic input increases and drives spiking, the facilitatory influences wane; then, as evoked firing increases, activity-dependent

depressive mechanisms may come into effect. Thus, the integration of inputs may transition smoothly from facilitation to depression as synaptic input varies from subthreshold to suprathreshold intensities. Further work is necessary to experimentally validate this proposed relationship, and to explicate the mechanisms that underlie the response facilitation and depression that we observed.

6.1.3 Effects of anesthesia on neuronal responses to conditioned cues

We observed NAcc and mPFC neuronal responses to Pavlovian conditioned cues in chloral hydrated-anesthetized rats. In mPFC, a subset of neurons was excited by the conditioned cues (consistent with responses observed in awake rats (Baeg et al. 2001; Gilmartin and McEchron 2005)), suggesting that some cue-encoding mechanisms in mPFC are preserved in our anesthetized preparation. Cortical neurons under anesthesia and during natural sleep exhibit slow, synchronized oscillatory activity that becomes non-synchronized upon wakefulness (Amzica and Steriade 1998). Interestingly, the balance between excitatory and local inhibitory transmission appears to be maintained during this transition, as wakefulness is associated with both higher spontaneous firing in (fast spiking) putative inhibitory interneurons and an increase in input resistance in pyramidal neurons (Steriade et al. 2001). This consistent balance may allow excitatory affective information from BLA to activate the same ensembles of mPFC neurons in both the anesthetized and awake states. Indeed, the proportion of cue-responsive mPFC neurons in the present study (Chapter 2) is comparable to previous recordings in awake rats (Baeg et al. 2001; Gilmartin and McEchron 2005).

In contrast, NAcc neurons recorded under anesthesia in the present study showed only negligible excitation to conditioned cues, unlike reports in awake rats (Nicola et al. 2004; Roitman et al. 2005). Thus, chloral hydrate anesthesia appears to disrupt the processing of affective information to a much greater extent in the NAcc than in the mPFC. Dopamine release may be necessary for cue-evoked excitatory responses in the NAcc (Nicola et al. 2005), and we have hypothesized that this dopamine signal may be absent in our preparation (see 4.5). However, non-dopaminergic mechanisms are also likely to contribute to the decreased excitability of NAcc neurons. For example, striatal neurons recorded under anesthesia exhibit less excitation to somatic sensory stimulation and iontophoretically applied glutamate than those recorded in awake rats treated with dopamine D1 and D2 receptor antagonists (Kiyatkin and Brown 2007). This may be explained by strong, rhythmic hyperpolarizations that occur during natural sleep and anesthesia, but that are absent in the awake state (O'Donnell and Grace 1995; Mahon et al. 2006). Thus, cue-evoked excitatory activity may be depressed under anesthesia due to medium spiny neuron membrane polarization and insufficient dopaminergic tone.

6.2 THE MPFC, NACC AND CONDITIONED FEAR

The present findings and previous work in our lab implicate the mPFC-to-NAcc projection in learned fear responses, such as freezing to a conditioned stimulus (Laviolette et al. 2005). While the mPFC outputs to hypothalamus and brainstem would be expected to contribute to defensive behavior (Price 1999), the role of the mPFC-to-NAcc pathway (and the mPFC in general) to classical conditioned fear responses is not clear (Pezze and Feldon 2004; Quirk et al. 2006). We

propose two hypotheses that are consistent with the current results, and that may explain some of the seemingly contradictory observations of the mPFC and fear.

First, we propose that the many independent efferent projections of the mPFC support multiple actions in response to fear conditioned stimuli. For example, we have shown a role for mPFC in the expression of conditioned fear, while others have shown its role in fear extinction (Milad and Quirk 2002). While extinction may rely on the mPFC innervation of the amygdala (Quirk et al. 2003; Berretta et al. 2005), fear expression may rely on the mPFC output to the NAcc (Chapter 2, Laviolette et al. 2005). Because there is minimal overlap between these two efferent systems (Pinto and Sesack 2000), they are independent and thus may be activated at different times under different circumstances. Indeed, we have shown that anatomical segregation of mPFC projections corresponds to a functional segregation, as the BLA and conditioned odors activated mPFC-to-NAcc projecting neurons, but not mPFC-to-contralateral mPFC projecting neurons.

The second hypothesis is that the mPFC is usually involved in – but is not absolutely necessary for – fear responses to conditioned stimuli. Somatic and autonomic fear reactions are mediated by brainstem and hypothalamic nuclei, such as the lateral hypothalamus (LHA) and the periaqueductal gray (PAG) (LeDoux et al. 1988). These regions are innervated (both directly and hierarchically) by a network of telencephalic nuclei, including the amygdala central nucleus, mPFC, BLA, and NAcc (Price 1999; LeDoux 2000). We propose that Pavlovian conditioning normally recruits all of these nuclei, rather than only those that are strictly necessary for conditioned responses. As a result, all of the nodes in this network respond to conditioned stimuli in a way that promotes (or is permissive for) fear responses. For example, the mPFC (possibly via the NAcc) may bring a halt to ongoing motor behaviors that are incompatible with

freezing and other defenses (similar to the way orbitofrontal cortex neurons encode "no-go" responses to aversive instrumental cues (Schoenbaum et al. 1999)). When mPFC activity is suddenly disrupted (e.g. Laviolette et al. 2005; Corcoran and Quirk 2007b), the loss of its influence on the amygdala, NAcc, LHA and PAG results in weak or aberrant activity throughout the network, disrupting the behavioral response. Permanent lesions of the mPFC, however, result in no long-lasting deficit (Quirk et al. 2000), due to compensatory mechanisms in the other nuclei in the network.

In summary, the segregated output pathways from the mPFC may allow this one region to mediate diverse responses to conditioned cues. Outputs to the brainstem, hypothalamus and NAcc may be recruited during classical conditioning and participate in defensive fear responses. Although the mPFC may not be necessary for these responses, its involvement may confer behavioral flexibility, as it receives inputs from hippocampus, orbital prefrontal cortex, and the VTA (Conde et al. 1995). Thus, the mPFC may be a site where contextual or other motivational information can intervene to modify conditioned fear (Carnicella et al. 2006; Corcoran and Quirk 2007a).

6.3 INPUT INTEGRATION IN NACC NEURONS: REMAINING QUESTIONS

The mechanisms underlying spike generation are one of the most intensely studied topics in striatal physiology. In the NAcc, the influence of converging subcortical and cortical afferents is of particular interest, as they may mediate action selection based on cognitive, contextual and affective constraints. By characterizing the spiking activity due to BLA and mPFC activation,

we have shown one set of interactions that may explain how multiple inputs influence NAcc output. However, many details and underlying mechanisms remain to be studied.

6.3.1 Mechanisms of spike generation in NAcc neurons

Given the intrinsic properties of NAcc medium spiny neurons, multiple synaptic inputs appear necessary for them to fire (Wilson and Kawaguchi 1996; Blackwell et al. 2003). While the study shown in Chapter 3 demonstrated some properties of coincidentally evoked spikes, the mechanisms that underlie these properties are not entirely known. Furthermore, our observations are not entirely congruent with previous observations of evoked subthreshold responses. For example, Goto and O'Donnell (2002) measured BLA- and mPFC-evoked EPSPs, and reported reduced variability at short ISIs, as well as facilitatory and depressive interactions at 100ms ISIs; however, the comparable experiments in the present studies showed no changes in spike variability, and no facilitation or depression beyond 20ms ISIs. Thus, there appears to be an explanatory gap between the subthreshold and suprathreshold effects of amygdala and cortical afferent integration.

Resolving this discrepancy will require systematic study of synaptic inputs at both subthreshold and suprathreshold intensities. For example, a current/response study (e.g. Figure 3.7) using intracellular recording could show how sublinear summation of subthreshold inputs (Goto and O'Donnell 2002) evolves into spiking with greater stimulation. In addition, such work could take into account the powerful intrinsic conductances (Wilson and Kawaguchi 1996) and extrinsic afferent activity (O'Donnell and Grace 1995) that operate at subthreshold voltages. Finally, veridical computational models of medium spiny neurons (Wolf et al. 2005; Moyer et al.

2007) may also be useful for determining the contributions of specific conductances to multi-input-evoked spike discharge.

6.3.2 Common and distinct features of limbic and cortical inputs to the NAcc

Activation of the BLA changed the latency and probability of mPFC-evoked spiking. These afferent interactions may reflect the unique properties of the BLA and mPFC inputs, or may be due to intrinsic NAcc neuron properties. Thus, it is unknown whether other glutamatergic afferent inputs exhibit interactions similar to those between BLA and mPFC. There is clear evidence for structural and functional differences among the inputs to the NAcc. For example, although the NAcc receives multiple sources of excitatory input, the hippocampal input alone appears to be necessary and sufficient for the production of bistable states (O'Donnell and Grace 1995). At the anatomical level, cortical, amygdalar and hippocampal afferent terminals can be distinguished based on vesicle size (French and Totterdell 2004), suggesting possible differences in synaptic glutamate release. Despite this evidence, the distinct functional properties of the different inputs are not known. These distinct properties correspond to the differential influence of affective, contextual and goal-related information on NAcc output; thus, discovering asymmetrical or differential interactions among NAcc afferents is crucial to understanding NAcc information flow.

While we demonstrated symmetrical facilitation between BLA and mPFC inputs, this symmetry was not tested in all experiments. Non-symmetrical interactions have been observed in amygdalar- and cortically-evoked EPSPs (Goto and O'Donnell 2002), but as we have noted above, subthreshold observations may not be sufficient to explain spiking. In Chapter 5, we

observed BLA-mediated depression of mPFC-to-NAcc transmission, similar to a hippocampal-mediated depression reported previously (Floresco et al. 2001b). Because these effects were activity-dependent, the underlying mechanism may rely on calcium influx or active membrane properties, allowing any sufficient depolarizing input to produce decreased responsivity. Thus, it will be necessary to explicitly test whether the BLA/mPFC interactions we have observed are common among the many glutamatergic afferents to the NAcc, or are exclusive to the mPFC and BLA. In addition, anatomical descriptions of afferent synapse patterns within the medium spiny dendritic tree may also be informative, as input summation appears to depend on the distance between activated synapses (Carter et al. 2007). While recent evidence has shown convergence of multiple inputs into the same NAcc neurons, these studies did not attempt to find the spatial distribution of these inputs (French and Totterdell 2002, 2003).

6.3.3 Dopamine interactions with glutamatergic inputs

In addition to glutamatergic afferents, dopamine input appears to be obligatory for NAcc neurons to signal salient cues and guide appropriate behavioral responses (Yun et al. 2004; Nicola et al. 2005; Ambroggi et al. 2007). Because dopamine is a modulator of glutamatergic inputs and because multiple glutamatergic inputs are necessary to elicit spiking, it follows that the mechanisms underlying multi-input synaptic integration may themselves be modulated by dopamine during ongoing NAcc activity. We saw no effect of dopamine antagonists on BLA facilitation of mPFC-evoked spiking; however this result is not definitive evidence that dopamine does not modulate excitatory BLA/mPFC interactions. Indeed, it may be necessary to observe the intracellular correlates of dopamine/glutamate interactions (West and Grace 2002),

or to stimulate dopamine release above baseline levels (Brady and O'Donnell 2004) in order to determine its effects. Recent NAcc field potential recordings (Goto and Grace 2005a) and computational models (Moyer et al. 2007) have suggested that dopamine modulates both ongoing synaptic integration and long term limbic/cortical plasticity; however this has yet to be observed in single neurons. Despite the extensive study of dopamine's effects on excitatory transmission, (Nicola et al. 2000; West et al. 2003), there is little understanding of how dopamine influences multi-input synaptic integration in the striatum. Given that dense dopamine innervation and multi-input convergence are perhaps the most conspicuous features of the NAcc, it will be ultimately necessary to account for both of these phenomena in order to understand NAcc function.

6.4 EMOTION, ACTION, AND PRIMATE MEDIAL FRONTAL CORTEX

The human brain contains an amygdala-ventral striatum-medial frontal cortex circuit that has similarities to the rodent circuit in the current study (Ongur and Price 2000). Thus, the interactions we have observed in the rodent may be applicable to human emotion and motivation. While the primate and rodent BLA appear to have similar roles in processing emotional stimuli (Baxter and Murray 2002), the comparability of primate and rodent mPFC is less clear. Human and non-human primate medial frontal cortex comprises many more distinct cytoarchitectonic regions than rodent mPFC (Ongur and Price 2000; Palomero-Gallagher et al. 2008), and areas that may be comparable on anatomical bases do not always appear to be functionally equivalent. For example, human subgenual anterior cingulate cortex (sACC) is agranular and receives dense

BLA input (Price 2007; Palomero-Gallagher et al. 2008), similar to rodent PL and IL; however, unlike the rodent mPFC, sACC does not appear to be involved in goal-directed behavior[†]. Instead, other medial frontal regions exhibit goal-related encoding (Matsumoto et al. 2003), suggesting that the cognitive functions performed by PL and IL in rodent mPFC is supported by regions unlike PL and IL within the elaborated medial frontal cortex of primates.

Because much of primate medial frontal cortex receives BLA input and projects to ventral striatum (Ongur and Price 2000; Price 2007), it is possible that these areas use learned emotional information to guide behavior in the same way as PL and IL do in the rodent (e.g. (Baxter et al. 2000; Schoenbaum et al. 2003)). Indeed, humans with focal amygdala lesions exhibit weaker choice- and reward-related activity in medial frontal areas (Hampton et al. 2007). Thus, despite the anatomical differences between species, the preserved function of medial frontal cortex suggests that it is critical for emotion and goal-directed action in both rodents and primates – and that data obtained from rodent models may show neuronal interactions that are relevant to limbic-cortical-striatal circuitry in humans.

[†] Human sACC is associated with negative mood and clinical depression (Mayberg et al. 1999), and responds to images that depict painful or "disgusting" situations (Benuzzi et al. 2008). Like in the rodent, sACC appears to also have autonomic and visceromotor functions (Nagai et al. 2004; Wong et al. 2007).

6.5 PATHOLOGICAL AND HEALTHY INFORMATION FLOW WITHIN THE BLA-MPFC-NACC CIRCUIT

6.5.1 Information integration in healthy cognitive function

Affective, contextual and goal-related motor signals innervate single NAcc neurons. NAcc neurons can be driven to fire by a single strong excitatory input, or by multiple weaker inputs. This suggests that NAcc neuron firing (and behavior) may be influenced by a single cue with high predictive value, or by multiple, less predictive pieces of information (cues, contexts, prepotent motor responses, etc.) impinging upon a single cell. In this way, integration of inputs in the NAcc may be necessary for optimal behavior in the face of complex or incomplete information. Furthermore, because input timing and intensity was critical for facilitatory BLA/mPFC interactions, the NAcc may only be capable of integrating information when its afferent nuclei are undamaged and fully functional. In several psychiatric disorders, pathological changes in afferent activity to the NAcc (in particular the mPFC and BLA) may disrupt the balance of inputs to NAcc neurons. This disruption may lead to unbalanced information flow, and to actions that are driven inappropriately by affect or by preservative goal-seeking, rather than by the coordinated influence of affect, context, and goals.

6.5.2 Deficits in inhibitory transmission in schizophrenia

We have previously proposed that misregulation of NAcc by the hippocampus and the concomitant effects on dopaminergic tone contribute to the pathology of schizophrenia (Grace

2000). However, cortical pathology also plays a significant role in the disease. In individuals with schizophrenia there are consistent reductions in protein and mRNA markers for GABAergic transmission throughout the cortex (Lewis et al. 2005; Hashimoto et al. 2008). These deficits may also be present in rodent models of the disease (DJ Lodge, AA Grace, M Behrens, in preparation). This loss of interneuronal signaling could impact BLA-to-mPFC transmission, as we and others have observed a BLA-evoked inhibition of mPFC projection neurons (Floresco and Tse 2007) that is likely dependent on activation of local interneurons (Swadlow 1994; Dilgen and O'Donnell 2004; Gabbott et al. 2006).

Consistent with the role of inhibitory interneurons in generating fast oscillatory activity (Bragin et al. 1995), schizophrenic individuals exhibit altered gamma band EEG activity compared to unaffected controls (Spencer et al. 2004). We have hypothesized that fast synchronized oscillations between BLA and mPFC may permit these areas to drive NAcc neuron firing (see 6.1.1). If this is the case, schizophrenia could result in a reduced ability of cortical and amygdalar afferents to activate NAcc neurons, form ensembles and influence behavior. Such a deficit in excitatory synaptic integration could lead to the impaired motivation and goal-directed behavior exhibited by those suffering from the disease (Brown and Pluck 2000).

6.5.3 Synaptic plasticity in the NAcc and drug addiction

Exposure to psychostimulant drugs changes the excitability of NAcc neurons. While the specific effects can depend on several experimental factors (route of administration, length of withdrawal, recording site, etc.), it has been proposed that drug sensitization leads to increased efficacy of cortico-accumbens transmission with an accompanying decrease in intrinsic medium

spiny neuron excitability (Kalivas and Hu 2006). Despite clear evidence that the BLA-to-NAcc pathway is critical for drug seeking (Ledford et al. 2003; Di Ciano and Everitt 2004), it is not known if this pathway also experiences plasticity due to sensitization. Sensitization increases both spines and branches in medium spiny neuron dendrites (Kolb et al. 2003; Li et al. 2003), suggesting that drug exposure can induce a dramatic restructuring of synaptic inputs. Furthermore, cocaine sensitization potentiates hippocampal-to-NAcc transmission (Goto and Grace 2005a) as measured by field potentials, suggesting that drug effects are not limited to cortical inputs.

Importantly, plastic changes in mPFC-to-NAcc and/or BLA-to-NAcc transmission could disrupt input integration. Potentiation of these pathways could reduce facilitatory effects between these inputs, as we have shown that weak inputs produce the greatest increase in evoked firing (Figure 3.7). Furthermore, unequal potentiation of one input pathway could bias the spike timing in NAcc ensembles, as we have shown that mPFC inputs dictate response latency when stimulated at higher intensity (Figure 3.10, Table 3.1). These disruptions could have multiple effects on the processing of motor, contextual and affective information by the NAcc, and lead to the compulsion and lack of behavioral flexibility (Goto and Grace 2005a) seen in addicted individuals.

6.5.4 Elevated amygdala activity in schizophrenia, drug addiction and PTSD

We have proposed that spike timing may be a key factor that defines neuronal ensembles within the ongoing activity in the NAcc; and we have shown evidence that input strength can influence spike timing. Therefore, in individuals with pathologically elevated amygdala activity (sufferers

of addiction, schizophrenia and PTSD (Kilts et al. 2001; Shin et al. 2005; Kalivas and Hu 2006; Hall et al. 2008)), increased synaptic activity in BLA-to-NAcc afferents could subtly shift the dynamics of ensemble formation and timing. In this way, the BLA may persistently dictate NAcc activity, resulting in behavior that inappropriately reflects affect – to the detriment of goal-directed or contextual constraints (Grace 2000).

6.6 CONCLUSIONS: THE PHYSIOLOGICAL BASIS FOR THE LIMBIC/MOTOR INTERFACE

The idea that the NAcc forms a link between motivation and action was inspired by an anatomical finding: that the NAcc is richly supplied with limbic afferents, and projects densely to the basal ganglia (Mogenson et al. 1980). Even though this hypothesis and the evidence supporting it have been updated and refined, many studies of the NAcc (including the present studies) are anchored by this anatomical view of the limbic-motor interface. We showed physiological interactions in the NAcc and associated circuitry that may be critical for the integration of motivational and motor-related information. One of the striking findings we encountered was the sensitivity of NAcc neurons to the state of its afferent inputs: the BLA facilitated, depressed, or had no effect on mPFC-evoked spiking depending on when and how strongly it was these inputs were activated. These physiological constraints suggest that processing in NAcc neurons depends on the specific activity taking place in it afferents. Thus, the physiological interactions we have observed may be selective, transient phenomena, limited in time and magnitude by sensory stimuli, attentional capacity, cognitive demands, and other

factors. In this sense, the limbic-motor interface is more than an anatomically defined circuit; it is a circuit that has entered an activity state conducive to the integration of affective and motor signals. Furthermore, while the etiology of motivational disorders (such as addiction) can be anatomical or genetic in nature, the core pathology may be a failure of limbic-motor circuits to maintain activity states that support healthy motivations and adaptive actions.

REFERENCES

Ambroggi F, Ishikawa A, Seroussi A, Fields HL, Nicola SM (2007) Evidence that dopamine enhances nucleus accumbens responses to incentive cues by gating an excitatory input from the basolateral amygdala. In: Society for Neuroscience Annual Meeting, p Program No. 310.318. San Diego, CA: Neuroscience Meeting Planner.

Amzica F, Steriade M (1998) Electrophysiological correlates of sleep delta waves. Electroencephalogr Clin Neurophysiol 107:69-83.

Angel A, Gratton DA (1982) The effect of anaesthetic agents on cerebral cortical responses in the rat. Br J Pharmacol 76:541-549.

Anglada-Figueroa D, Quirk GJ (2005) Lesions of the basal amygdala block expression of conditioned fear but not extinction. J Neurosci 25:9680-9685.

Bacon SJ, Headlam AJ, Gabbott PL, Smith AD (1996) Amygdala input to medial prefrontal cortex (mPFC) in the rat: a light and electron microscope study. Brain Res 720:211-219.

Baeg EH, Kim YB, Jang J, Kim HT, Mook-Jung I, Jung MW (2001) Fast spiking and regular spiking neural correlates of fear conditioning in the medial prefrontal cortex of the rat. Cereb Cortex 11:441-451.

Barrot M, Olivier JD, Perrotti LI, DiLeone RJ, Berton O, Eisch AJ, Impey S, Storm DR, Neve RL, Yin JC, Zachariou V, Nestler EJ (2002) CREB activity in the nucleus accumbens shell controls gating of behavioral responses to emotional stimuli. Proc Natl Acad Sci U S A 99:11435-11440.

Bauer EP, Paz R, Pare D (2007) Gamma oscillations coordinate amygdalo-rhinal interactions during learning. J Neurosci 27:9369-9379.

Baxter MG, Murray EA (2002) The amygdala and reward. Nat Rev Neurosci 3:563-573.

Baxter MG, Parker A, Lindner CC, Izquierdo AD, Murray EA (2000) Control of response selection by reinforcer value requires interaction of amygdala and orbital prefrontal cortex. J Neurosci 20:4311-4319.

Berretta S, Pantazopoulos H, Caldera M, Pantazopoulos P, Pare D (2005) Infralimbic cortex activation increases c-Fos expression in intercalated neurons of the amygdala. Neuroscience 132:943-953.

Bibbig A, Traub RD, Whittington MA (2002) Long-range synchronization of gamma and beta oscillations and the plasticity of excitatory and inhibitory synapses: a network model. J Neurophysiol 88:1634-1654.

Biondo A-M, Clements R, Hayes D, Eshpeter B, Greenshaw A (2005) NMDA or AMPA/kainate receptor blockade prevents acquisition of conditioned place preference induced by D2/3 dopamine receptor stimulation in rats. Psychopharmacology 179:189-197.

Birrell JM, Brown VJ (2000) Medial frontal cortex mediates perceptual attentional set shifting in the rat. J Neurosci 20:4320-4324.

Bisley JW, Krishna BS, Goldberg ME (2004) A rapid and precise on-response in posterior parietal cortex. J Neurosci 24:1833-1838.

Blackwell KT, Czubayko U, Plenz D (2003) Quantitative estimate of synaptic inputs to striatal neurons during up and down states in vitro. J Neurosci 23:9123-9132.

Block AE, Dhanji H, Thompson-Tardif SF, Floresco SB (2007) Thalamic-prefrontal cortical-ventral striatal circuitry mediates dissociable components of strategy set shifting. Cereb Cortex 17:1625-1636.
Brady AM, O'Donnell P (2004) Dopaminergic modulation of prefrontal cortical input to nucleus accumbens neurons in vivo. J Neurosci 24:1040-1049.
Bragin A, Jando G, Nadasdy Z, Hetke J, Wise K, Buzsaki G (1995) Gamma (40-100 Hz) oscillation in the hippocampus of the behaving rat. J Neurosci 15:47-60.
Brinley-Reed M, Mascagni F, McDonald AJ (1995) Synaptology of prefrontal cortical projections to the basolateral amygdala: an electron microscopic study in the rat. Neurosci Lett 202:45-48.
Brown RG, Pluck G (2000) Negative symptoms: the 'pathology' of motivation and goal-directed behaviour. Trends Neurosci 23:412-417.
Buffalari DM, Grace AA (2007) Noradrenergic modulation of basolateral amygdala neuronal activity: opposing influences of alpha-2 and beta receptor activation. J Neurosci 27:12358-12366.
Burgos-Robles A, Vidal-Gonzalez I, Santini E, Quirk GJ (2007) Consolidation of fear extinction requires NMDA receptor-dependent bursting in the ventromedial prefrontal cortex. Neuron 53:871-880.
Burhans LB, Gabriel M (2007) Contextual modulation of conditioned responses: role of the ventral subiculum and nucleus accumbens. Behav Neurosci 121:1243-1257.
Caine SB, Koob GF (1994) Effects of dopamine D-1 and D-2 antagonists on cocaine self-administration under different schedules of reinforcement in the rat. J Pharmacol Exp Ther 270:209-218.
Canini F, Bourdon L (1998) Dopamine involvement in thermoregulatory responses to heat in rats. Neuroscience Letters 241:91-94.
Cardinal RN, Parkinson JA, Hall J, Everitt BJ (2002) Emotion and motivation: the role of the amygdala, ventral striatum, and prefrontal cortex. Neurosci Biobehav Rev 26:321-352.
Carelli RM (2002) The nucleus accumbens and reward: neurophysiological investigations in behaving animals. Behav Cogn Neurosci Rev 1:281-296.
Carnicella S, de Vasconcelos AP, Pain L, Majchrzak M, Oberling P (2006) Fos immunolabelling evidence for brain regions involved in the Pavlovian degraded contingency effect and in its disruption by atropine. Neuropharmacology 51:102-111.
Carter AG, Sabatini BL (2004) State-dependent calcium signaling in dendritic spines of striatal medium spiny neurons. Neuron 44:483-493.
Carter AG, Soler-Llavina GJ, Sabatini BL (2007) Timing and location of synaptic inputs determine modes of subthreshold integration in striatal medium spiny neurons. J Neurosci 27:8967-8977.
Cassaday HJ, Horsley RR, Norman C (2005) Electrolytic lesions to nucleus accumbens core and shell have dissociable effects on conditioning to discrete and contextual cues in aversive and appetitive procedures respectively. Behav Brain Res 160:222-235.
Cervo L, Carnovali F, Stark JA, Mennini T (2003) Cocaine-seeking behavior in response to drug-associated stimuli in rats: involvement of D3 and D2 dopamine receptors. Neuropsychopharmacology 28:1150-1159.
Chang HT, Kitai ST (1985) Projection neurons of the nucleus accumbens: an intracellular labeling study. Brain Res 347:112-116.

Charpier S, Deniau JM (1997) In vivo activity-dependent plasticity at cortico-striatal connections: Evidence for physiological long-termÂ potentiation. Proceedings of the National Academy of Sciences 94:7036-7040.
Christakou A, Robbins TW, Everitt BJ (2004) Prefrontal cortical-ventral striatal interactions involved in affective modulation of attentional performance: implications for corticostriatal circuit function. J Neurosci 24:773-780.
Collins DR, Pelletier JG, Pare D (2001) Slow and fast (gamma) neuronal oscillations in the perirhinal cortex and lateral amygdala. J Neurophysiol 85:1661-1672.
Conde F, Maire-Lepoivre E, Audinat E, Crepel F (1995) Afferent connections of the medial frontal cortex of the rat. II. Cortical and subcortical afferents. J Comp Neurol 352:567-593.
Conover WJ, Johnson ME, Johnson MM (1981) A comparative study of tests for homogeneity of variances, with applications to the outer continental shelf bidding data. Technometrics 23:351-361.
Corcoran KA, Quirk GJ (2007a) Recalling safety: cooperative functions of the ventromedial prefrontal cortex and the hippocampus in extinction. CNS Spectr 12:200-206.
Corcoran KA, Quirk GJ (2007b) Activity in prelimbic cortex is necessary for the expression of learned, but not innate, fears. J Neurosci 27:840-844.
Coutureau E, Dix SL, Kilcross AS (2000) Involvement of the medial prefrontal cortex--basolateral amygdala pathway in fear--related behaviour in rats. European Journal of Neuroscience 12(Suppl 11.):156.
Cruikshank SJ, Lewis TJ, Connors BW (2007) Synaptic basis for intense thalamocortical activation of feedforward inhibitory cells in neocortex. Nat Neurosci 10:462-468.
Dalley JW, Cardinal RN, Robbins TW (2004) Prefrontal executive and cognitive functions in rodents: neural and neurochemical substrates. Neurosci Biobehav Rev 28:771-784.
Day J, Wheeler R, Roitman M, Carelli R (2006a) Nucleus accumbens neurons encode Pavlovian approach behaviors: evidence from an autoshaping paradigm. European Journal of Neuroscience 23:1341-1351.
Day M, Wang Z, Ding J, An X, Ingham CA, Shering AF, Wokosin D, Ilijic E, Sun Z, Sampson AR, Mugnaini E, Deutch AY, Sesack SR, Arbuthnott GW, Surmeier DJ (2006b) Selective elimination of glutamatergic synapses on striatopallidal neurons in Parkinson disease models. Nat Neurosci 9:251-259.
Degenetais E, Thierry AM, Glowinski J, Gioanni Y (2003) Synaptic influence of hippocampus on pyramidal cells of the rat prefrontal cortex: an in vivo intracellular recording study. Cereb Cortex 13:782-792.
Delfs JM, Zhu Y, Druhan JP, Aston-Jones GS (1998) Origin of noradrenergic afferents to the shell subregion of the nucleus accumbens: anterograde and retrograde tract-tracing studies in the rat. Brain Res 806:127-140.
Di Ciano P, Everitt BJ (2004) Direct interactions between the basolateral amygdala and nucleus accumbens core underlie cocaine-seeking behavior by rats. J Neurosci 24:7167-7173.
Dilgen JE, O'Donnell PO (2004) Basolateral amygdala and ventral hippocampal stimulation evoke complex synaptic responses in prefrontal cortex pyramidal neurons recorded in vivo. In: Society for Neuroscience Annual Meeting. San Diego, CA.
Ding DC, Gabbott PL, Totterdell S (2001) Differences in the laminar origin of projections from the medial prefrontal cortex to the nucleus accumbens shell and core regions in the rat. Brain Res 917:81-89.

Engel AK, Singer W (2001) Temporal binding and the neural correlates of sensory awareness. Trends Cogn Sci 5:16-25.
Finch DM (1996) Neurophysiology of converging synaptic inputs from the rat prefrontal cortex, amygdala, midline thalamus, and hippocampal formation onto single neurons of the caudate/putamen and nucleus accumbens. Hippocampus 6:495-512.
Floresco SB, Grace AA (2003) Gating of hippocampal-evoked activity in prefrontal cortical neurons by inputs from the mediodorsal thalamus and ventral tegmental area. J Neurosci 23:3930-3943.
Floresco SB, Tse MT (2007) Dopaminergic regulation of inhibitory and excitatory transmission in the basolateral amygdala-prefrontal cortical pathway. J Neurosci 27:2045-2057.
Floresco SB, Ghods-Sharifi S (2007) Amygdala-prefrontal cortical circuitry regulates effort-based decision making. Cereb Cortex 17:251-260.
Floresco SB, Seamans JK, Phillips AG (1997) Selective roles for hippocampal, prefrontal cortical, and ventral striatal circuits in radial-arm maze tasks with or without a delay. J Neurosci 17:1880-1890.
Floresco SB, Braaksma DN, Phillips AG (1999) Thalamic-cortical-striatal circuitry subserves working memory during delayed responding on a radial arm maze. J Neurosci 19:11061-11071.
Floresco SB, Yang CR, Phillips AG, Blaha CD (1998) Basolateral amygdala stimulation evokes glutamate receptor-dependent dopamine efflux in the nucleus accumbens of the anaesthetized rat. Eur J Neurosci 10:1241-1251.
Floresco SB, Blaha CD, Yang CR, Phillips AG (2001a) Dopamine D1 and NMDA receptors mediate potentiation of basolateral amygdala-evoked firing of nucleus accumbens neurons. J Neurosci 21:6370-6376.
Floresco SB, Blaha CD, Yang CR, Phillips AG (2001b) Modulation of hippocampal and amygdalar-evoked activity of nucleus accumbens neurons by dopamine: cellular mechanisms of input selection. J Neurosci 21:2851-2860.
Floyd NS, Price JL, Ferry AT, Keay KA, Bandler R (2000) Orbitomedial prefrontal cortical projections to distinct longitudinal columns of the periaqueductal gray in the rat. J Comp Neurol 422:556-578.
Floyd NS, Price JL, Ferry AT, Keay KA, Bandler R (2001) Orbitomedial prefrontal cortical projections to hypothalamus in the rat. J Comp Neurol 432:307-328.
French SJ, Totterdell S (2002) Hippocampal and prefrontal cortical inputs monosynaptically converge with individual projection neurons of the nucleus accumbens. J Comp Neurol 446:151-165.
French SJ, Totterdell S (2003) Individual nucleus accumbens-projection neurons receive both basolateral amygdala and ventral subicular afferents in rats. Neuroscience 119:19-31.
French SJ, Totterdell S (2004) Quantification of morphological differences in boutons from different afferent populations to the nucleus accumbens. Brain Res 1007:167-177.
Fuller JH, Schlag JD (1976) Determination of antidromic excitation by the collision test: problems of interpretation. Brain Res 112:283-298.
Gabbott PL, Warner TA, Busby SJ (2006) Amygdala input monosynaptically innervates parvalbumin immunoreactive local circuit neurons in rat medial prefrontal cortex. Neuroscience 139:1039-1048.

Gale GD, Anagnostaras SG, Fanselow MS (2001) Cholinergic modulation of pavlovian fear conditioning: effects of intrahippocampal scopolamine infusion. Hippocampus 11:371-376.
Garcia R, Chang CH, Maren S (2006) Electrolytic lesions of the medial prefrontal cortex do not interfere with long-term memory of extinction of conditioned fear. Learn Mem 13:14-17.
Garcia R, Vouimba RM, Baudry M, Thompson RF (1999) The amygdala modulates prefrontal cortex activity relative to conditioned fear. Nature 402:294-296.
Gifford GW, 3rd, MacLean KA, Hauser MD, Cohen YE (2005) The neurophysiology of functionally meaningful categories: macaque ventrolateral prefrontal cortex plays a critical role in spontaneous categorization of species-specific vocalizations. J Cogn Neurosci 17:1471-1482.
Gilmartin MR, McEchron MD (2005) Single neurons in the medial prefrontal cortex of the rat exhibit tonic and phasic coding during trace fear conditioning. Behav Neurosci 119:1496-1510.
Goto Y, O'Donnell P (2002) Timing-dependent limbic-motor synaptic integration in the nucleus accumbens. Proc Natl Acad Sci U S A 99:13189-13193.
Goto Y, Grace AA (2005a) Dopamine-dependent interactions between limbic and prefrontal cortical plasticity in the nucleus accumbens: disruption by cocaine sensitization. Neuron 47:255-266.
Goto Y, Grace AA (2005b) Dopaminergic modulation of limbic and cortical drive of nucleus accumbens in goal-directed behavior. Nat Neurosci 8:805-812.
Grace AA (2000) Gating of information flow within the limbic system and the pathophysiology of schizophrenia. Brain Res Brain Res Rev 31:330-341.
Gray CM, Engel AK, Konig P, Singer W (1990) Stimulus-Dependent Neuronal Oscillations in Cat Visual Cortex: Receptive Field Properties and Feature Dependence. Eur J Neurosci 2:607-619.
Groenewegen HJ, Berendse HW, Wolters JG, Lohman AH (1990) The anatomical relationship of the prefrontal cortex with the striatopallidal system, the thalamus and the amygdala: evidence for a parallel organization. Prog Brain Res 85:95-116; discussion 116-118.
Hall J, Whalley HC, McKirdy JW, Romaniuk L, McGonigle D, McIntosh AM, Baig BJ, Gountouna VE, Job DE, Donaldson DI, Sprengelmeyer R, Young AW, Johnstone EC, Lawrie SM (2008) Overactivation of Fear Systems to Neutral Faces in Schizophrenia. Biol Psychiatry.
Hampton AN, Adolphs R, Tyszka MJ, O'Doherty J P (2007) Contributions of the amygdala to reward expectancy and choice signals in human prefrontal cortex. Neuron 55:545-555.
Hanes DP, Thompson KG, Schall JD (1995) Relationship of presaccadic activity in frontal eye field and supplementary eye field to saccade initiation in macaque: Poisson spike train analysis. Exp Brain Res 103:85-96.
Hasenstaub A, Shu Y, Haider B, Kraushaar U, Duque A, McCormick DA (2005) Inhibitory postsynaptic potentials carry synchronized frequency information in active cortical networks. Neuron 47:423-435.
Hashimoto T, Bazmi HH, Mirnics K, Wu Q, Sampson AR, Lewis DA (2008) Conserved Regional Patterns of GABA-Related Transcript Expression in the Neocortex of Subjects With Schizophrenia. Am J Psychiatry 165:479-489.
Holt W, Maren S (1999) Muscimol inactivation of the dorsal hippocampus impairs contextual retrieval of fear memory. J Neurosci 19:9054-9062.

Howland JG, Taepavarapruk P, Phillips AG (2002) Glutamate receptor-dependent modulation of dopamine efflux in the nucleus accumbens by basolateral, but not central, nucleus of the amygdala in rats. J Neurosci 22:1137-1145.
Hur EE, Zaborszky L (2005) Vglut2 afferents to the medial prefrontal and primary somatosensory cortices: a combined retrograde tracing in situ hybridization study [corrected]. J Comp Neurol 483:351-373.
Ishikawa A, Nakamura S (2003) Convergence and interaction of hippocampal and amygdalar projections within the prefrontal cortex in the rat. J Neurosci 23:9987-9995.
Ishikawa A, Nakamura S (2006) Ventral hippocampal neurons project axons simultaneously to the medial prefrontal cortex and amygdala in the rat. J Neurophysiol 96:2134-2138.
Izaki Y, Akema T (2008) Gamma-band power elevation of prefrontal local field potential after posterior dorsal hippocampus-prefrontal long-term potentiation induction in anesthetized rats. Exp Brain Res 184:249-253.
Jackson ME, Moghaddam B (2001) Amygdala regulation of nucleus accumbens dopamine output is governed by the prefrontal cortex. J Neurosci 21:676-681.
Jiang ZG, North RA (1991a) Membrane properties and synaptic responses of rat striatal neurones in vitro. J Physiol 443:533-553.
Jiang ZG, North RA (1991b) Membrane properties and synaptic responses of rat striatal neurones in vitro. J Physiol 443:533-553.
Jones JL, Wheeler RA, Day JJ, Carelli RM (2007) Examination of basolateral amygdala inactivation on nucleus accumbens cell firing during goal-directed behaviors. In: Society for Neuroscience Annual Meeting, p Program Number 530.535. San Diego, CA: Neuroscience Meeting Planner.
Jones MW, Wilson MA (2005) Theta rhythms coordinate hippocampal-prefrontal interactions in a spatial memory task. PLoS Biol 3:e402.
Jongen-Relo AL, Kaufmann S, Feldon J (2003) A differential involvement of the shell and core subterritories of the nucleus accumbens of rats in memory processes. Behav Neurosci 117:150-168.
Kalivas PW, Duffy P (1995) Selective activation of dopamine transmission in the shell of the nucleus accumbens by stress. Brain Res 675:325-328.
Kalivas PW, Volkow ND (2005) The neural basis of addiction: a pathology of motivation and choice. Am J Psychiatry 162:1403-1413.
Kalivas PW, Hu XT (2006) Exciting inhibition in psychostimulant addiction. Trends Neurosci 29:610-616.
Kaufman JN, Ross TJ, Stein EA, Garavan H (2003) Cingulate hypoactivity in cocaine users during a GO-NOGO task as revealed by event-related functional magnetic resonance imaging. J Neurosci 23:7839-7843.
Kawaguchi Y, Kubota Y (1997) GABAergic cell subtypes and their synaptic connections in rat frontal cortex. Cereb Cortex 7:476-486.
Kemp JM, Powell TP (1971) The structure of the caudate nucleus of the cat: light and electron microscopy. Philos Trans R Soc Lond B Biol Sci 262:383-401.
Kerr JN, Plenz D (2002) Dendritic calcium encodes striatal neuron output during up-states. J Neurosci 22:1499-1512.
Killcross S, Robbins TW, Everitt BJ (1997) Different types of fear-conditioned behaviour mediated by separate nuclei within amygdala. Nature 388:377-380.

Kilts CD, Schweitzer JB, Quinn CK, Gross RE, Faber TL, Muhammad F, Ely TD, Hoffman JM, Drexler KP (2001) Neural activity related to drug craving in cocaine addiction. Arch Gen Psychiatry 58:334-341.

Kiyatkin EA, Brown PL (2007) I.v. cocaine induces rapid, transient excitation of striatal neurons via its action on peripheral neural elements: single-cell, iontophoretic study in awake and anesthetized rats. Neuroscience 148:978-995.

Kolb B, Gorny G, Li Y, Samaha AN, Robinson TE (2003) Amphetamine or cocaine limits the ability of later experience to promote structural plasticity in the neocortex and nucleus accumbens. Proc Natl Acad Sci U S A 100:10523-10528.

Krettek JE, Price JL (1977a) The cortical projections of the mediodorsal nucleus and adjacent thalamic nuclei in the rat. J Comp Neurol 171:157-191.

Krettek JE, Price JL (1977b) Projections from the amygdaloid complex to the cerebral cortex and thalamus in the rat and cat. J Comp Neurol 172:687-722.

Kubos KL, Moran TH, Robinson RG (1987) Differential and asymmetrical behavioral effects of electrolytic or 6-hydroxydopamine lesions in the nucleus accumbens. Brain Res 401:147-151.

Lape R, Dani JA (2004) Complex response to afferent excitatory bursts by nucleus accumbens medium spiny projection neurons. J Neurophysiol 92:1276-1284.

Laviolette SR, Grace AA (2006) Cannabinoids Potentiate Emotional Learning Plasticity in Neurons of the Medial Prefrontal Cortex through Basolateral Amygdala Inputs. J Neurosci 26:6458-6468.

Laviolette SR, Lipski WJ, Grace AA (2005) A subpopulation of neurons in the medial prefrontal cortex encodes emotional learning with burst and frequency codes through a dopamine D4 receptor-dependent basolateral amygdala input. J Neurosci 25:6066-6075.

Ledford CC, Fuchs RA, See RE (2003) Potentiated reinstatement of cocaine-seeking behavior following D-amphetamine infusion into the basolateral amygdala. Neuropsychopharmacology 28:1721-1729.

LeDoux JE (2000) Emotion circuits in the brain. Annu Rev Neurosci 23:155-184.

LeDoux JE, Iwata J, Cicchetti P, Reis DJ (1988) Different projections of the central amygdaloid nucleus mediate autonomic and behavioral correlates of conditioned fear. J Neurosci 8:2517-2529.

LeDoux JE, Cicchetti P, Xagoraris A, Romanski LM (1990) The lateral amygdaloid nucleus: sensory interface of the amygdala in fear conditioning. J Neurosci 10:1062-1069.

Levesque M, Charara A, Gagnon S, Parent A, Deschenes M (1996) Corticostriatal projections from layer V cells in rat are collaterals of long-range corticofugal axons. Brain Res 709:311-315.

Levita L, Dalley JW, Robbins TW (2002) Disruption of Pavlovian contextual conditioning by excitotoxic lesions of the nucleus accumbens core. Behav Neurosci 116:539-552.

Lewis DA, Hashimoto T, Volk DW (2005) Cortical inhibitory neurons and schizophrenia. Nat Rev Neurosci 6:312-324.

Lewis DA, Cruz DA, Melchitzky DS, Pierri JN (2001) Lamina-specific deficits in parvalbumin-immunoreactive varicosities in the prefrontal cortex of subjects with schizophrenia: evidence for fewer projections from the thalamus. Am J Psychiatry 158:1411-1422.

Li Y, Kolb B, Robinson TE (2003) The location of persistent amphetamine-induced changes in the density of dendritic spines on medium spiny neurons in the nucleus accumbens and caudate-putamen. Neuropsychopharmacology 28:1082-1085.

Likhtik E, Pelletier JG, Paz R, Pare D (2005) Prefrontal control of the amygdala. J Neurosci 25:7429-7437.
MacLean PD (1952) Some psychiatric implications of physiological studies on frontotemporal portion of limbic system (visceral brain). Electroencephalogr Clin Neurophysiol 4:407-418.
Mahon S, Delord B, Deniau JM, Charpier S (2000) Intrinsic properties of rat striatal output neurones and time-dependent facilitation of cortical inputs in vivo. J Physiol 527 Pt 2:345-354.
Mahon S, Vautrelle N, Pezard L, Slaght SJ, Deniau JM, Chouvet G, Charpier S (2006) Distinct patterns of striatal medium spiny neuron activity during the natural sleep-wake cycle. J Neurosci 26:12587-12595.
Maren S, Quirk GJ (2004) Neuronal signalling of fear memory. Nat Rev Neurosci 5:844-852.
Maren S, Aharonov G, Fanselow MS (1997) Neurotoxic lesions of the dorsal hippocampus and Pavlovian fear conditioning in rats. Behav Brain Res 88:261-274.
Matsumoto K, Suzuki W, Tanaka K (2003) Neuronal correlates of goal-based motor selection in the prefrontal cortex. Science 301:229-232.
Maunsell JH, Gibson JR (1992) Visual response latencies in striate cortex of the macaque monkey. J Neurophysiol 68:1332-1344.
McGinty V, Grace A (2007) Selective Activation of Medial Prefrontal-to-Accumbens Projection Neurons by Amygdala Stimulation and Pavlovian Conditioned Stimuli. Cereb Cortex:bhm223.
McQuade RD, Chipkin R, Amlaiky N, Caron M, Iorio L, Barnett A (1988) Characterization of the radioiodinated analogue of SCH 23390: in vitro and in vivo D-1 dopamine receptor binding studies. Life Sci 43:1151-1160.
Meredith GE (1999) The synaptic framework for chemical signaling in nucleus accumbens. Ann N Y Acad Sci 877:140-156.
Milad MR, Quirk GJ (2002) Neurons in medial prefrontal cortex signal memory for fear extinction. Nature 420:70-74.
Milad MR, Vidal-Gonzalez I, Quirk GJ (2004) Electrical stimulation of medial prefrontal cortex reduces conditioned fear in a temporally specific manner. Behav Neurosci 118:389-394.
Mogenson GJ, Jones DL, Yim CY (1980) From motivation to action: functional interface between the limbic system and the motor system. Prog Neurobiol 14:69-97.
Moyer JT, Wolf JA, Finkel LH (2007) Effects of dopaminergic modulation on the integrative properties of the ventral striatal medium spiny neuron. J Neurophysiol 98:3731-3748.
Mulder AB, Hodenpijl MG, Lopes da Silva FH (1998) Electrophysiology of the hippocampal and amygdaloid projections to the nucleus accumbens of the rat: convergence, segregation, and interaction of inputs. J Neurosci 18:5095-5102.
Muller JF, Mascagni F, McDonald AJ (2005) Coupled networks of parvalbumin-immunoreactive interneurons in the rat basolateral amygdala. J Neurosci 25:7366-7376.
Neafsey EJ (1990) Prefrontal cortical control of the autonomic nervous system: anatomical and physiological observations. Prog Brain Res 85:147-165; discussion 165-146.
Neter J, Wasserman W, Kutner M (1990) Applied Linear Statistical Models, Third Edition. Burr Ridge, Illinoise: Irwin.
Nicola SM (2007) The nucleus accumbens as part of a basal ganglia action selection circuit. Psychopharmacology (Berl) 191:521-550.

Nicola SM, Deadwyler SA (2000) Firing rate of nucleus accumbens neurons is dopamine-dependent and reflects the timing of cocaine-seeking behavior in rats on a progressive ratio schedule of reinforcement. J Neurosci 20:5526-5537.
Nicola SM, Surmeier J, Malenka RC (2000) Dopaminergic modulation of neuronal excitability in the striatum and nucleus accumbens. Annu Rev Neurosci 23:185-215.
Nicola SM, Yun IA, Wakabayashi KT, Fields HL (2004) Cue-evoked firing of nucleus accumbens neurons encodes motivational significance during a discriminative stimulus task. J Neurophysiol 91:1840-1865.
Nicola SM, Taha SA, Kim SW, Fields HL (2005) Nucleus accumbens dopamine release is necessary and sufficient to promote the behavioral response to reward-predictive cues. Neuroscience 135:1025-1033.
Nisenbaum ES, Xu ZC, Wilson CJ (1994) Contribution of a slowly inactivating potassium current to the transition to firing of neostriatal spiny projection neurons. J Neurophysiol 71:1174-1189.
Norman DR, Streiner DL (2000) Biostatistics: The Bare Essentials. Hamilton, Ontario: B.C. Decker, Inc.
O'Donnell P, Grace AA (1993) Physiological and morphological properties of accumbens core and shell neurons recorded in vitro. Synapse 13:135-160.
O'Donnell P, Grace AA (1995) Synaptic interactions among excitatory afferents to nucleus accumbens neurons: hippocampal gating of prefrontal cortical input. J Neurosci 15:3622-3639.
O'Donnell P, Greene J, Pabello N, Lewis BL, Grace AA (1999) Modulation of cell firing in the nucleus accumbens. Ann N Y Acad Sci 877:157-175.
O'Neill MF, Shaw G (1999) Comparison of dopamine receptor antagonists on hyperlocomotion induced by cocaine, amphetamine, MK-801 and the dopamine D1 agonist C-APB in mice. Psychopharmacology (Berl) 145:237-250.
Ongur D, Price JL (2000) The organization of networks within the orbital and medial prefrontal cortex of rats, monkeys and humans. Cereb Cortex 10:206-219.
Orozco-Cabal L, Pollandt S, Liu J, Vergara L, Shinnick-Gallagher P, Gallagher JP (2006) A novel rat medial prefrontal cortical slice preparation to investigate synaptic transmission from amygdala to layer V prelimbic pyramidal neurons. J Neurosci Methods 151:148-158.
Ostlund SB, Balleine BW (2005) Lesions of medial prefrontal cortex disrupt the acquisition but not the expression of goal-directed learning. J Neurosci 25:7763-7770.
Otto T, Cousens G, Rajewski K (1997) Odor-guided fear conditioning in rats: 1. Acquisition, retention, and latent inhibition. Behav Neurosci 111:1257-1264.
Palomero-Gallagher N, Mohlberg H, Zilles K, Vogt B (2008) Cytology and receptor architecture of human anterior cingulate cortex. J Comp Neurol 508:906-926.
Parkinson JA, Willoughby PJ, Robbins TW, Everitt BJ (2000) Disconnection of the anterior cingulate cortex and nucleus accumbens core impairs Pavlovian approach behavior: further evidence for limbic cortical-ventral striatopallidal systems. Behav Neurosci 114:42-63.
Paton JJ, Belova MA, Morrison SE, Salzman CD (2006) The primate amygdala represents the positive and negative value of visual stimuli during learning. Nature 439:865-870.
Paxinos G, Watson C (1998) The Rat Brain in Stereotaxic Coordinates: Fourth Edition: Academic Press.

Paxinos G, Watson C (2005) The Rat Brain in Stereotaxic Coordinates: Fifth Edition. San Diego, CA: Elsevier Academic Press.
Pennartz CM, Lopes da Silva FH (1994) Muscarinic modulation of synaptic transmission in slices of the rat ventral striatum is dependent on the frequency of afferent stimulation. Brain Res 645:231-239.
Perez-Jaranay JM, Vives F (1991) Electrophysiological study of the response of medial prefrontal cortex neurons to stimulation of the basolateral nucleus of the amygdala in the rat. Brain Res 564:97-101.
Petrovich GD, Holland PC, Gallagher M (2005) Amygdalar and prefrontal pathways to the lateral hypothalamus are activated by a learned cue that stimulates eating. J Neurosci 25:8295-8302.
Pezze MA, Feldon J (2004) Mesolimbic dopaminergic pathways in fear conditioning. Prog Neurobiol 74:301-320.
Pinto A, Sesack SR (2000) Limited collateralization of neurons in the rat prefrontal cortex that project to the nucleus accumbens. Neuroscience 97:635-642.
Pitkanen A (2000) Connectivity of the rat amygdaloid complex. In: The Amygdala: A functional analysis (Aggleton JP, ed), pp 31-116. New York, NY: Oxford University Press.
Pratt WE, Mizumori SJ (1998) Characteristics of basolateral amygdala neuronal firing on a spatial memory task involving differential reward. Behav Neurosci 112:554-570.
Price JL (1999) Prefrontal cortical networks related to visceral function and mood. Ann N Y Acad Sci 877:383-396.
Price JL (2007) Definition of the orbital cortex in relation to specific connections with limbic and visceral structures and other cortical regions. Ann N Y Acad Sci 1121:54-71.
Quirk G, Garcia R, Gonzalez-Lima F (2006) Prefrontal Mechanisms in Extinction of Conditioned Fear. Biological Psychiatry 60:337-343.
Quirk GJ, Russo GK, Barron JL, Lebron K (2000) The role of ventromedial prefrontal cortex in the recovery of extinguished fear. J Neurosci 20:6225-6231.
Quirk GJ, Likhtik E, Pelletier JG, Pare D (2003) Stimulation of medial prefrontal cortex decreases the responsiveness of central amygdala output neurons. J Neurosci 23:8800-8807.
Resstel LB, Joca SR, Guimaraes FG, Correa FM (2006a) Involvement of medial prefrontal cortex neurons in behavioral and cardiovascular responses to contextual fear conditioning. Neuroscience 143:377-385.
Resstel LBM, Joca SRL, Guimaraes FG, Correa FMA (2006b) Involvement of medial prefrontal cortex neurons in behavioral and cardiovascular responses to contextual fear conditioning. Neuroscience 143:377-385.
Riedel G, Harrington NR, Hall G, Macphail EM (1997) Nucleus accumbens lesions impair context, but not cue, conditioning in rats. Neuroreport 8:2477-2481.
Robbins TW, Everitt BJ (1996) Neurobehavioural mechanisms of reward and motivation. Curr Opin Neurobiol 6:228-236.
Roitman MF, Wheeler RA, Carelli RM (2005) Nucleus accumbens neurons are innately tuned for rewarding and aversive taste stimuli, encode their predictors, and are linked to motor output. Neuron 45:587-597.
Rosenkranz JA, Grace AA (1999) Modulation of basolateral amygdala neuronal firing and afferent drive by dopamine receptor activation in vivo. J Neurosci 19:11027-11039.

Rosenkranz JA, Grace AA (2002) Dopamine-mediated modulation of odour-evoked amygdala potentials during pavlovian conditioning. Nature 417:282-287.
Rosenkranz JA, Grace AA (2003) Affective conditioning in the basolateral amygdala of anesthetized rats is modulated by dopamine and prefrontal cortical inputs. Ann N Y Acad Sci 985:488-491.
Rosenkranz JA, Moore H, Grace AA (2003) The prefrontal cortex regulates lateral amygdala neuronal plasticity and responses to previously conditioned stimuli. J Neurosci 23:11054-11064.
Schoenbaum G, Chiba AA, Gallagher M (1998) Orbitofrontal cortex and basolateral amygdala encode expected outcomes during learning. Nat Neurosci 1:155-159.
Schoenbaum G, Chiba AA, Gallagher M (1999) Neural encoding in orbitofrontal cortex and basolateral amygdala during olfactory discrimination learning. J Neurosci 19:1876-1884.
Schoenbaum G, Setlow B, Saddoris MP, Gallagher M (2003) Encoding predicted outcome and acquired value in orbitofrontal cortex during cue sampling depends upon input from basolateral amygdala. Neuron 39:855-867.
Schulz D, Staples L, Mailman R (1985) SCH23390 causes persistent antidopaminergic effects in vivo: Evidence for longterm occupation of receptors. Life Sciences 36:1941-1948.
Schwienbacher I, Schnitzler HU, Westbrook RF, Richardson R, Fendt M (2006) Carbachol injections into the nucleus accumbens disrupt acquisition and expression of fear-potentiated startle and freezing in rats. Neuroscience 140:769-778.
Sesack SR, Deutch AY, Roth RH, Bunney BS (1989) Topographical organization of the efferent projections of the medial prefrontal cortex in the rat: an anterograde tract-tracing study with Phaseolus vulgaris leucoagglutinin. J Comp Neurol 290:213-242.
Sesack SR, Carr DB, Omelchenko N, Pinto A (2003) Anatomical substrates for glutamate-dopamine interactions: evidence for specificity of connections and extrasynaptic actions. Ann N Y Acad Sci 1003:36-52.
Setlow B, Holland PC, Gallagher M (2002) Disconnection of the basolateral amygdala complex and nucleus accumbens impairs appetitive pavlovian second-order conditioned responses. Behav Neurosci 116:267-275.
Setlow B, Schoenbaum G, Gallagher M (2003) Neural encoding in ventral striatum during olfactory discrimination learning. Neuron 38:625-636.
Shin LM, Wright CI, Cannistraro PA, Wedig MM, McMullin K, Martis B, Macklin ML, Lasko NB, Cavanagh SR, Krangel TS, Orr SP, Pitman RK, Whalen PJ, Rauch SL (2005) A functional magnetic resonance imaging study of amygdala and medial prefrontal cortex responses to overtly presented fearful faces in posttraumatic stress disorder. Arch Gen Psychiatry 62:273-281.
Shinonaga Y, Takada M, Mizuno N (1994) Topographic organization of collateral projections from the basolateral amygdaloid nucleus to both the prefrontal cortex and nucleus accumbens in the rat. Neuroscience 58:389-397.
Shipley RH (1974) Extinction of conditioned fear in rats as a function of several parameters of CS exposure. J Comp Physiol Psychol 87:699-707.
Sierra-Mercado D, Jr., Corcoran KA, Lebron-Milad K, Quirk GJ (2006) Inactivation of the ventromedial prefrontal cortex reduces expression of conditioned fear and impairs subsequent recall of extinction. Eur J Neurosci 24:1751-1758.

Spencer KM, Nestor PG, Perlmutter R, Niznikiewicz MA, Klump MC, Frumin M, Shenton ME, McCarley RW (2004) Neural synchrony indexes disordered perception and cognition in schizophrenia. Proc Natl Acad Sci U S A 101:17288-17293.
Steriade M, Contreras D (1998) Spike-wave complexes and fast components of cortically generated seizures. I. Role of neocortex and thalamus. J Neurophysiol 80:1439-1455.
Steriade M, Timofeev I, Grenier F (2001) Natural waking and sleep states: a view from inside neocortical neurons. J Neurophysiol 85:1969-1985.
Steriade M, Amzica F, Neckelmann D, Timofeev I (1998) Spike-wave complexes and fast components of cortically generated seizures. II. Extra- and intracellular patterns. J Neurophysiol 80:1456-1479.
Surmeier DJ, Bargas J, Kitai ST (1989) Two types of A-current differing in voltage-dependence are expressed by neurons of the rat neostriatum. Neurosci Lett 103:331-337.
Swadlow HA (1994) Efferent neurons and suspected interneurons in motor cortex of the awake rabbit: axonal properties, sensory receptive fields, and subthreshold synaptic inputs. J Neurophysiol 71:437-453.
Swanson LW, Petrovich GD (1998) What is the amygdala? Trends Neurosci 21:323-331.
Team RDC (2005) R: A language and environment for statistical computing. In. Vienna, Austria: R Foundation for Statistical Computing.
Tepper JM, Bolam JP (2004) Functional diversity and specificity of neostriatal interneurons. Curr Opin Neurobiol 14:685-692.
Traub RD, Whittington MA, Stanford IM, Jefferys JG (1996) A mechanism for generation of long-range synchronous fast oscillations in the cortex. Nature 383:621-624.
Tye KM, Janak PH (2007) Amygdala neurons differentially encode motivation and reinforcement. J Neurosci 27:3937-3945.
Wan X, Peoples L (2006) Firing Patterns of Accumbal Neurons During a Pavlovian-Conditioned Approach Task. J Neurophysiol 96:652-660.
Wang XJ, Buzsaki G (1996) Gamma oscillation by synaptic inhibition in a hippocampal interneuronal network model. J Neurosci 16:6402-6413.
West AR, Grace AA (2002) Opposite influences of endogenous dopamine D1 and D2 receptor activation on activity states and electrophysiological properties of striatal neurons: studies combining in vivo intracellular recordings and reverse microdialysis. J Neurosci 22:294-304.
West AR, Floresco SB, Charara A, Rosenkranz JA, Grace AA (2003) Electrophysiological interactions between striatal glutamatergic and dopaminergic systems. Ann N Y Acad Sci 1003:53-74.
Wickens JR, Wilson CJ (1998) Regulation of action-potential firing in spiny neurons of the rat neostriatum in vivo. J Neurophysiol 79:2358-2364.
Wilson CJ, Kawaguchi Y (1996) The origins of two-state spontaneous membrane potential fluctuations of neostriatal spiny neurons. J Neurosci 16:2397-2410.
Wilson CJ, Chang HT, Kitai ST (1990) Firing patterns and synaptic potentials of identified giant aspiny interneurons in the rat neostriatum. J Neurosci 10:508-519.
Wilson DI, Bowman EM (2005) Rat nucleus accumbens neurons predominantly respond to the outcome-related properties of conditioned stimuli rather than their behavioral-switching properties. J Neurophysiol 94:49-61.
Wolf JA, Moyer JT, Lazarewicz MT, Contreras D, Benoit-Marand M, O'Donnell P, Finkel LH (2005) NMDA/AMPA ratio impacts state transitions and entrainment to oscillations in a

computational model of the nucleus accumbens medium spiny projection neuron. J Neurosci 25:9080-9095.
Wright CI, Groenewegen HJ (1995) Patterns of convergence and segregation in the medial nucleus accumbens of the rat: relationships of prefrontal cortical, midline thalamic, and basal amygdaloid afferents. J Comp Neurol 361:383-403.
Yim CY, Mogenson GJ (1982) Response of nucleus accumbens neurons to amygdala stimulation and its modification by dopamine. Brain Res 239:401-415.
Young AM, Ahier RG, Upton RL, Joseph MH, Gray JA (1998) Increased extracellular dopamine in the nucleus accumbens of the rat during associative learning of neutral stimuli. Neuroscience 83:1175-1183.
Yun IA, Wakabayashi KT, Fields HL, Nicola SM (2004) The ventral tegmental area is required for the behavioral and nucleus accumbens neuronal firing responses to incentive cues. J Neurosci 24:2923-2933.